NAVAL POSTGRADUATE SCHOOL
Monterey, California

THESIS

AN ANALYSIS OF COHERENT DIGITAL RECEIVERS IN THE PRESENCE OF COLORED NOISE INTERFERENCE

by

Avraham Hasarchi

June 1985

Thesis Advisor: Daniel Bukofzer

REPORT DOCUMENTATION PAGE

READ INSTRUCTIONS BEFORE COMPLETING FORM

1. REPORT NUMBER
2. GOVT ACCESSION NO.
3. RECIPIENT'S CATALOG NUMBER

4. TITLE (and Subtitle)
An Analysis of Coherent Digital Receivers in the Presence of Colored Noise Interference

5. TYPE OF REPORT & PERIOD COVERED
Master's Thesis
June 1985

6. PERFORMING ORG. REPORT NUMBER

7. AUTHOR(s)
Avraham Hasarchi

8. CONTRACT OR GRANT NUMBER(s)

9. PERFORMING ORGANIZATION NAME AND ADDRESS
Naval Postgraduate School
Monterey, California 93943-5100

10. PROGRAM ELEMENT, PROJECT, TASK AREA & WORK UNIT NUMBERS

11. CONTROLLING OFFICE NAME AND ADDRESS
Naval Postgraduate School
Monterey, California 93943-5100

12. REPORT DATE
June 1985

13. NUMBER OF PAGES
141

14. MONITORING AGENCY NAME & ADDRESS (If different from Controlling Office)

15. SECURITY CLASS. (of this report)
Unclassified

15a. DECLASSIFICATION/DOWNGRADING SCHEDULE

16. DISTRIBUTION STATEMENT (of this Report)
Approved for public release; distribution unlimited

17. DISTRIBUTION STATEMENT (of the abstract entered in Block 20, if different from Report)

18. SUPPLEMENTARY NOTES

19. KEY WORDS (Continue on reverse side if necessary and identify by block number)
Colored Noise, Colored Noise Digital Receiver, Jamming

20. ABSTRACT (Continue on reverse side if necessary and identify by block number)

Optimum receivers for detecting binary signals in additive colored Gaussian noise are analyzed and their performance evaluated in terms of bit error probabilities (P_e). Implementation and practical design implications of such receivers is discussed. Evaluation of P_e for receivers that are optimum for additive white Gaussian noise (WGN) environments but due to jamming or "friendly" ECM interferers, must operate in a colored Gaussian

#20 - ABSTRACT - (CONTINUED)

noise environment has been carried out. It was generally found that such receivers do not perform significantly worse than receivers specifically designed to operate in a colored noise environment. Examples were considered in which the colored noise interference was modeled as the output of a one-pole filter driven by WGN. Additional work has been carried out on the jamming of binary (colored noise) receivers using a deterministic jammer model. While this modeling assumption needs to be refined, it has been demonstrated that a power constrained jammer can seriously degrade the performance of a receiver designed to operate in a colored noise environment.

Approved for public release; distribution unlimited.

An Analysis of Coherent Digital Receivers in the Presence of Colored Noise Interference

by

Avraham Hasarchi
Major, Israel Air Force
B.Sc.E.E., Technion, Haifa, Israel, 1973
M.B.A., University of Tel-Aviv, Israel, 1981

Submitted in partial fulfillment of the
requirements for the degree of

MASTER OF SCIENCE IN ELECTRICAL ENGINEERING

from the

NAVAL POSTGRADUATE SCHOOL

June 1985

ABSTRACT

Optimum receivers for detecting binary signals in additive colored Gaussian noise are analyzed and their performance evaluated in terms of bit error probabilities (P_e). Implementation and practical design implications of such receivers is discussed. Evaluation of P_e for receivers that are optimum for additive white Gaussian noise (WGN) environments but due to jamming or "friendly" ECM interferers, must operate in a colored Gaussian noise environment has been carried out. It was generally found that such receivers do not perform significantly worse than receivers specifically designed to operate in a colored noise environment. Examples were considered in which the colored noise interference was modeled as the output of a one-pole filter driven by WGN. Additional work has been carried out on the jamming of binary (colored noise) receivers using a deterministic jammer model. While this modeling assumption needs to be refined, it has been demonstrated that a power constrained jammer can seriously degrade the performance of a receiver designed to operate in a colored noise environment.

TABLE OF CONTENTS

LIST OF FIGURES

ACKNOWLEDGMENT

I wish to express my appreciation to my thesis advisor Prof. Daniel Bukofzer for his efforts and guidance which contributed to the completion of this work.

I. INTRODUCTION

The theory of statistical signal detection and estimation in the presence of colored noise is described in many textbooks [Refs. 1,2, 3]. However, applications and practical system design considerations as well as implementations based on the developed theory are not often discussed.

There are some [Refs. 4,5,6] DOD research publications which deal with signal reception in colored noise. None of these publications uses colored noise thoery as developed in textbooks or analyzes advantages and disadvantages of signal designs that account for the presence of colored noise.

The goals of this thesis are to:

1. Discuss some practical applications that can be derived from colored noise signal detection theory.
2. Analyze practical design implications of the theory.
3. Present advantages as well as disadvantages of using theoretical results involving colored noise interferences as compared to results dealing with white noise interference models.

Specifically, the following problems will be analyzed:

1. The design of a binary communication receiver in the presence of colored noise interference when the signals used to transmit the binary information are completely known.
2. Design of an optimum signal set for a receiver operation under the same conditions as in 1. above.
3. Comparison of the performance of the receivers analyzed in 1. and 2. above relative to an equivalent receiver designed to operate in white noise interference.

4. Evaluation of the effect of an RF prefilter on the performance of a binary communication receiver.

5. Evaluation of the performance of receivers designed for colored noise interference operating in the presence of jammers.

This thesis is divided up as follows.

In Chapter II we present briefly colored noise theory and the integral equations governing the receiver design. In Chapter III we analyze Fredholm Integral Equations and the techniques used for solving them for baseband signals and bandpass signals. In Chapter IV we discuss receiver design and performance in the presence of colored noise interference, according to the rules of colored noise theory. We also compare these results to the more conventional receiver designed to operate in a white noise only environment. In Chapter V we analyze the effect of using RF-preamplifiers in digital receivers. In Chapter VI the sensitivity of this receiver is evaluated when operating in the presence of colored noise interference and a deterministic jammer signal which is optimum in a specific sense. Performance comparisons to equivalent white noise environment receivers are presented. The Conclusions and interpretations of the results obtained are presented in Chapter VII.

II. THEORY OF COHERENT SIGNAL DETECTION IN THE PRESENCE OF COLORED NOISE

A. DETECTION IN THE PRESENCE OF WHITE GAUSSIAN NOISE

The design of coherent signal receivers in the presence of additive white Gaussian noise (WGN) is widely dealt with in the literature [Refs. 7,8,9,10]. The optimum receiver (in the sense of producing minimum probability of error) for discriminating between two different yet completely known signals in additive WGN is shown in Fig. 2.1.

The receiver of Fig. 2.1 is optimum (i.e., minimum probability of error) when the received signal z(t) is either

$$\text{Hypothesis } H_1: \quad z(t) = y_1(t) + n(t) \qquad 0 \leq t \leq T$$

$$\text{Hypothesis } H_0: \quad z(t) = y_0(t) + n(t) \qquad 0 \leq t \leq T$$

where y_1 and $y_0(t)$ are known deterministic signals and n(t) is a sample function of a WGN process. For convenience we define

$$y_d(t) \triangleq y_1(t) - y_0(t)$$

The threshold level shown in Fig. 2.1 is given by [Refs. 7,8,9,10].

$$\gamma = \frac{N_0}{2} \ln \frac{(1-P)}{P} + \frac{1}{2}(E_1 - E_0) \qquad (2.1)$$

where

$$E_i = \int_0^T y_i^2(t)dt \qquad i = 0,1$$

and $\frac{N_0}{2}$ is the two-sided power spectral density level of the WGN interference. Also, P is the prior probability that signal $y_1(t)$ was sent.

If equiprobably and equal energy signals are transmitted, then P = 1/2 and the threshold γ becomes zero.

Assuming equiprobable signals, the performance of this receiver is given by

$$P_e = ERFC_*\left(\sqrt{\frac{E(1-\rho)}{N_0}}\right) \qquad (2.1A)$$

where

$$E = \frac{1}{2}\int_0^T [y_0^2(t) + y_1^2(t)]\,dt = \text{AVG Bit Energy}$$

and

$$\rho = \frac{1}{E}\int_0^T y_0(t)y_1(t)dt$$

The complementary function $ERFC_*(\cdot)$ used throughout this thesis is defined as

$$ERFC_*(v) = \int_v^\infty \frac{1}{\sqrt{2\pi}}\,\varepsilon^{-x^2/2}\,dx$$

For the so-called antipodal signals, $y_1(t)$ and $y_0(t)$ are related by

$$y_1(t) = -y_0(t)$$

Hence $\rho = -1$ and Eq. 2.1A becomes

$$P_e = \text{ERFC}_*(\sqrt{(2E)/N_0}) \tag{2.2}$$

It is important to notice that P_e is independent of the particular waveform shapes used. Equation (2.1A) demonstrates that the signal-to-noise ratio (SNR) E/N_0 and the normalized signal correlation coefficient ρ are the only factors affecting P_e. Such will not be the case when the noise interference is colored.

B. DETECTION IN THE PRESENCE OF COLORED NOISE

In certain cases, the transmitted signals can encounter a nonwhite colored Gaussian interference. The most common such cases arise when:

1. Between the actual white noise source and the signal processing part of the receiver, there are some bandpass elements such as antennas or RF filters which shape the noise spectrum so that it no longer is white.

2. In addition to the desired signal at the front end of the receiver, there is an interfering signal which may be some ECM jammer or may be a "friendly" electronic emitter causing interference in the communication channel. In radar/sonar systems such interference is frequently caused by multiple targets.

3. Multipath channel interferences arise which effectively add a colored noise component to the channel.

The basic decision model can now be specified as follows

$$\text{Hypothesis } H_1: \quad z(t) = y_1(t) + n_w(t) + n_c(t) \qquad 0 \leq t \leq T$$

$$\text{Hypothesis } H_0: \quad z(t) = y_0(t) + n_w(t) + n_c(t) \qquad 0 \leq t \leq T$$

where $n_c(t)$ is the colored noise component and $n_w(t)$ is the white noise component. Notice that a white noise component is present in the model. It is appropriate to assume that the interference contains also an independent white component due to the fact that:

1. Practical systems always will contain a nonzero thermal white noise component. Even shot noise which is dominant in the optical range of the spectrum is also practically a white noise.

2. As will be discussed in Appendix A, the white noise component enables us to guarantee that our mathematical solutions will be meaningful.

The conventional approach in the design of an optimum receiver is to take "samples" of the received signal, express the joint probability density function of these samples and then to determine the limiting form as the samples are taken closer together and their number increases to infinity. These operations become more difficult in the case of colored noise since the samples may no longer be statistically independent [Refs. 1,2,10].

The approaches taken when colored noise interference is present are to:

1. Introduce a "Whitening" filter to transform the interference into a white Gaussian noise so that use of

the white Gaussian interference analysis to solve the problem is possible [Refs. 1,2].

2. Use the Karhunen-Loeve expansion [Ref. 3].

The advantage of the Karhunen-Loeve expansion is that it leads to a series of elements, the coefficients of which are uncorrelated. These coefficients represent the signal "samples" or components along the dimensions associated with each eigenfunction $g_i(t)$.

Clearly both the "Whitening Filter" approach and the Karhunen-Loeve expansion approach lead to exactly the same results.

C. DERIVATION OF THE OPTIMUM RECEIVER IN COLORED NOISE VIA THE KARHUNEN-LOEVE EXPANSION METHOD

Let us assume that the noise is colored with covariance function $K_v(t,u)$. We expand the noise covariance function in terms of a set of orthogonal functions. We use the Karhunen-Loeve expansion in which the orthogonal functions are the eigenfunctions of the integral equation

$$\int_0^T K_v(t,u)g_i(u)du = \lambda_i g_i(t) \quad i = 1,2,... \tag{2.3}$$

We are now able to expand the received signal $z(t)$, the signals $y_i(t)$, $i = 0,1$, and the noise $n(t)$ in the coordinate system specified by the set $\{g_i(t)\}$. That is

$$z(t) = \underset{K\to\infty}{\ell.i.m} \sum_{i=1}^{K} z_i g_i(t) \tag{2.4}$$

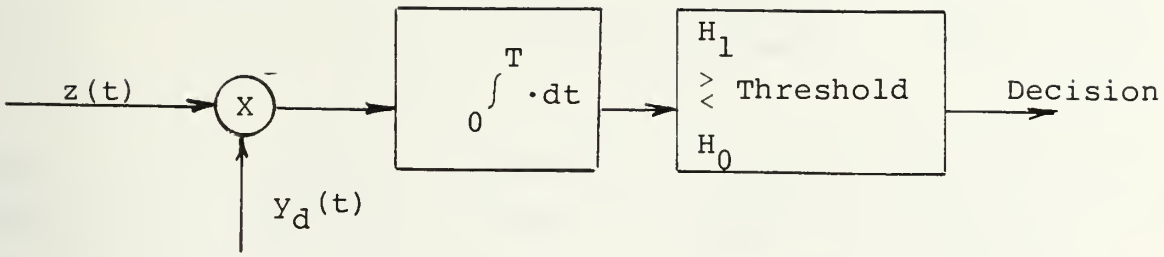

Figure 2.1 Coherent Correlator Receiver

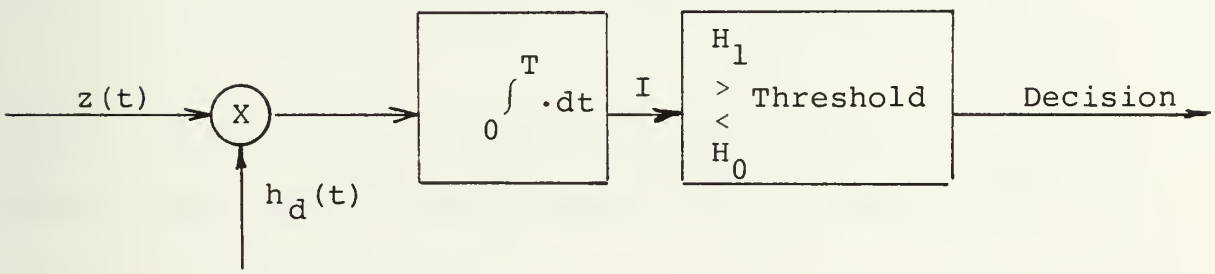

Figure 2.2 Coherent Colored Noise Correlator Receiver

$$n(t) = \underset{K\to\infty}{\ell.i.m} \sum_{i=1}^{K} n_i g_i(t) \tag{2.5}$$

$$y_j(t) = \underset{K\to\infty}{\ell.i.m} \sum_{i=1}^{K} y_{ji} g_i(t) \qquad j = 0,1 \tag{2.6}$$

where

$$z_i = \int_0^T z(t) g_i(t) dt \qquad i = 1,2,... \tag{2.7}$$

$$n_i = \int_0^T n(t) g_i(t) dt \qquad i = 1,2,... \tag{2.8}$$

$$y_{ji} = \int_0^T y_j(t) g_i(t) dt \qquad \begin{matrix} i = 1,2,... \\ j = 0,1 \end{matrix} \tag{2.9}$$

It is reasonable to assume that the noise is zero mean. Then

$$E(n_i) = 0 \qquad i = 1,2,... \tag{2.10}$$

The covariance of n_i and n_j will become

$$E(n_i n_j) = E\left[\int_0^T n(t) g_i(t) dt \cdot \int_0^T n(u) g_j(u) du\right]$$

$$= \int_0^T g_i(t) \int_0^T K_v(t,u) g_j(u)\, du\, dt \tag{2.11}$$

Substituting Eq. (2.3) into (2.11) yields

$$E(n_i n_j) = \lambda_i \delta_{ij} \tag{2.12}$$

where δ_{ij} is the Kroenecker delta. Equation (2.12) demonstrates that the Karhunen-Loeve expansion leads to noise "samples" that are statistically independent since the noise has been assumed Gaussian.

We can now express the likelihood ratio test involving the K signal "samples" as follows [Refs. 4,5,6]

$$\Lambda(z_k(t)) = \frac{\prod_{i=1}^{K} \frac{1}{\sqrt{2\pi\lambda_i}} \exp\{-\frac{1}{2}\frac{(z_i - y_{1i})^2}{2\lambda_i}\}}{\prod_{i=1}^{K} \frac{1}{\sqrt{2\pi\lambda_i}} \exp\{-\frac{1}{2}\frac{(z_i - y_{0i})^2}{2\lambda_i}\}} \underset{H_0}{\overset{H_1}{\gtrless}} \gamma \tag{2.13}$$

where γ is the threshold defined by Eq. (2.1). Cancelling common terms, taking the logarithm and letting K to infinity yields the decision rule

$$\ell n(\Lambda(z(t))) = \sum_{i=1}^{\infty} \frac{z_i}{\lambda_i}(y_{1i} - y_{0i}) - \frac{1}{2}\sum_{i=1}^{\infty} \frac{1}{\lambda_i}(y_{0i}^2 - y_{1i}^2)$$

$$\underset{H_0}{\overset{H_1}{\gtrless}} \ell n\ \gamma \tag{2.14}$$

If equiprobable antipodal signals are used, then $\ell n\ \gamma = 0$. Expressing the likelihood ratio in terms of the signals z(t),

$y_1(t)$, and $y_0(t)$ by using Equations (2.8), (2.9), (2.10), respectively, yields

$$\int_0^T \int_0^T [y_1(u)-y_0(u)]z(t) \sum_{i=1}^{\infty} \frac{g_i(t)g_i(u)}{\lambda_i} du\, dt$$

$$+ \frac{1}{2} \int_0^T \int_0^T [y_0(t)y_0(u)-y_1(t)y_1(u)] \sum_{i=1}^{\infty} \frac{g_i(t)g_i(u)}{\lambda_i} du\, dt \underset{H_0}{\overset{H_1}{>}} 0 \tag{2.15}$$

We define

$$h_1(t) - h_0(t) \triangleq h_d(t) = \int_0^T (y_1(u)-y_0(u)) \sum_{i=1}^{\infty} \frac{g_i(t)g_i(u)}{\lambda_i} du \tag{2.16}$$

Substituting Eq. (2.16) in Eq. (2.15) yields the simplified decision rule

$$\int_0^T z(t)h_d(t)dt \underset{H_0}{\overset{H_1}{>}} \frac{1}{2} \int_0^T [y_1(t)h_1(t)-y_0(t)h_0(t)]dt \triangleq \gamma' \tag{2.17}$$

where $h_d(t)$ is defined by Eq. (2.16). The term on the right-hand side of the inequality sign is a constant and may be considered as a new threshold γ'.

We can get a different mathematical form for $h_d(t)$ by multiplying Eq. (2.16) by $K_v(t,u)$ and then integrating over the interval (0,T). We thus obtain

$$\int_0^T K_v(t,u)h_d(u)du = \int_0^T \int_0^T K_v(t,u)(y_1(u) - y_0(u)) \cdot \sum_{i=1}^{\infty} \frac{g_i(t)g_i(u)}{\lambda_i} dt\,du$$

$$= y_1(t) - y_0(t) \ . \qquad (2.18)$$

Therefore $h_d(u)$ is now defined by the integral equation

$$\int_0^T K_v(t,u)h_d(u)du = y_1(t) - y_0(t) \qquad (2.19)$$

An optimum receiver structure can now be obtained as a direct consequence of the decision rule of Eq. (2.17). Eq. (2.19) defines $h_d(t)$ implicitly and the receiver structure is shown in Fig. 2.2. We refer to this receiver as a "Colored Noise Receiver." Fig. 2.2 shows that this receiver is a correlation detection receiver much like a "White Noise Receiver," except that the correlating signal is no longer of the same form as that of the transmitted signal but instead is given by the solution to the integral equation of Eq. (2.19).

D. RECEIVER PERFORMANCE

The performance of a binary communication receiver can be quantified as the probability of making an erroneous decision labeled P_e. This involves finding the probabilities that the

output, I, of the correlator (Fig. 2.2) exceeds or is exceeded by the threshold given knowledge of which signal was transmitted. This can be accomplished since I is a linear combination of a Gaussian noise and therefore is a Gaussian random variable. Thus, P_e is given by

$$P_e = P\{H_0\}P\{I>\gamma'|H_0\} + P\{H_1\}P\{I<\gamma'|H_1\}$$

$$= P\{H_0\} \int_{\gamma'}^{\infty} P\{I|H_0\}dI + P\{H_1\} \int_{-\infty}^{\gamma'} P\{I|H_1\}dI$$

where $P\{H_0\}$, $P\{H_1\}$ are the prior probabilities of sending signal y_0 or y_1, respectively. Since we assume equiprobable antipodal signals, $P\{H_0\} = P\{H_1\} = \frac{1}{2}$ and γ' as defined by Eq. (2.17) is zero. Since $I|H_0$ and $I|H_1$ are Gaussian variables, their mean and variance only need to be found in order to evaluate the P_e. The mean value of $I|H_0$ is given by

$$E\{I|H_0\} = E\{\int_0^T [y_0(t)+n(t)]h_d(t)dt\} = \int_0^T y_0(t)h_d(t)dt$$

$$\triangleq m_0. \qquad (2.21)$$

Similarly

$$E\{I|H_1\} = \int_0^T y_1(t)h_d(t)dt \triangleq m_1. \qquad (2.21A)$$

For antipodal signals, that is $y_0(t) = -y_1(t)$, we have

$$m_1 = -m_0 . \tag{2.22}$$

It can be easily shown that the variance of random variable I conditioned by H_0 or H_1 is given by

$$\text{Var}\{I|H_1\} = \text{Var}\{I|H_0\} = E\{[\int_0^T n(t)h_d(t)dt]^2\} \triangleq \sigma_I^2 \tag{2.23}$$

Eq. (2.23) can be written in the form

$$\sigma_I^2 = \int_0^T \int_0^T h_d(t)K_v(t,u)h_d(u)\, du dt \tag{2.23A}$$

Substituting Eq. (2.19) in Eq. (2.23A) yields

$$\sigma_I^2 = \int_0^T h_d(t)y_d(t)\, dt = 2m_1 \tag{2.24}$$

From Eq. (2.21) and Eq. (2.24) and since $\gamma' = 0$ for antipodal equiprobable signals, P_e becomes

$$P_e = \frac{1}{2}\int_0^\infty \frac{1}{\sqrt{2\pi\sigma_I^2}} \exp\{-\frac{(I-m_1)^2}{2\sigma_I^2}\}\, dI + \frac{1}{2}\int_{-\infty}^0 \frac{1}{\sqrt{2\pi\sigma_I^2}} \exp\{-\frac{(I-m_0)^2}{2\sigma_I^2}\}\, dI \tag{2.25}$$

A change of variables in Eq. (2.25) and use of Eqs. (2.21-2.23) yields

$$P_e = \mathrm{ERFC}_*\left(\sqrt{\frac{1}{4}\int_0^T y_d(t)h_d(t)dt}\right) = \mathrm{ERFC}_*\left(\sqrt{\frac{1}{4}\cdot 2m_1}\right) \quad (2.26)$$

Observe that the performance of the "Colored noise" receiver does depend on the signal waveforms. For white noise interference P_e was shown to be independent of the signal waveforms. (See Eq. (2.2).)

E. OPTIMUM SIGNAL DESIGN

Since the performance of the receiver analyzed in the previous sections depends on $y_d(t)$, there may be an optimum waveform set for minimum probability of error. From Eq. (2.26) it is clear that by making $y_d(t)$ large, P_e can be made small. Thus, to make the optimization problem meaningful an energy constraint is placed on the signal set. That is, with fixed

$$E = \frac{1}{2}\int_0^T (y_0^2(t) + y_1^2(t))dt$$

$$J = \int_0^T y_d(t)h_d(t)dt - \mu\left[\int_0^T (y_0^2(t)+y_1^2(t))dt - 2E\right) \quad (2.27)$$

is to be maximized, where μ is the Lagrange multiplier. It then follows from the calculus of variations [Refs. 1,2] that

the optimum signal set obeys

$$y_1(t) = -y_0(t) \tag{2.28}$$

and

$$\int_0^T K_v(t,u)y_1(u)du = \lambda_i y_1(t) \tag{2.29}$$

or equivalently

$$\int_0^T K_v(t,u)y_d(u)du = \lambda_i y_d(t) \tag{2.30}$$

There are many solutions to Eq. (2.30) and the one which corresponds to the minimal λ_i should be chosen [Refs. 2,14].

F. SUMMARY

This chapter discusses the theory of designing a receiver in the presence of colored noise interference. Figure 2.2 shows the block diagram of this receiver and reveals the fact that this receiver is basically a correlation detection receiver. The only difference is that the correlating signal $h_d(t)$ which is given by the solution of the integral equation

$$\int_0^T K_v(t,u)h_d(u)du = y_1(t) - y_0(t) = y_d(t) \tag{2.19}$$

must be used in place of $y_d(t)$ as is done for an optimum receiver operating in WGN interference. The performance of this receiver assuming equiprobable antipodal signals is given by equation

$$P_e = \text{ERFC}^*\left(\sqrt{\frac{1}{4}\int_0^T y_d(t)h_d(t)\,dt}\right) \tag{2.26}$$

The performance depends heavily on the signal waveforms. An optimum signal waveform set is given by the solution of the integral equation

$$\int_0^T K_v(t,u)y_d(u)\,du = \frac{1}{\lambda_i} y_d(t) \ . \tag{2.30}$$

The design procedure of a colored noise receiver will then consist of the following steps:

1. Identifying the environmental noise and formulating its correlation function.
2. Solving Eq. (2.19) for the correlating signal $h_d(t)$ when $y_1(t)$ and $y_0(t)$ are known.
3. If $y_1(t)$ or $y_0(t)$ are not given, then Eq. (2.30) must be solved first for an optimal signal set and only then can Eq. (2.19) be solved for the optimum correlating signal.

III. SOLUTION OF FREDHOLM INTEGRAL EQUATIONS

A. FREDHOLM INTEGRAL EQUATIONS

As demonstrated in the previous chapter, an important step in the design of the colored noise receiver involves solving an integral equation in order to obtain $h_d(t)$. That is, a solution to the following equation must be found.

$$\int_0^T K_v(t,u)h_d(u)du = y_d(t) \qquad 0 \leq t \leq T \tag{2.19}$$

This equation is called a Fredholm Equation of the First Kind. The function $K_v(t,u)$, namely the noise covariance, is called the kernel of the equation. If the kernel of Eq. (2.19) contains singularities, or equivalently if the colored noise contains an additive white noise component, then $K_v(t,u)$ takes on the mathematical form

$$K_v(t,u) = \frac{N_1}{2}\delta(t-u) + K_c(t,u) \qquad (*)(3.1)$$

which when substituted in Eq. (2.19), yields

$$\frac{N_1}{2} h_d(t) + \int_0^T K_c(t,u)h_d(u)du = y_d(t) \quad 0 \leq t \leq T \tag{3.2}$$

(*) Throughout this thesis, $\delta(t)$ denotes the Dirac Delta Function.

This equation is called a Fredholm Equation of the Second Kind.

The properties satisfied by these equations have been discussed and proved in many textbooks [Refs. 2,11,12]. We shall state here only those properties that are important to the present work.

Property 1: If the kernel does not contain singularities (i.e., no white noise component) a finite square integrable solution to the Fredholm I equation will not exist.

Property 2: In this case of kernel singularities, a solution to the Fredholm I equation will exist only if we allow it to contain singularity functions (impulses).

The solution will then be of the form

$$h_d(t) = h_p(t) + \sum_i a_i h_{hi}(t) + \sum_k b_k \delta^{(k)}(t) \qquad (3.3)$$

where $h_p(t)$ and $h_{hi}(t)$ are the particular and homogeneous solutions, respectively, to a differential equation derived from the Fredholm I equation and $\delta^{(k)}(t)$ is the k-th derivative of $\delta(t)$ [Ref. 1].

Property 3: The solution to Fredholm equations are at best tedious to obtain and in many cases solutions are very difficult or impossible to obtain. In two specific cases there is a straightforward procedure for solving Fredholm II equations.

1. If the kernel is separable, the solution is quite easy to obtain [Ref. 11].
2. If the noise power spectral density is a ratio of two polynomials, a solution can be obtained after following a specific procedure. This situation occurs when the colored noise is the steady state response of a linear time invariant system excited by white noise.

In this research, we shall deal only with Fredholm II equations for the following reasons.

1. From a practical standpoint, we do not want to deal with the problem of trying to generate impulse functions.
2. In real physical systems there will always be some white noise component, however small, due to thermal effects in the electronic circuitry. One is never able to totally eliminate the white noise component.

Also, we will deal only with colored noise having a rational spectra since it best models the output of real physical systems.

B. GENERAL SOLUTION TO FREDHOLM II EQUATIONS FOR BASEBAND SIGNALS

The Fredholm II equation of interest is

$$\frac{N_1}{2} h_d(t) + \int_0^T K_c(t,u) h_d(u) du = y_d(t) \quad 0 \leq t \leq T \qquad (3.2)$$

We assume that:

1. The white noise component has power spectral density level $N_1/2$ watts/Hz.

2. The noises are wide-sense stationary (W.S.S.)

3. The Power Spectral Density (P.S.D.) of the colored noise can be expressed as a ratio of two polynomials that are functions of the complex variables, namely

$$\phi_c(s) = \frac{N(s^2)}{D(s^2)}$$

($\phi_c(s)$ and $K_c(\tau)$ are a two sided Laplace transform pair). Multiplying both sides of the above equation by $D(s^2)$ yields

$$D(s^2)\phi_c(s) = N(s^2) \tag{3.4}$$

Multiplication by s corresponds to differentiation with respect to t in the time domain. So, Eq. (3.4) becomes

$$D(p^2)K_c(t-u) = N(p^2)\delta(t-u) \tag{3.5}$$

where $p = d/dt$. Operating on Eq. (3.2) with $D(p^2)$ yields

$$D(p^2)\left[\frac{N_1}{2} h_d(t)\right] + \int_0^T h_d(u) D(p^2)[K_c(t,u)]du$$

$$= D(p^2)[y_d(t)] \tag{3.6}$$

Substituting Eq. (3.5) in (3.6) and performing the integration yields

$$D(p^2)\left[\frac{N_1}{2} h_d(t)\right] + N(p^2)[h_d(t)] = D(p^2)y_d(t) \tag{3.7}$$

Eq. (3.7) is a differential equation that must be solved completely. In this research we deal with a simple colored noise model in which the output of a lst order Butterworth filter driven by white noise is taken as the source of colored noise. Thus its P.S.D. is given by

$$\phi_c(s) = \frac{N(s^2)}{D(s^2)} = \frac{2\alpha\beta}{-s^2+\beta^2} \tag{3.8}$$

Equivalently in the time domain

$$K_c(\tau) = \alpha\varepsilon^{-\beta|\tau|} \tag{3.9}$$

Substituting Eq. (3.8) into (3.7) yields

$$D(p^2)[\frac{N_1}{2} h_d(t)] + 2\alpha\beta[h_d(t)] = D[p^2]y_d(t)$$

Operating with $D(p^2)$ yields

$$-\frac{N_1}{2}\ddot{h}_d(t) + (\frac{N_1}{2}\beta^2 + 2\alpha\beta)h_d(t) = -\ddot{y}_d(t) + \beta^2 y_d(t) \; . \tag{3.10}$$

Eq. (3.10) is a second order differential equation. Its solution is of the form

$$h_d(t) = h_p(t) + K_1 h_{h1}(t) + K_2 h_{h2}(t) \tag{3.11}$$

where $h_p(t)$ is the particular solution and $h_{h1}(t)$ and $h_{h2}(t)$ form the homogeneous solution. Substitution of Eq. (3.11)

into Eq. (3.2) leads to two simultaneous equations that K_1 and K_2 must satisfy. Solving for K_1 and K_2 explicitly gives the complete solution.

A similar procedure must be applied when the noise is modeled as the output of a higher order Butterworth filter. For such a case (Nth order Butterworth filter), the noise P.S.D. is

$$\phi_c(s) = \frac{\beta^{2N}}{(\beta)^{2N} + s^{2N}} = \frac{N(s^2)}{D(s^2)} \tag{3.12}$$

Substituting Eq. (3.12) in Eq. (3.2) yields

$$\frac{N_1}{2}\left[\frac{d^{2N}}{dt^{2N}} h_d(t)\right] + \left[\frac{N_1}{2}(\beta)^{2N} + (\beta)^{2N}\right] h_d(t) = \frac{d^{2N}}{dt^{2N}} y_d(t) + (\beta)^{2N} y_d(t) \tag{3.13}$$

There will now be 2N homogeneous solutions and a particular solution. Substitution into the Fredholm II equation will lead to 2N simultaneous equations from which the constants associated with the homogeneous solutions must be determined.

The complete solution for the case in which $y_d(t)$ is rectangular or sinusoidal is worked out in detail in Appendices A and B. The procedure is long and tedious so that for higher order filters numerical techniques must be utilized.

C. GENERAL SOLUTION TO FREDHOLM II EQUATIONS FOR BANDPASS SIGNALS

In practice, the communication signals are baseband signals which modulate a carrier prior to transmission. The received signals can be modeled as

$$\text{Hypothesis } H_1: \quad z(t) = y_1(t)\cos \omega_0 t + n(t) \quad 0 \leq t \leq T$$

$$\text{Hypothesis } H_0: \quad z(t) = y_0(t)\cos \omega_0 t + n(t) \quad 0 \leq t \leq T \tag{3.14}$$

$$y_d(t) \cos \omega_0 t = [y_1(t)-y_0(t)]\cos \omega_0 t \tag{3.15}$$

where ω_0 is the carrier frequency and $y_1(t)$, and $y_0(t)$ are the baseband signals.

The Fredholm II equation now becomes

$$\frac{N_1}{2} \tilde{h}_d(t) + \int_0^T \tilde{K}_c(t,u)\tilde{h}_d(u)du = y_d(t) \cos\omega_0 t \tag{3.16}$$

where $\tilde{h}(t)$, $\tilde{K}(t-u)$ represent bandpass waveforms.

The bandpass autocorrelation function $\tilde{K}_c(t,u)$ can be expressed as

$$\tilde{K}_c(t-u) = K_c(t-u)\cos \omega_0(t-u) \tag{3.17}$$

where $K_c(t-u)$ is the baseband autocorrelation function.

The solution of this equation follows the same procedure as the one used in the solution of Eq. (3.2) but is considerably more tedious.

In Appendix C, we prove that if the carrier frequency ω_0 is much bigger than the bandwidth of the noise or the bandwidth of the information signals, then the solution to Eq. (3.16) is approximated by

$$\tilde{h}_d(t) \cong h_d(t)\cos \omega_0 t \tag{3.18}$$

where $h_d(t)$ is the solution to the Fredholm II (Baseband) equation of Eq. (3.2).

Since in practical cases the carrier frequency is much bigger than the bandwidth of the data or of the colored noise, we will only solve the Fredholm II equation for baseband signals and will use this solution as the solution for the bandpass case using Eq. (3.18).

IV. RECEIVER DESIGN AND PERFORMANCE IN THE PRESENCE OF COLORED NOISE INTERFERENCE

A. INTRODUCTION

This chapter presents the analysis of a typical case in which the communication receiver operates in an environment which consists of colored noise interference. This interference can be due to an ECM jammer, a 'friendly' electronic emitter, or some multipath interference. This chapter presents the design of the colored noise receiver which is optimized to the presence of the interference. The performance of this receiver is analyzed and compared to the performance of a coherent digital communication receiver (designed for white noise only interference) operating in the same environment. The most important parameter in the design procedure is the interference P.S.D. This fact creates problems when designing a colored noise receiver whose function is to suppress hostile interferences. However there are many applications in which the P.S.D. of the colored noise is either known or can be measured sufficiently accurately. A typical such application occurs when a digital communication receiver has to operate on board a ship or an aircraft in the presence of other friendly emitters such as radars, ECM transmitters, or navigational equipment. Those emitters whose characteristics are known, often cause significant degradation in the quality of the digital communication channel. Even multipath interference can

be measured and modeled as colored noise interference whose power spectral density or autocorrelation function are known. The results of this chapter demonstrate that in such situations, utilization of a colored noise receiver with "proper" signal waveforms can improve the P_e performance.

B. THE MODEL

The system model consists of a digital coherent communication receiver operating in the presence of both colored noise and additive white noise interference as shown in Fig. 4.1. Both noises are assumed Gaussian.

The signals are binary, at baseband, and encounter baseband interference. Extensions to bandpass signal analysis is straightforward, given the results described in Chapter III, Section C.

The colored noise source block diagram is shown in Fig. 4.2. This is the typical block diagram of a noise jammer [Ref. 13].

The output P.S.D. of the colored noise source is

$$N_c(f) = \frac{N_0}{2} H(f)H^*(f) \tag{4.1}$$

where H(f) is the transfer function of the amplifier chain. For the sake of simplicity, we model the amplifier chain as a one-stage amplifier of gain G followed by a first order Butterworth filter with 3 db bandwidth 2β. If the input to that source is a white noise with P.S.D. level $N_0'/2$, then the output P.S.D. is

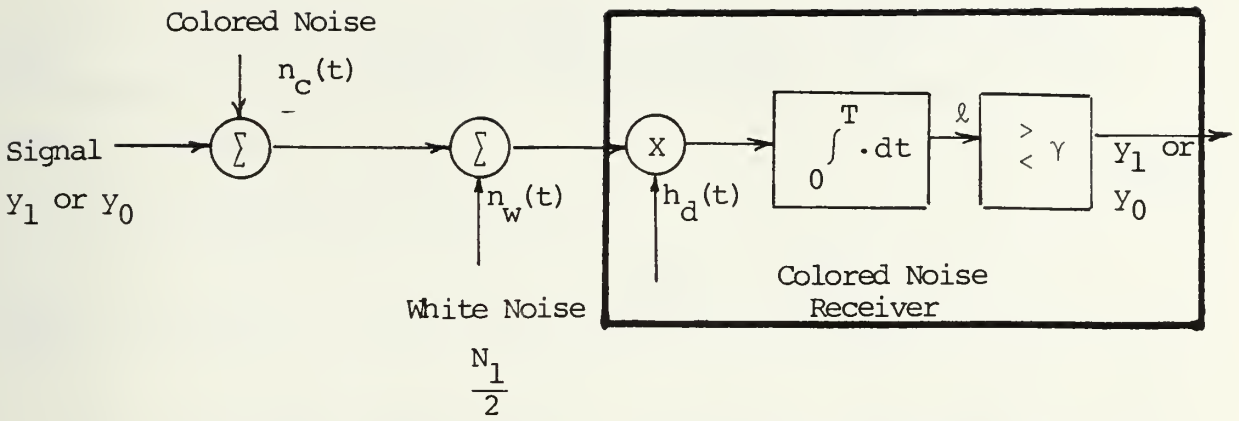

Figure 4.1 Colored Noise Receiver and Colored Noise Interference

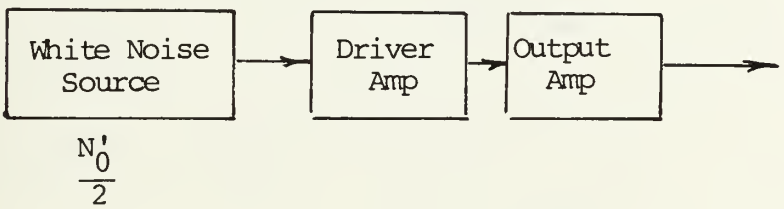

Figure 4.2 Colored Noise Source

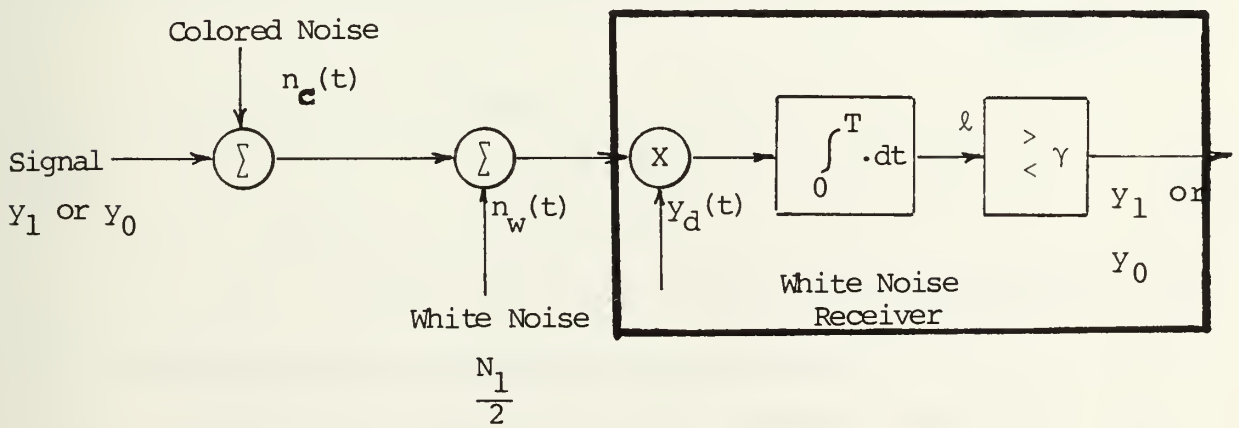

Figure 4.3 White Noise Receiver and Colored Noise Interference

$$\phi_c(s) = \frac{N_0'}{2} G^2 \frac{\beta^2}{-s^2+\beta^2} = \frac{N_0}{2} \frac{\beta^2}{-s^2+\beta^2} \tag{4.2}$$

where

$$\frac{N_0}{2} = \frac{N_0'}{2} G^2 \tag{4.3}$$

The P.S.D. can also be written in accordance with the notation of Appendix A as

$$\phi_c(s) = \frac{2\alpha\beta}{-s^2+\beta^2} \tag{4.4}$$

where

$$\alpha = \frac{N_0}{4} \beta. \tag{4.5}$$

In the time domain, the autocorrelation of the colored noise is given by

$$K_c(\tau) = \alpha \exp(-\beta|\tau|) . \tag{4.6}$$

and the power of the colored noise is given by

$$P_j = K_c(0) = \alpha = \frac{N_0}{4} \beta \tag{4.7}$$

One should notice that since a constant power source is assumed, an increase in the bandwidth β must be accompanied by

a drop in the gain G so that P_j in Eq. (4.7) will remain unchanged as β is varied. The colored noise receiver structure is shown in Fig. 4.1.

The input to the receiver is

$$\text{Hypothesis } H_0: \quad z(t) = y_0(t) + n_c(t) + n_w(t) \qquad 0 \leq t \leq T$$

$$\text{Hypothesis } H_1: \quad z(t) = y_1(t) + n_c(t) + n_w(t)$$

where $y_1^{(t)}$ and $y_0^{(t)}$ are defined as

$$y_0(t) = \begin{cases} -A & 0 \leq t \leq T \\ 0 & 0 > t,\ t > T \end{cases} \tag{4.8}$$

$$y_1(t) = \begin{cases} A & 0 \leq t \leq T \\ 0 & 0 > t,\ t > T \end{cases} \tag{4.9}$$

and for convenience we define (as before)

$$y_d(t) = y_1(t) - y_0(t) \tag{4.10}$$

C. RECEIVER DESIGN FOR RECTANGULAR PULSES

As discussed in Chapter II, the optimum receiver is (as can be seen in Fig. 4.1) a correlation detection receiver. The correlating signal, $h_d(t)$, is the solution of the Fredholm II Integral equation

$$\frac{N_1}{2} h_d(t) + \int_0^T K_c(t,u) h_d(u) du = y_d(t) \qquad (3.2)$$

The detailed solution of Eq. (3.2) for the specific autocorrelation function and signals given by Eqs. (4.6) and (4.8), (4.9) respectively, is worked out in Appendix A. The solution is given by Eq. (A.13), namely

$$h_d(t) = C(1 + K_1 \varepsilon^{\gamma t} + K_2 \varepsilon^{-\gamma t}) \quad 0 \leq t \leq T \qquad (A.13)$$

where K_1, K_2, C, and γ are constants defined by Eqs. (A.15), (A.16), (A.17) respectively. Defining now

$$m_1 \triangleq \sqrt{1 + \frac{N_0}{N_1}} \qquad (4.11)$$

where N_0 is given by Eq. (4.3) and $N_1/2$ is the white noise P.S.D. level and also defining

$$E \triangleq \beta T \qquad (4.12)$$

where T is the length of the integration time in the receiver, it is now possible to specify $h_d(t)$ in compact form. Observe that the factor 1/T can be interpreted as the bandwidth of the receiver, so that E can be viewed as the ratio of the interference bandwidth to the receiver bandwidth. Substituting into the results of Appendix A the above definitions as well

as the definition of α as given by Eq. (4.5), we can express $h_d(t)$ as a function of A, N_0, N_1, m_1, and E as follows

$$C = \frac{4A}{N_0 + N_1} \tag{4.13}$$

$$K_1 = \left[\frac{(m_1+1)\left[\varepsilon^{-Em_1} + \frac{m_1-1}{m_1+1}\varepsilon^{-2Em_1}\right]}{\frac{m_1+1}{m_1-1} - \frac{m_1-1}{m_1+1}\varepsilon^{-2Em_1}} \right] \tag{4.14}$$

$$K_2 = \frac{(m_1-1)\left[\frac{m_1+1}{m_1-1} + \varepsilon^{-Em_1}\right]}{\frac{m_1+1}{m_1-1} - \varepsilon^{-2Em_1}\cdot\frac{m_1-1}{m_1+1}} \tag{4.15}$$

$$h_d(t) = C + CK_1\varepsilon^{+\beta m_1 t} + CK_2\varepsilon^{-\beta m_1 t} \tag{4.16}$$

Ignoring the constant of proportionality C, it is easy to see that $h_d(t)$ is a function of m_1 and E. Using Eqs. (4.7), (4.11), (4.12), m_1 can be written as

$$m_1 = \sqrt{1 + \frac{N_0}{N_1}} = \sqrt{1 + \frac{P_j 4A^2T}{\beta N_1 A^2 T}} = \sqrt{1 + \frac{4(JSR)(SNR)}{E}} \tag{4.17}$$

where

$$JSR = \frac{P_j}{A^2}, \qquad SNR = \frac{A^2T}{N_1} \tag{4.18}$$

The factor JSR is the ratio of the jamming power to signal power. The factor SNR is the ratio of bit energy to white noise power spectral density level. This factor can also be interpreted as the signal to noise ratio. The product (JSR)(SNR) represents implicitly the ratio of the interference power to the white noise power at the input to the receiver. It is independent of the signal power.

Figure 4.4 presents a plot of $h_d(t)$ as a function of time normalized to T for (JSR)(SNR) = 1, and different values of E. Figures 4.5 and 4.6 show similar plots for different (JSR)(SNR) values with E as a parameter.

These figures show that decreasing the interference power or increasing E tend to make the colored noise interference less dominant in comparison to the white noise. Effectively this makes the receiver behave very much like a white noise receiver. It is not particularly difficult to design a system whose output will be $h_d(t)$. Such an implementation is suggested in Appendix D. Furthermore, there are now programmable signal generators in the commercial market. However we should be aware that $h_d(t)$ depends on:

1. The colored noise autocorrelation function, and signal waveform.
2. The colored noise power relative to the white noise power.
3. The colored noise bandwidth relative to receiver bandwidth.

These factors must not only be known but must also remain time independent, unless adaptive techniques are used. This would

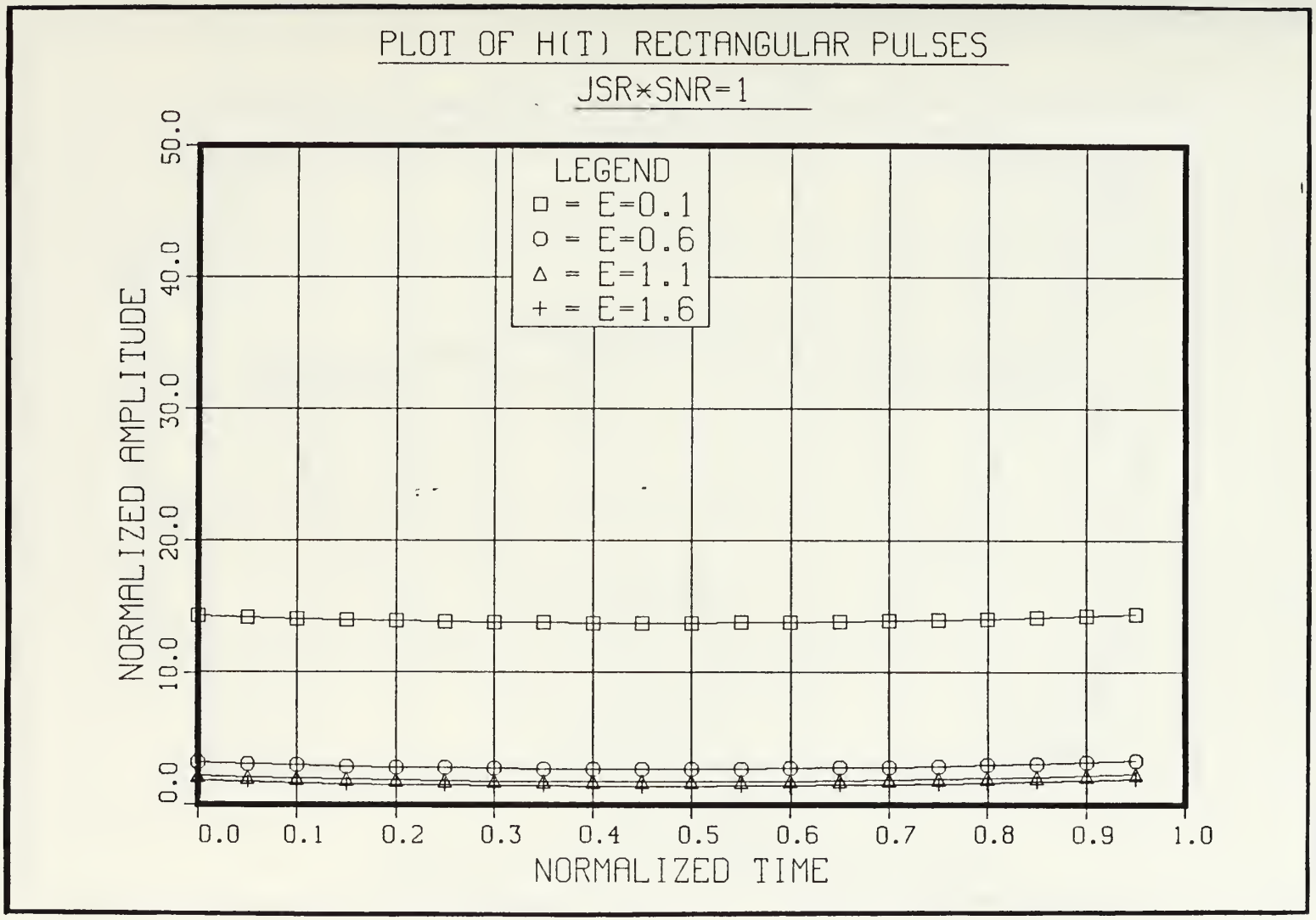

Figure 4.4 Plot of $h_d(t)$ for Rectangular Pulses Where (JSR)(SNR) = 1

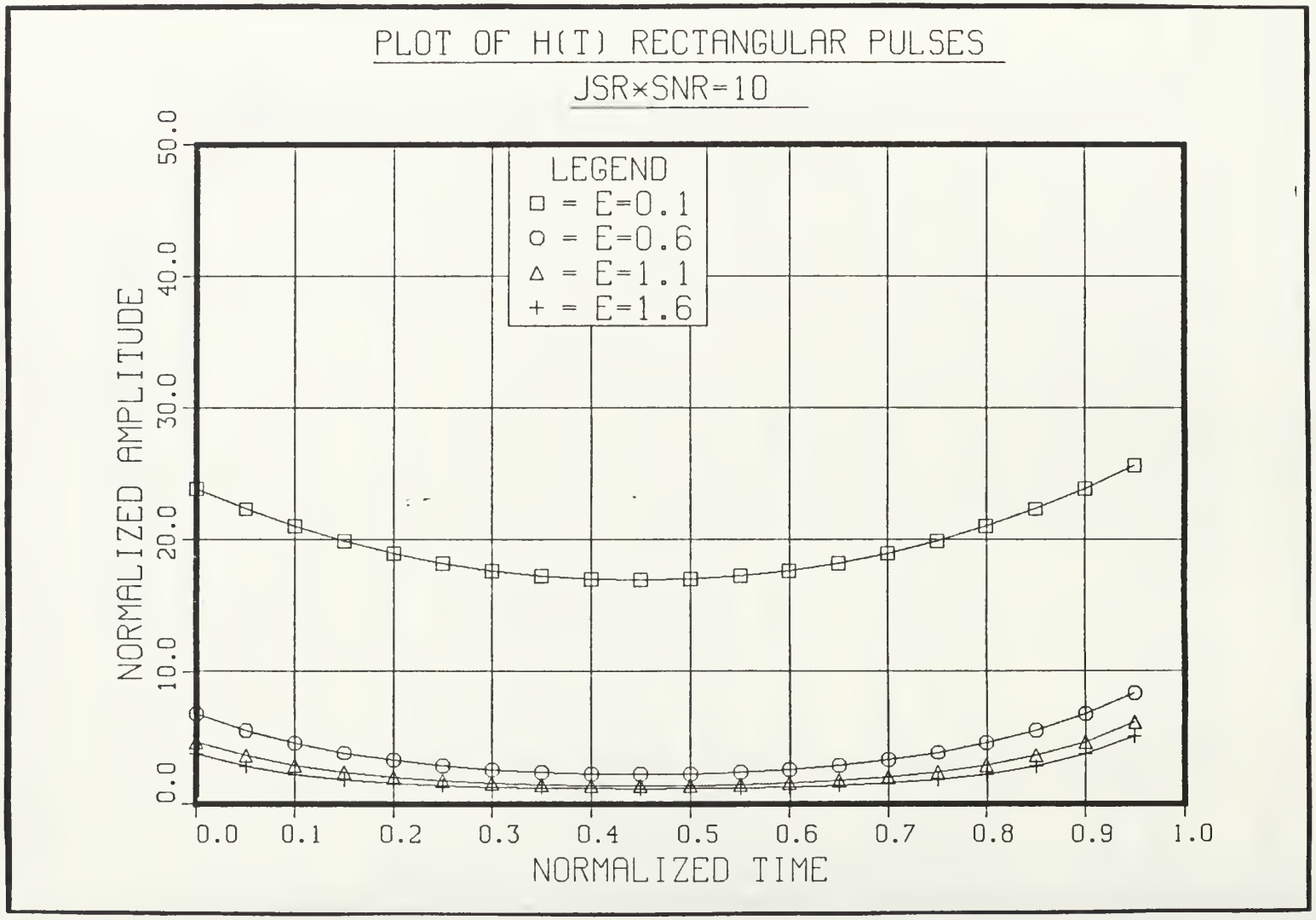

Figure 4.5 Plot of $h_d(t)$ for Rectangular Pulses Where (JSR)(SNR) = 10

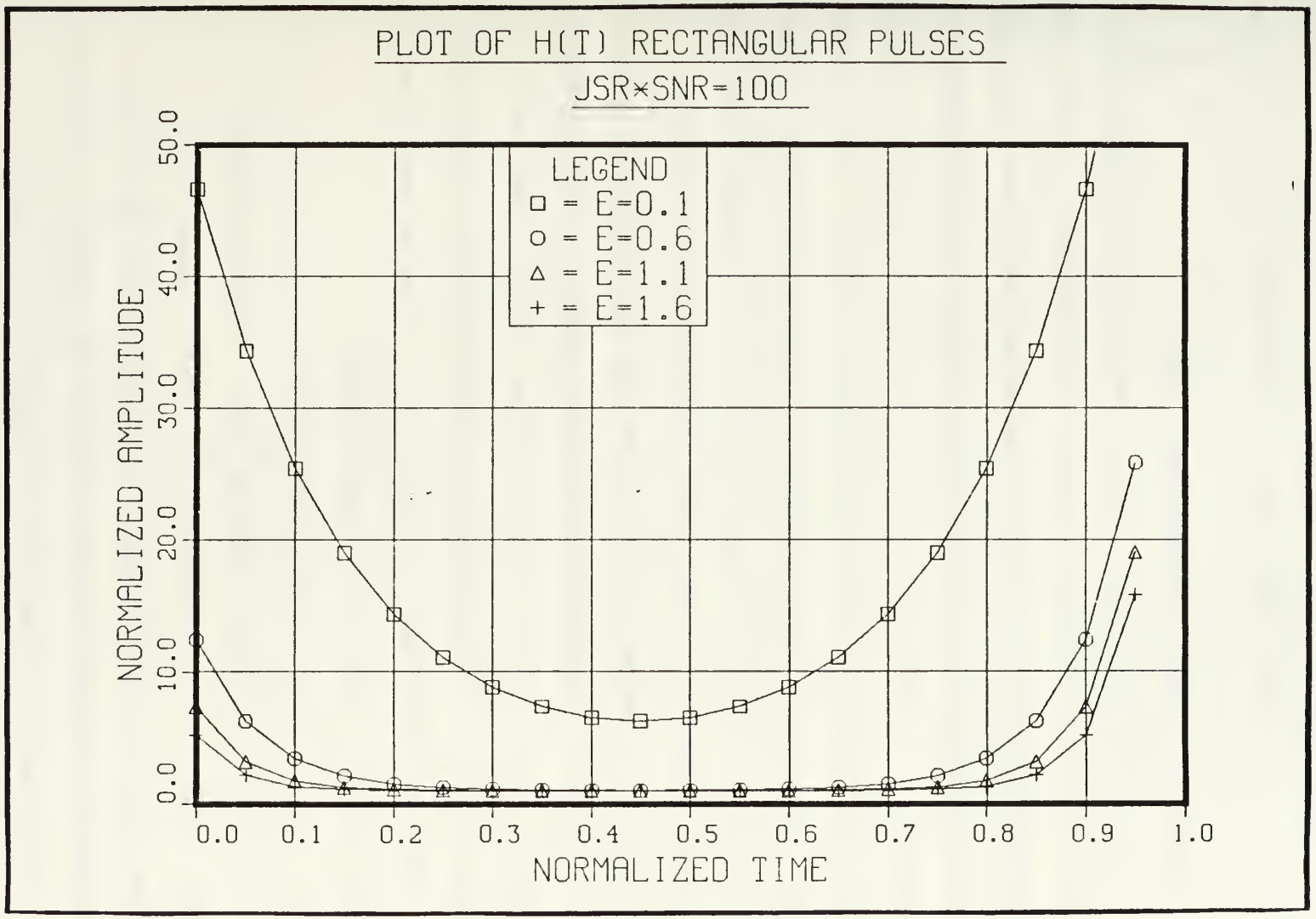

Figure 4.6 Plot of $h_d(t)$ for Rectangular Pulses Where (JSR)(SNR) = 100

otherwise seriously complicate the electronic circuitry. These $h_d(t)$ dependencies cause significant constraints on the application and use of colored noise theory to receiver design problems.

D. RECEIVER DESIGN FOR OPTIMAL PULSES

Colored noise theory results demonstrate that the performance of the optimal colored noise receiver, unlike the white noise receiver, depends on signal waveforms $y_0(t)$ and $y_1(t)$. The optimal choice for $y_0(t)$ and $y_1(t)$ is obtained as a solution of the integral equation given by Eq. (2.30). We now assume that the model described in Section IV.B is valid except that the binary communication signals are no longer rectangular pulses but can be chosen by the system designer. In other words the system designer has one more "degree of freedom." In order to determine the optimum waveforms to be utilized by the system designer, we solve the integral equation of Eq. (2.30) for the case in which the kernel is defined by Eq. (4.6). The solution is worked out in detail in [Ref. 14] and consists of a set of cosines and sines of frequencies b_i which are the solutions

$$(\tan b_i T + \frac{b_i}{\beta})(\tan b_i T - \frac{\beta}{b_i}) = 0, \quad i = 1,2,... \tag{4.19}$$

There is an infinite number of solutions to Eq. (4.19). Since antipodal signaling can be shown to be optimum, we choose one solution for $y_1(t)$ and $y_0(t)$ given by

$$\begin{cases} y_1(t) = A \sin bt & 0 \leq t \leq T \\ y_0(t) = -A \sin bt & 0 \leq t \leq T \\ y_d(t) = 2A \sin bt & 0 \leq t \leq T \\ y_1(t) = y_0(t) = 0 & t > T \text{ or } t < 0 \end{cases} \tag{4.20}$$

and analyze its effect on receiver design and performance. Having specified $y_d(t)$, the correlating signal $h_d(t)$ must be found as a solution to

$$\frac{N_0}{2} h_d(t) + \int_0^T K_c(t-u) h_d(u) du = 2A \sin bt \ . \tag{4.21}$$

The detailed solution of Eq. (4.21) is worked out in Appendix B. The solution is given by Eq. (B.6), namely

$$h_d(t) = C \sin bt + CK_1 \varepsilon^{\gamma t} + CK_2 \varepsilon^{-\gamma t} \qquad 0 \leq t \leq T \tag{B.6}$$

where K_1, K_2, C, and γ are defined by Eqs. (B.8), (B.9), (B.5) and (A.17) respectively. With m_1 and E defined by Eq. (4.11) and Eq. (4.12) respectively, we can express $h_d(t)$ as a function of A, N_0, N_1, m_1, E, and b/β, the latter being the ratio of the signal's frequency to the bandwidth of the interference. Thus, the constants of Eq. (B.6) are given by

$$C = \frac{4A[(\frac{b}{\beta})^2 + 1]}{N_0 + N_1 + N_1(\frac{b}{\beta})^2} \tag{4.22}$$

$$K_1 = \frac{[\sin bT + (\frac{b}{\beta})\cos bT](m_1+1)\varepsilon^{-Em_1} - (\frac{b}{\beta})(m_1-1)\varepsilon^{-2Em_1}}{[1 + (\frac{b}{\beta})^2][\frac{m_1+1}{m_1-1} - \frac{m_1-1}{m_1+1}\varepsilon^{-2Em_1}]} \tag{4.23}$$

$$K_2 = \frac{-(\frac{b}{\beta})(m_1+1) + (m_1-1)\varepsilon^{-Em_1}[\sin bT + \frac{b}{\beta}\cos bT]}{[1 + (\frac{b}{\beta})^2][\frac{m_1+1}{m_1-1} - \varepsilon^{2Em_1}\frac{m_1-1}{m_1+1}]} \tag{4.24}$$

Ignoring the constant of proportionality C, it can be seen that $h_d(t)$ is a function of m_1, E, and $\frac{b}{\beta}$. [Notice that sin bT can be expressed as $\sin(\frac{b}{\beta}\beta T) = \sin(\frac{b}{\beta}E)$.] The meaning of the factors m_1 and E has been discussed previously. Fig. 4.7 is a plot of $h_d(t)$ as a function of time normalized to T for (JSR)(SNR) = 1, b/β = 1 and various values of E. Fig. 4.8 is a similar plot except that (JSR)(SNR) = 10. Figs. 4.9-4.12 are repetitions of Figs. 4.7 and 4.8 for various values of b/β.

E. PERFORMANCE OF THE "COLORED NOISE RECEIVER"

Once the colored noise receiver has been designed, its performance must be evaluated. This section analyzes the performance of the colored noise receiver designed for the detection of rectangular binary signals.

The performance of a colored noise receiver with equiprobable binary antipodal signals was derived in Chapter II.C,

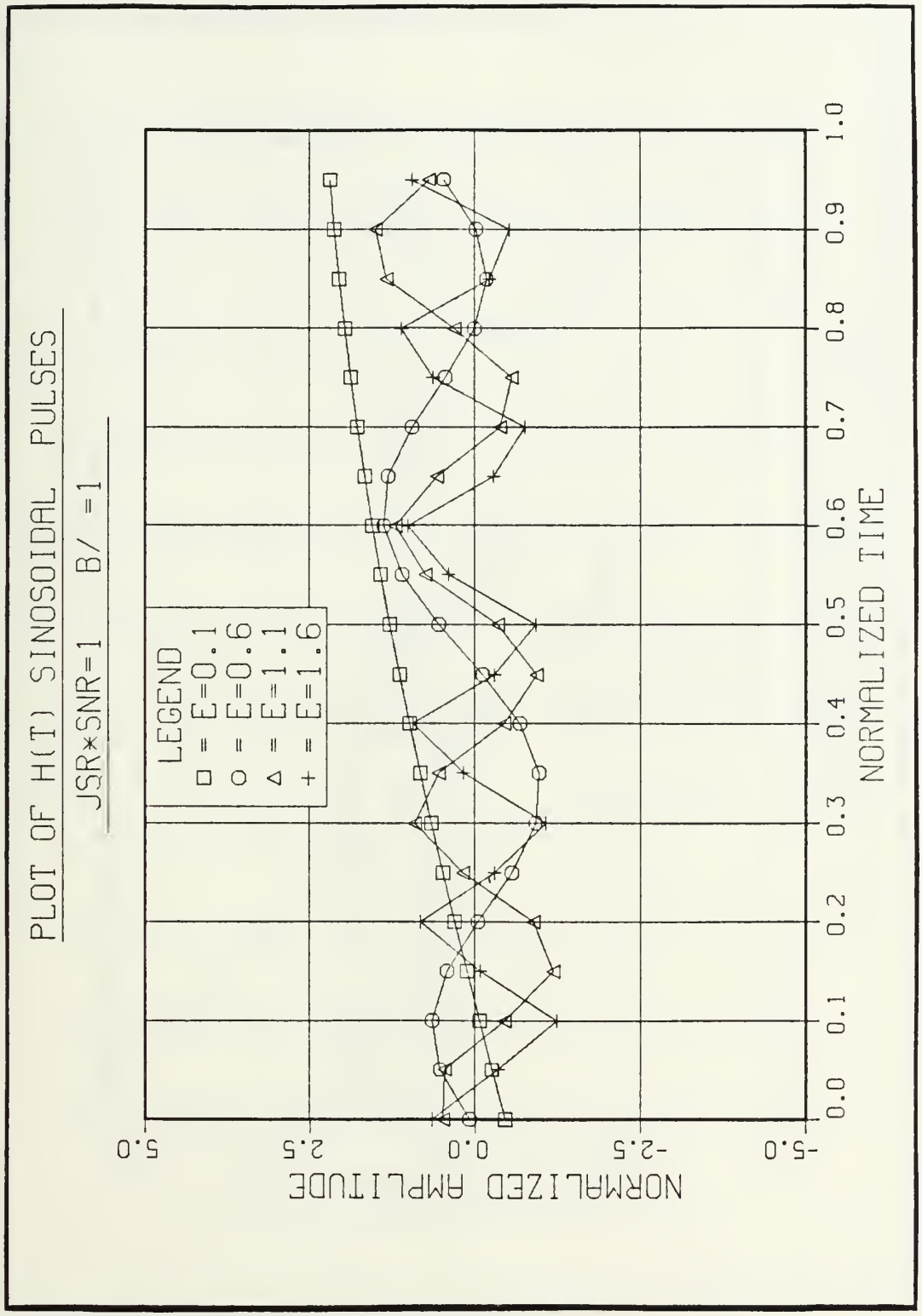

Figure 4.7 Plot of $h_d(t)$ for Sinusoidal Pulses Where (JSR)(SNR) = 1, b/β = 1

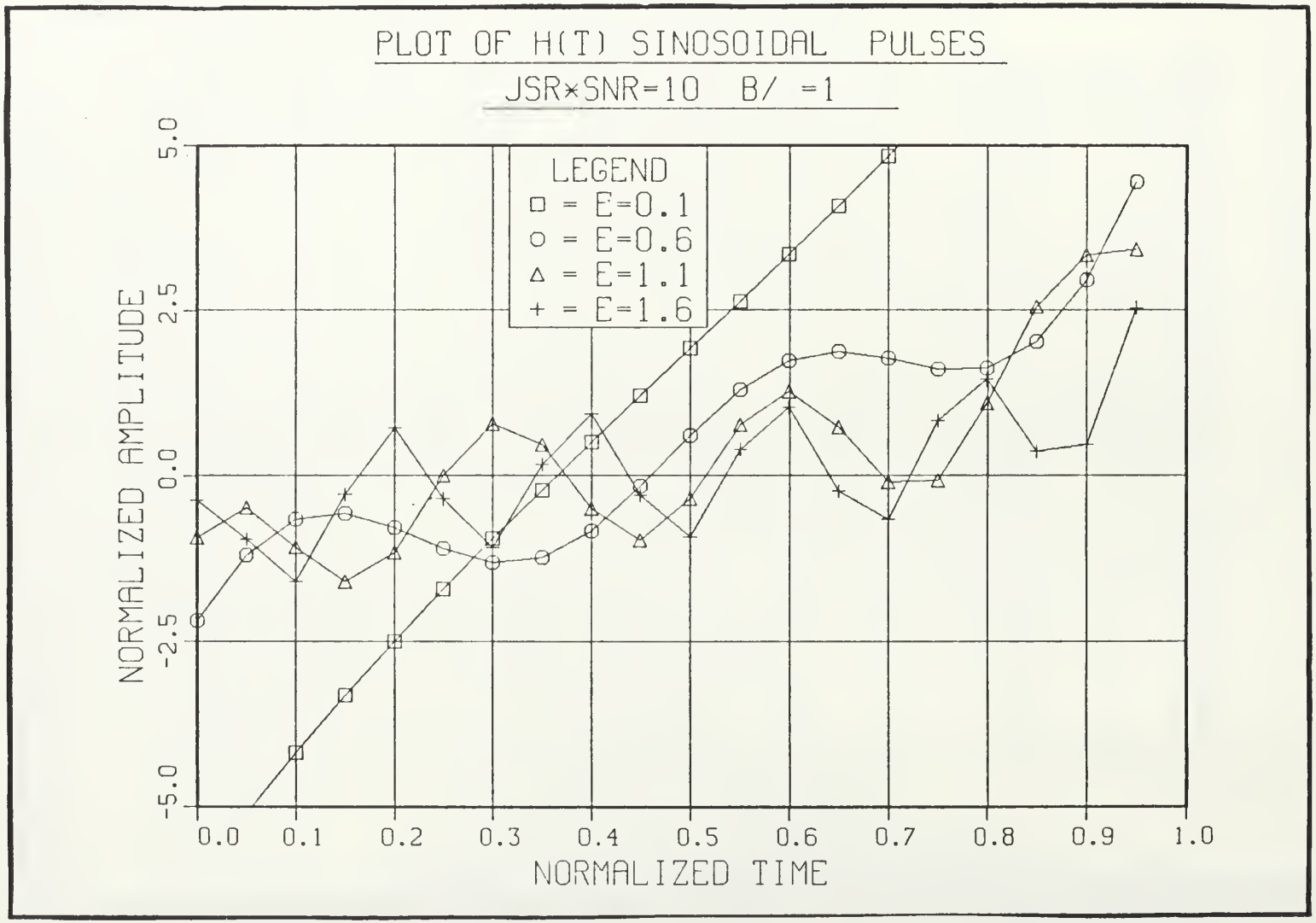

Figure 4.8 Plot of $h_d(t)$ for Sinusoidal Pulses Where (JSR)(SNR) = 10, b/β = 1

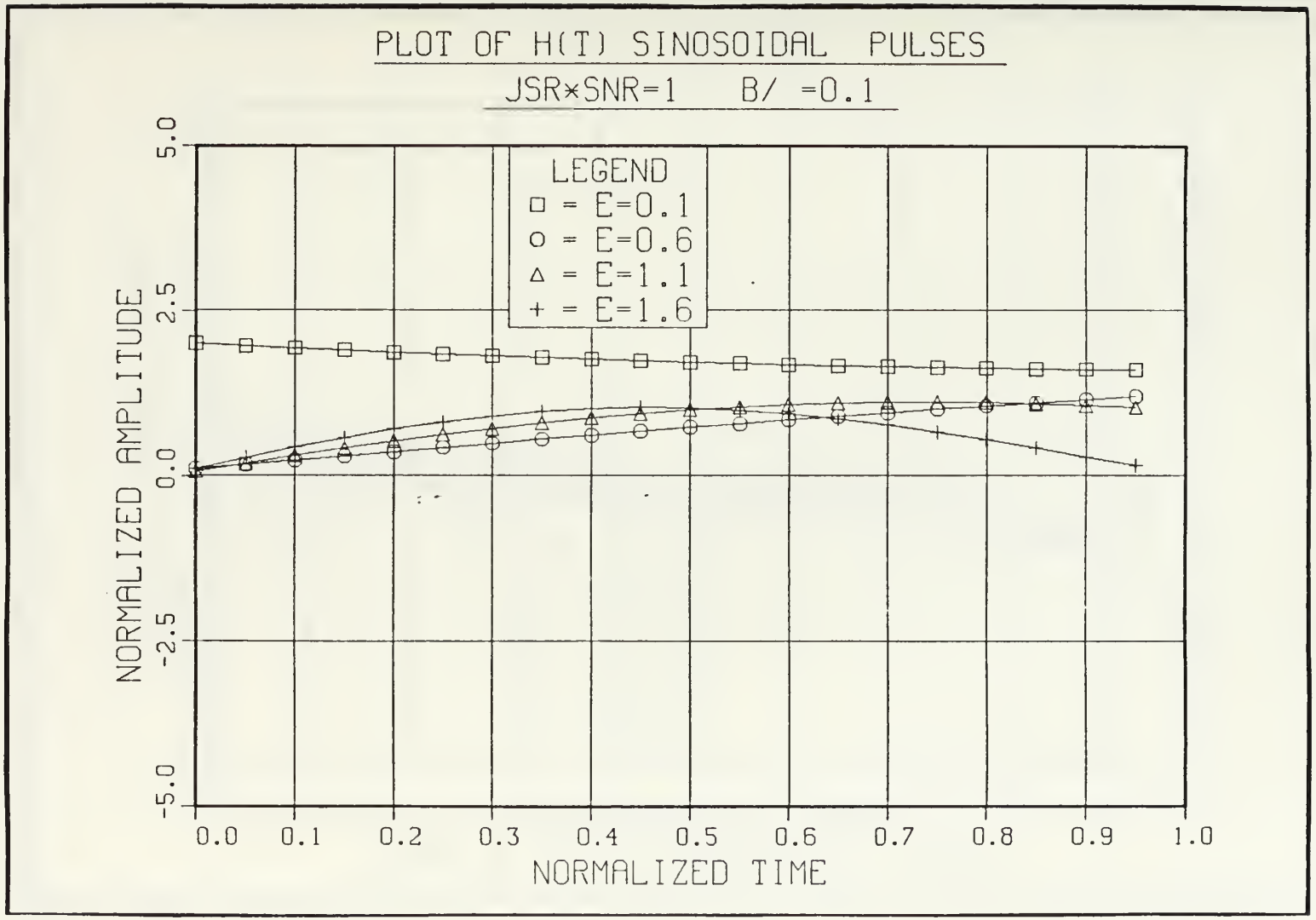

Figure 4.9 Plot of $h_d(t)$ for Sinusoidal Pulses Where (JSR)(SNR) = 10, $b/\beta = 0.1$

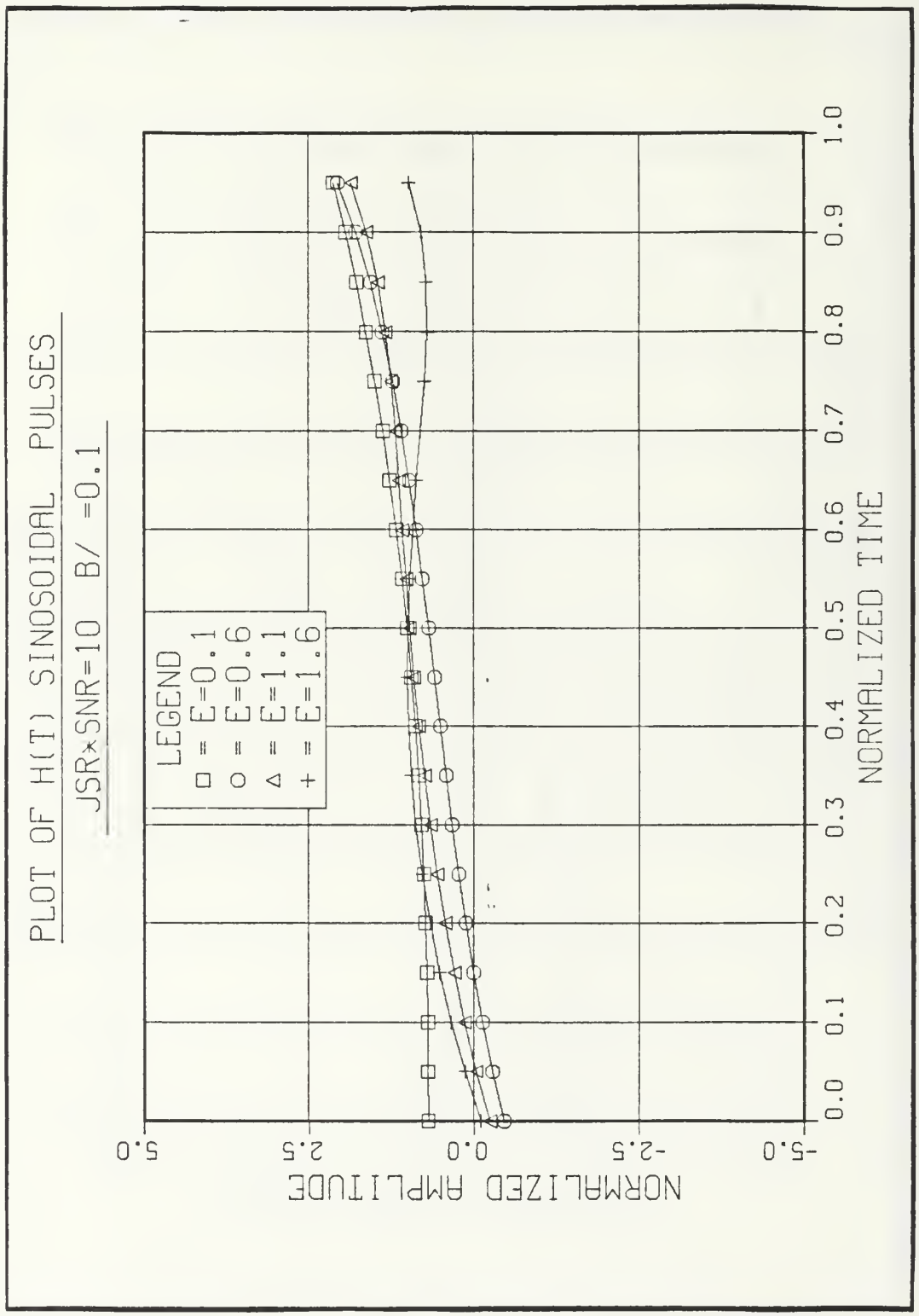

Figure 4.10 Plot of $h_d(t)$ for Sinusoidal Pulses Where (JSR)(SNR) = 10, b/β = 0.1

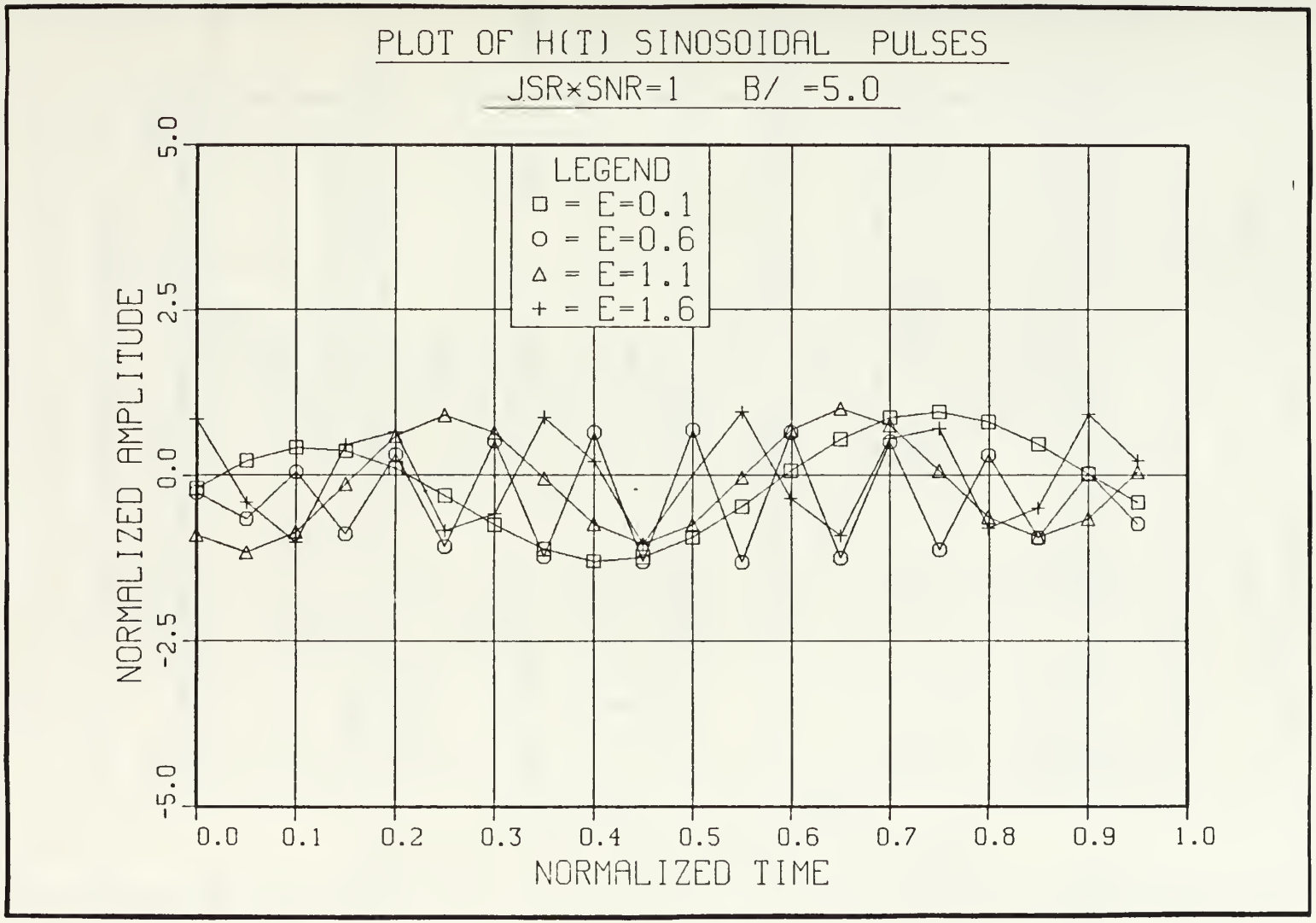

Figure 4.11 Plot of $h_d(t)$ for Sinusoidal Pulses Where (JSR)(SNR) = 1, $b/\beta = 0.5$

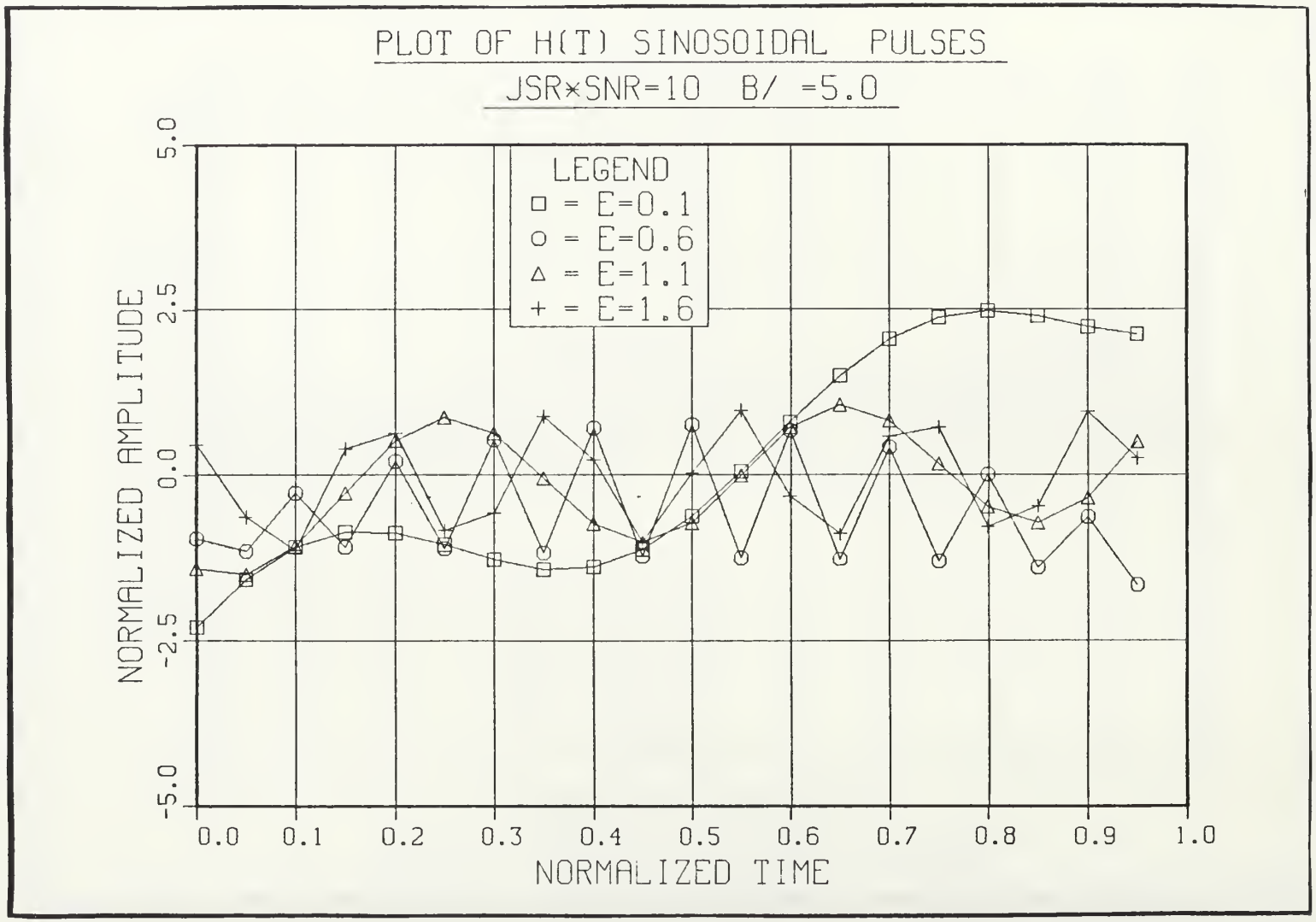

Figure 4.12 Plot of $h_d(t)$ for Sinusoidal Pulses Where (JSR)(SNR) = 10, b/β = 5

and its probability of error is given by Eq. (2.26), namely

$$P_e = \mathrm{ERFC}_*\left(\frac{1}{4}\int_0^T y_d(t)h_d(t)dt\right)^{1/2} \tag{2.26}$$

If we substitute $y_d(t)$ as defined by Eqs. (4.8) and (4.9) and substitute $h_d(t)$ as defined by Eq. (4.16), we obtain

$$P_e = \mathrm{ERFC}_*\left(\frac{1}{4}\int_0^T \frac{8A^2}{N_0+N_1}[1+K_1\varepsilon^{\beta m_1 t}+K_2\varepsilon^{-\beta m_1 t}]dt\right)^{1/2} \tag{4.25}$$

$$= \mathrm{ERFC}_*\left(\frac{2A^2T}{N_1(1+\frac{N_0}{N_1})}\left[1+\frac{K_1(\varepsilon^{\beta m_1 T}-1)}{\beta m_1 T}+\frac{K_2(1-\varepsilon^{-\beta m_1 T})}{\beta m_1 T}\right]\right)^{1/2}$$

Substituting Eqs. (4.12)-(4.16) in Eq. (4.25) yields

$$P_e = \mathrm{ERFC}_*\left(\frac{2(\mathrm{SNR})}{[1+(\mathrm{JSR})(\mathrm{SNR})\frac{4}{E}]}\left(1+\frac{2(m_1+1)-4\varepsilon^{-Em_1}-2\varepsilon^{-2E(m_1+1)}(m_1-1)}{Em_1(\frac{m_1+1}{m_1-1}-\frac{m_1-1}{m_1+1}\varepsilon^{-2Em_1})}\right)\right)^{1/2} \tag{4.26}$$

Observe that if E becomes unbounded, or equivalently if the colored noise has such a large bandwidth that its P.S.D. level is nearly zero for all frequencies, then the colored noise receiver should reach the performance of the white noise receiver. Indeed, letting $E \to \infty$ in Eq. (4.26) yields

$$P_e = ERFC_*(2SNR)^{1/2} \tag{4.27}$$

where Eq. (4.27) is the same as Eq. (2.2) for the white noise receiver.

Figs. 4.13 and 4.14 show the performance of this receiver for SNR = 10 and SNR = 1 respectively, for various values of JSR. It can be easily seen that as JSR increases, P_e increases also. In fact, if we define $P_e = 10^{-3}$ error/bit as the maximum probability of error tolerable, looking at Fig. 4.12, one can say that the receiver will not function properly for JSR greater than -12 db. These graphs show also the effect of increasing E. Increasing E spreads the jamming power over larger frequencies thus making the P.S.D. level lower at all frequencies. This causes a decrease in the amount of channel interference which in turn causes an improvement in the receiver performance.

F. PERFORMANCE OF THE WHITE NOISE RECEIVER

In order to better understand the performance of the colored noise receiver, it is desirable to compare its performance to that of the coherent digital white noise receiver when both operate under the same conditions. In other words, we deal with the model described in Section B. However, the colored noise receiver of Fig. 4.1 is replaced by the white noise receiver of Fig. 4.3.

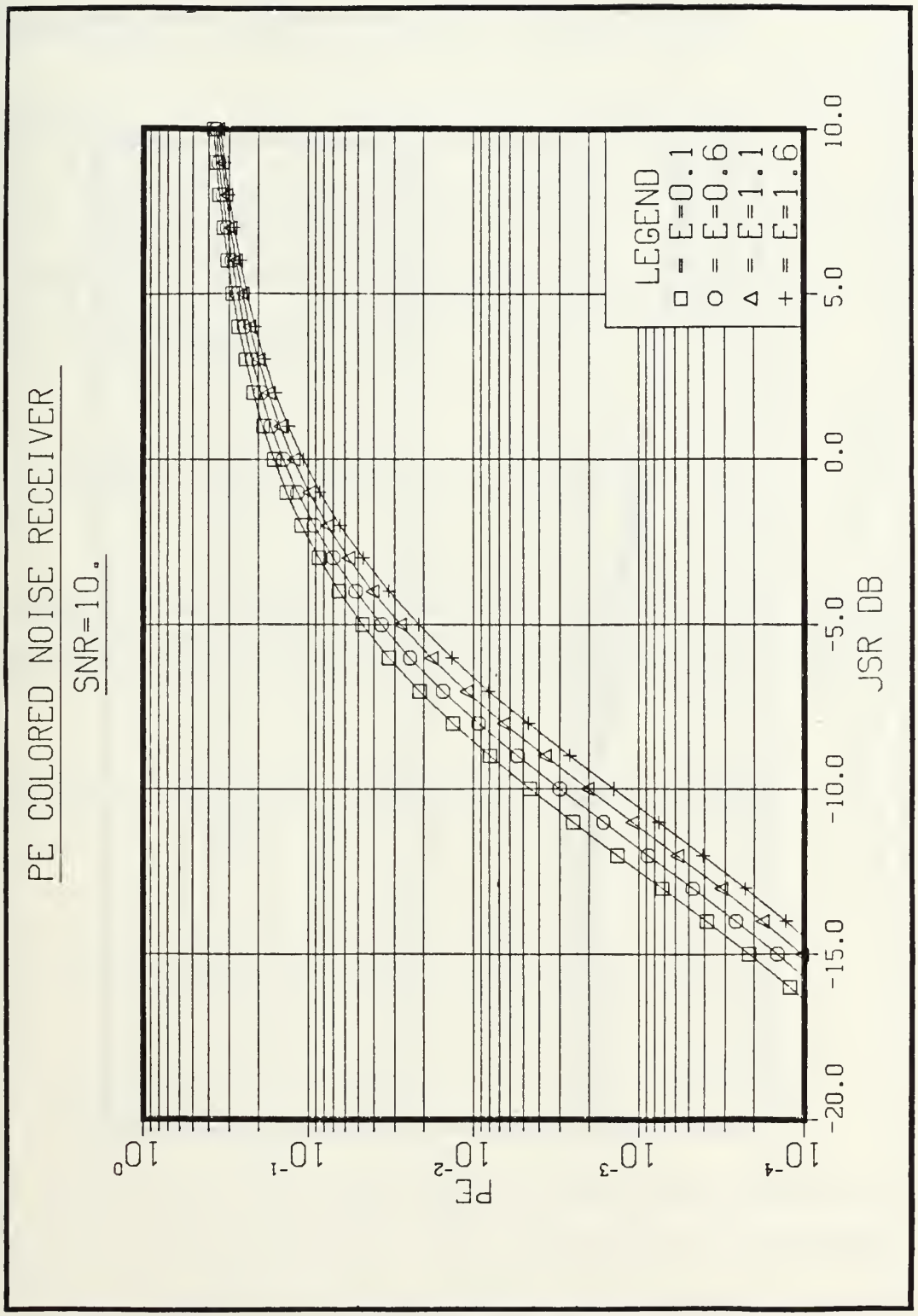

Figure 4.13 P_e for Colored Noise Receiver Where SNR = 10

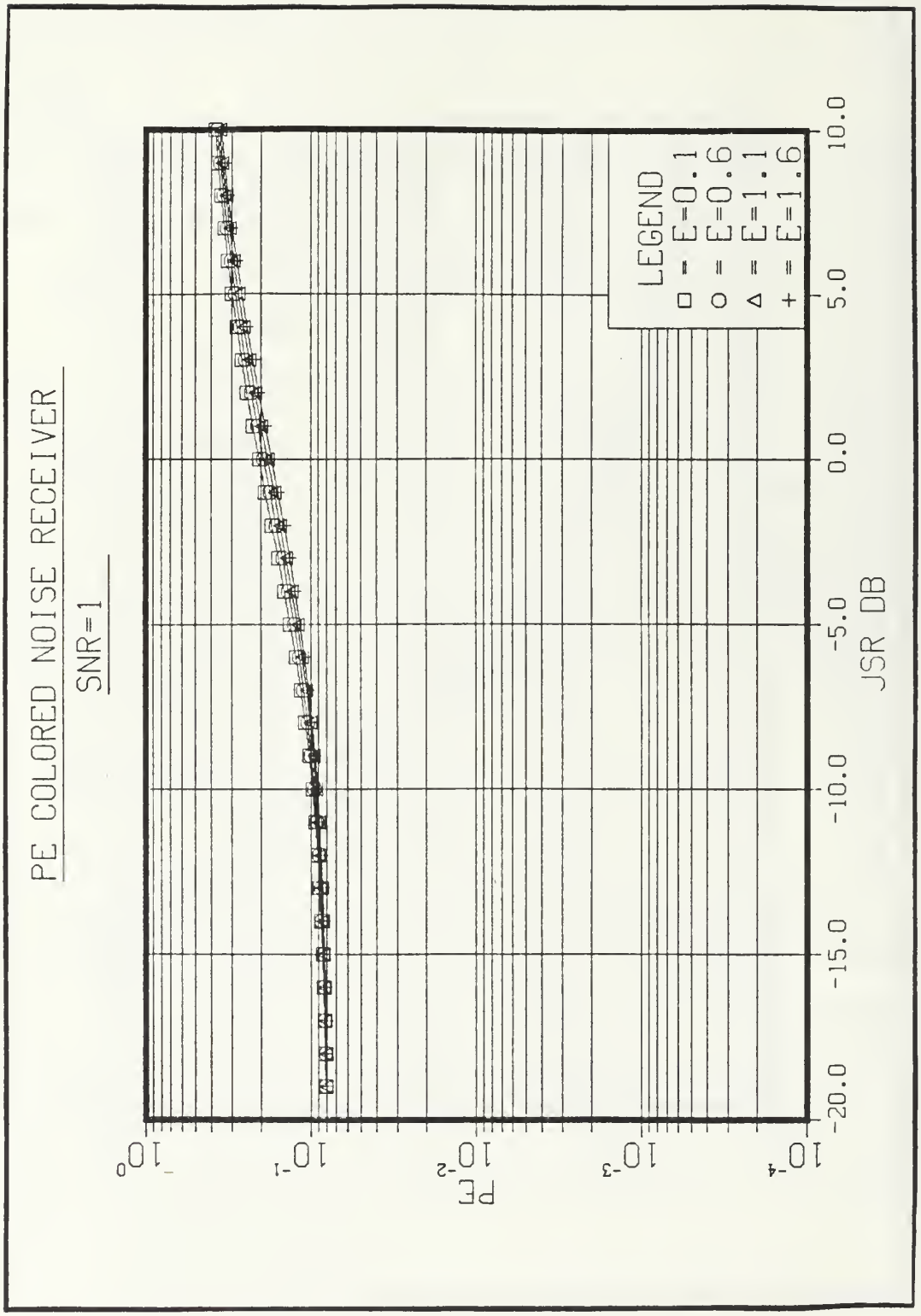

Figure 4.14 P_e for Colored Noise Receiver Where SNR = 1

The input to the receiver is

$$\text{Hypothesis } H_0: \quad z(t) = y_0(t) + n_c(t) + n_w(t)$$

$$\text{Hypothesis } H_1: \quad z(t) = y_1(t) + n_c(t) + n_w(t) \qquad 0 \leq t \leq T$$

where $y_0(t)$ and $y_1(t)$ are assumed to be two antipodal signals. The input signal $z(t)$ is correlated with the signal $y_d(t)/2\sqrt{E_s}$, where E_s is the energy of each signal. That is,

$$E_s = \int_0^T y_1^2(t)dt = \int_0^T y_0^2(t)dt \tag{4.28}$$

The receiver generates the statistic ℓ, which is a Gaussian random variable. Its mean under both hypotheses is given by

$$E[\ell|H_1] = E[\frac{1}{\sqrt{E_s}} \int_0^T y_1(t)[y_1(t)+n_c(t)+n_w(t)]dt]$$

$$= \frac{1}{\sqrt{E_s}} \int_0^T y_1^2(t)dt = \sqrt{E_s} \tag{4.29}$$

$$E[\ell|H_0] = -\sqrt{E_s} \tag{4.30}$$

Eqs. (4.29) and (4.30) were derived under the assumption that both noises are zero mean. This assumption is reasonable given the physical sources of most noises.

The conditional variance of ℓ is given by

$$\text{Var}[\ell|H_1] = E[(\ell - E(\ell|H_1))^2|H_1]$$

$$= E\{\left(\int_0^T \frac{y_1(t)}{\sqrt{E_s}}(y_1(t)+n_c(t)+n_w(t)dt - \sqrt{E_s}dt\right)^2\} \quad (4.32)$$

$$= \frac{1}{E_s}\int_0^T\int_0^T y_1(t)y_1(\tau)[E\{n_c(t)n_c(\tau)\}$$

$$+ E\{n_w(t)n_w(\tau)\} + E\{n_c(t)n_w(\tau)\}$$

$$+ E\{n_c(\tau)n_w(\tau)\}]dt\,d\tau$$

Since $n_c(t)$ and $n_w(t)$ are assumed to be statistically independent zero mean random processes, we have

$$E[n_c(\tau)n_w(t)] = E[n_c(t)n_w(\tau)] = 0 \quad (4.33)$$

Furthermore

$$E[n_c(t)n_c(\tau)] = \frac{N_0\beta}{4}\varepsilon^{-\beta|t-\tau|} \quad (4.34)$$

and

$$E\{n_w(\tau)n_w(t)\} = \frac{N_0}{2}\delta(t-\tau) \quad (4.35)$$

Substituting Eqs. (4.33), (4.34), (4.35) into Eq. (4.32) yields

$$\mathrm{Var}[\ell|H_1] = \frac{1}{E_s}\int_0^T\int_0^T [\frac{A^2N_0\beta\varepsilon^{-\beta|t-\tau|}}{4} + A^2\frac{N_1}{2}\delta(t-\tau)]dtd\tau \quad (4.36)$$

Performing the integration yields

$$\mathrm{Var}[\ell|H_1] = \frac{N_1}{2} + \frac{N_0}{2}[\frac{E-1+\exp(-E)}{E}] \quad (4.37)$$

where E is defined by Eq. (4.12).

Applying the same procedure for the evaluation of $\mathrm{Var}[\ell|H_0]$, we can easily show that

$$\mathrm{Var}[\ell|H_1] = \mathrm{Var}[\ell|H_0] \ . \quad (4.38)$$

Knowing the statistical behavior of ℓ, the performance of the receiver can now be derived. We obtain

$$P_e = \mathrm{ERFC}_*\{\sqrt{\frac{E_s}{\frac{N_1}{2}+\frac{N_0}{2}[\frac{E-1+\exp(-E)}{E}]}}\} \quad (4.39)$$

$$= \mathrm{ERFC}_*\{\sqrt{\frac{2E_s/N_1}{1+\frac{N_0}{N_1}[\frac{E-1+\exp(-E)}{E}]}}\}$$

The ratio N_0/N_1 can be written (using Eq. (4.18)) as

$$\frac{N_0}{N_1} = \frac{4P_j}{\beta N_1} = \frac{4P_j A^2 T}{\beta N_1 A^2 T} = \frac{4}{E}\left(\frac{P_j}{A^2}\right)\left(\frac{A^2 T}{N_1}\right) = \frac{4}{E}(JSR)(SNR) \qquad (4.40)$$

Substituting Eqs. (4.18) and (4.40) into Eq. (4.39) yields

$$P_e = ERFC_*\left\{\sqrt{\frac{2SNR}{1 + 4(JSR)(SNR)[E-1+\exp(-E)]/E^2}}\right\} \qquad (4.41)$$

Eq. (4.41) specifies the performance of the white noise receiver in the presence of colored noise interference as a function of signal to noise ratio, jamming (or interference) power to signal power, and E, which is defined by Eq. (4.12). As previously stated, E is the ratio of interference bandwidth to receiver bandwidth. Figs. 4.15 and 4.16 show the performance of the white noise receiver for SNR = 10 and 1, respectively, at various values of JSR and E. If we compare these figures to Figs. 4.13, 4.14 which show the performance of the colored noise receiver that has been optimized to the specific interference, we reach the conclusion that the performance of both receivers is almost the same. In fact, due to the limited resolution of the figures, one can hardly notice any difference in performance at all. In order to show the actual differences in performance, Tables 4.1-4.5 present numerical values for the performance of both receivers under various conditions. The tables show that the colored noise receiver always has better performance. However, this performance improvement is in the order of a few percent in the best cases.

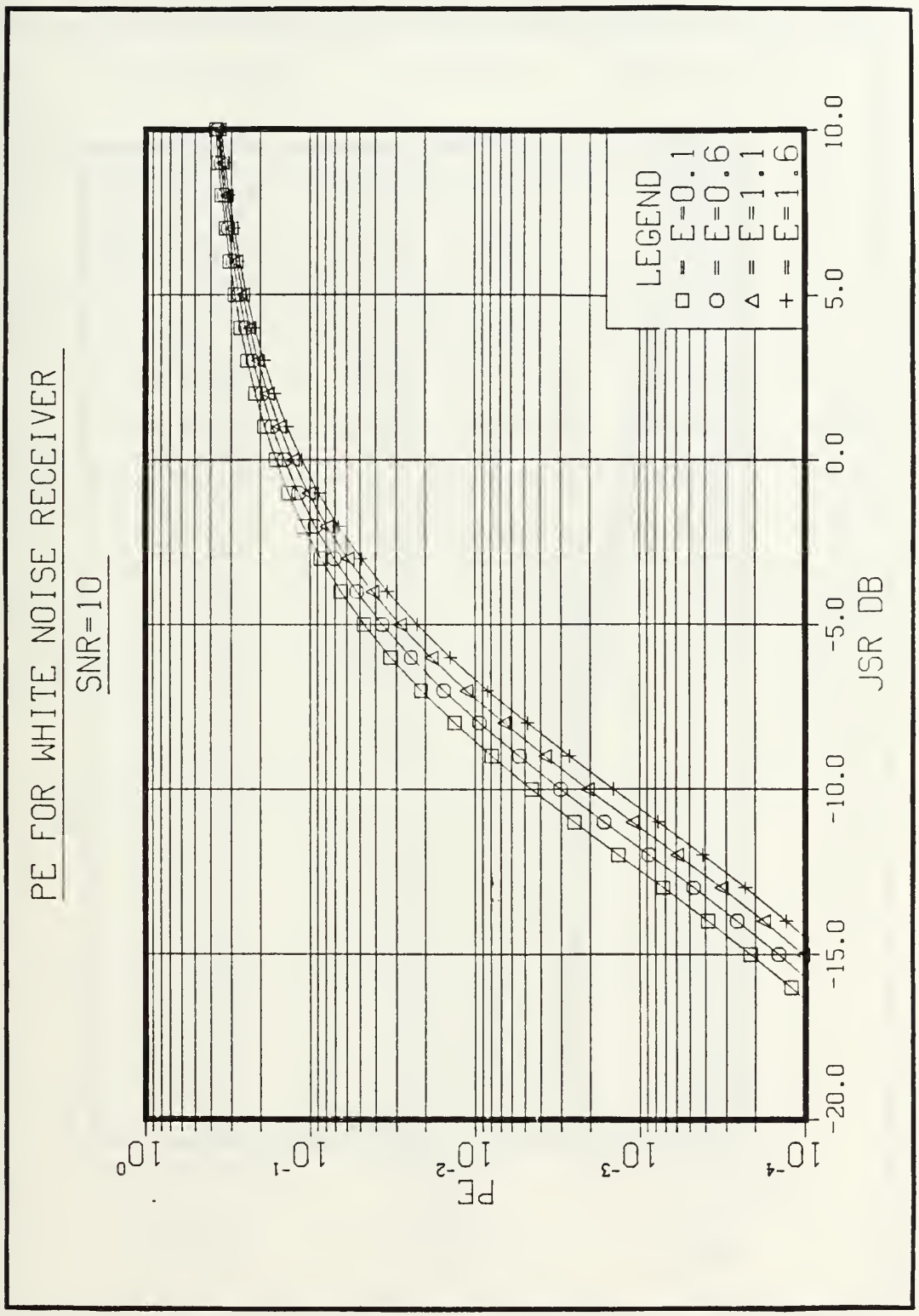

Figure 4.15 P_e for White Noise Receiver, SNR = 10

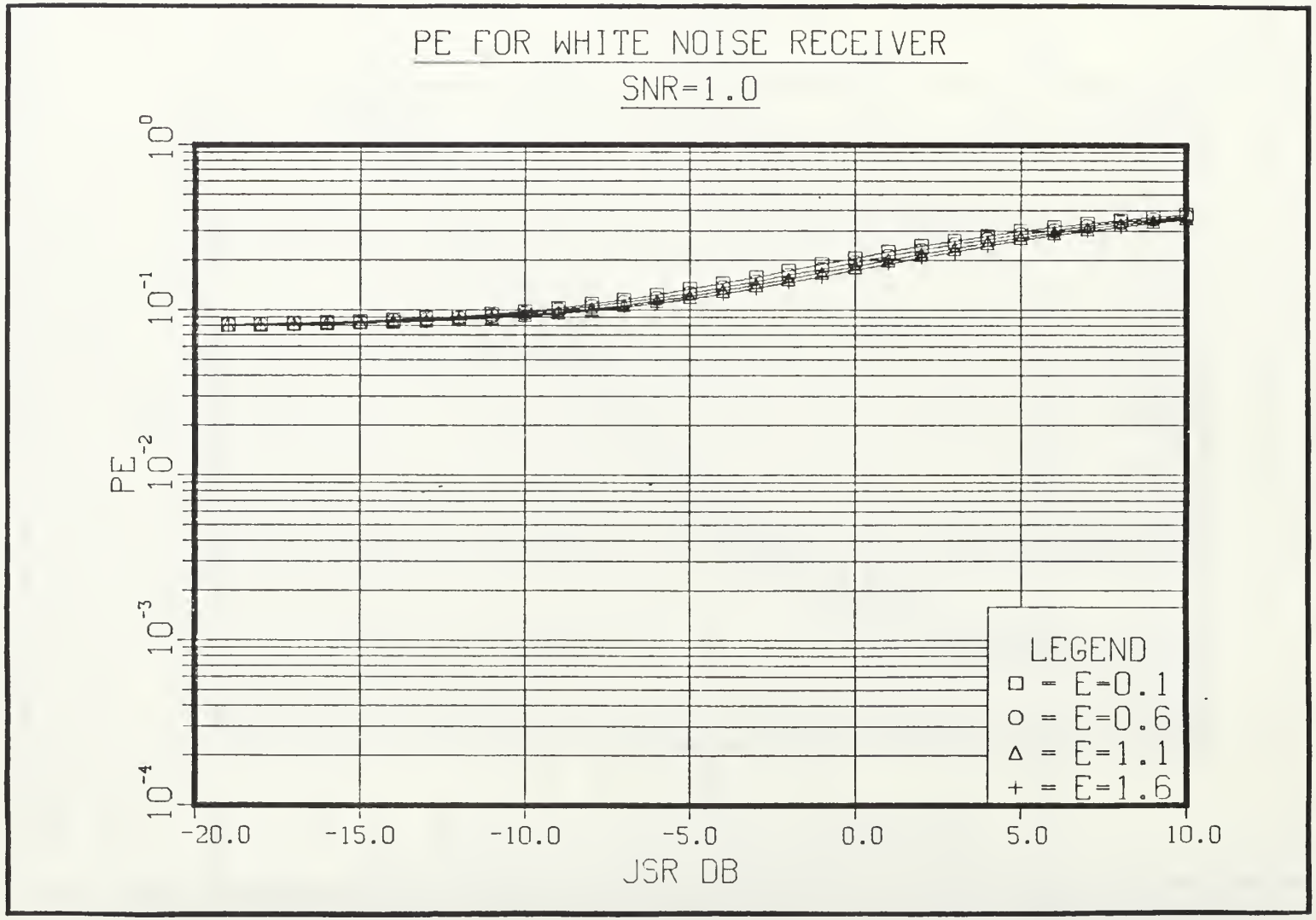

Figure 4.16 P_e for White Noise Receiver, SNR = 1.0

Table 4.1

SNR = 10.0 JSR = 0.1

E	P_e Colored	P_e White	Ratio of P_e
0.1	0.0043	0.0043	0.9997
0.5	0.0031	0.0031	0.9950
1.0	0.0021	0.0021	0.9859
1.5	0.0014	0.0015	0.9774
2.0	0.0010	0.0010	0.9712
2.5	0.0007	0.0008	0.9676
3.0	0.0006	0.0006	0.9661
3.5	0.0004	0.0004	0.9661
4.0	0.0003	0.0003	0.9671
4.5	0.0003	0.0003	0.9689
5.0	0.0002	0.0002	0.9709

Table 4.2

SNR = 10.0 JSR = 1.0

E	P_e Colored	P_e White	Ratio of P_e
0.1	0.1594	0.1595	0.9993
0.5	0.1434	0.1450	0.9892
1.0	0.1249	0.1284	0.9728
1.5	0.1089	0.1136	0.9586
2.0	0.0952	0.1005	0.9477
2.5	0.0835	0.0889	0.9400
3.0	0.0736	0.0787	0.9348
3.5	0.0651	0.0698	0.9315
4.0	0.0577	0.0621	0.9298
4.5	0.0514	0.0553	0.9292
5.0	0.0459	0.0493	0.9294

Table 4.3

SNR = 10.0 JSR = 10.0

E	P_e Colored	P_e White	Ratio of P_e
0.1	0.3733	0.3736	0.9991
0.5	0.3631	0.3657	0.9930
1.0	0.3511	0.3560	0.9865
1.5	0.3401	0.3465	0.9816
2.0	0.3298	0.3372	0.9780
2.5	0.3203	0.3283	0.9755
3.0	0.3114	0.3198	0.9738
3.5	0.3030	0.3115	0.9726
4.0	0.2951	0.3036	0.9719
4.5	0.2876	0.2960	0.9715
5.0	0.2805	0.2887	0.9713

Table 4.4

SNR = 1.0 JSR = 10.0

E	P_e Colored	P_e White	Ratio of P_e
0.1	0.3763	0.3763	0.9999
0.5	0.3681	0.3690	0.9978
1.0	0.3580	0.3600	0.9945
1.5	0.3484	0.3513	0.9917
2.0	0.3394	0.3429	0.9897
2.5	0.3311	0.3350	0.9884
3.0	0.3233	0.3274	0.9875
3.5	0.3161	0.3202	0.9871
4.0	0.3093	0.3134	0.9869
4.5	0.3029	0.3069	0.9870
5.0	0.2969	0.3008	0.9872

Table 4.5

SNR = 1.0 JSR = 1.0

E	P_e Colored	P_e White	Ratio of P_e
0.1	0.2033	0.2033	1.0000
0.5	0.1936	0.1937	0.9993
1.0	0.1826	0.1830	0.9979
1.5	0.1730	0.1735	0.9967
2.0	0.1647	0.1653	0.9959
2.5	0.1574	0.1582	0.9954
3.0	0.1512	0.1519	0.9952
3.5	0.1457	0.1464	0.9952
4.0	0.1410	0.1416	0.9954
4.5	0.1368	0.1374	0.9957
5.0	0.1330	0.1336	0.9960

One must conclude that under the given conditions, the colored noise receiver does not perform significantly better than the white noise receiver. The next logical step is to choose optimum signals and determine whether the colored noise receiver affords greater performance improvement over a white noise receiver operating in the same environment.

G. PERFORMANCE OF THE "COLORED NOISE RECEIVER" WITH OPTIMUM WAVEFORMS

As has been demonstrated the colored noise receiver does not perform significantly better than a white noise receiver for the signal choice of the previous section. However, the performance of a colored noise receiver, unlike that of a white noise receiver, depends on the signal waveforms. In this section we use the optimum signal waveforms derived in Section D (Eq. (4.20)) and analyze the performance of the receiver which is designed to match these waveforms.

The performance of the colored noise receiver with equiprobable binary antipodal signals is given by

$$P_e = \mathrm{ERFC}_*\left(\frac{1}{4}\int_0^T y_d(t)h_d(t)dt\right)^{1/2} \tag{2.26}$$

where $y_d(t)$ was defined by Eq. (4.20), namely

$$y_d(t) = 2A \sin bt \ . \tag{4.20}$$

The correlating signal $h_d(t)$ is defined by Eq. (B.6) and repeated here for convenience

$$h_d(t) = C \sin bt + CK_1\varepsilon^{\gamma t} + CK_2\varepsilon^{-\gamma t} \tag{B.6}$$

where the constants C, K_1, and K_2 are defined by Eqs. (4.22), (4.23), (4.24) respectively.

Substituting Eqs. (4.20) and (B.6) into the integral of Eq. (2.26), yields

$$P_e = \mathrm{ERFC}_*\left(\frac{1}{4}\int_0^T 2A \sin bt\,[C \sin bt + CK_1\varepsilon^{\gamma t} + CK_2\varepsilon^{-\gamma t}]\,dt\right)^{1/2} \tag{4.42}$$

Evaluating the integral yields

$$P_e = \mathrm{ERFC}_*\left\{AC\left[\frac{T}{2}\left(1 - \frac{\sin 2bT}{2bT}\right) + \frac{K_1}{\gamma^2+b^2}[\gamma \sin bT - b\cos bT] + \frac{K_1 b\varepsilon^{-\gamma T}}{\gamma^2+b^2} + \frac{K_2 b}{\gamma^2+b^2} - \frac{K_2\varepsilon^{-\gamma T}}{\gamma^2+b^2}(\gamma \sin bT - b\cos bT)\right]\right\}^{1/2} \tag{4.43}$$

We define a normalized frequency $\bar{b}$,

$$\bar{b} = \frac{b}{\beta} \tag{4.44}$$

The normalized frequency $\bar{b}$ is the ratio of the signal frequency to the noise bandwidth. Notice that when dealing with bandpass

signals, this is the ratio between the frequency of the modulation to the noise bandwidth.

Using Eqs. (4.44) and (4.12), the factor bT can be written as

$$bT = \frac{b}{\beta}\beta T = \bar{b}E \ . \tag{4.45}$$

Also, using Eqs. (A.17) and (4.11) yields

$$\gamma T = m_1 \beta T = m_1 E \tag{4.46}$$

Substituting Eqs. (4.46), (4.45), (4.44) and (4.22) into Eq. (4.43) yields

$$P_e = \text{ERFC}_* \left\{ \frac{\frac{4A^2}{N_1}\frac{T}{2}(1 - \frac{\sin 2\bar{b}E}{2\bar{b}E})(1+\bar{b}^2)}{\frac{N_0}{N_1} - 1 + \bar{b}^2} \left[1 + 2K_1 \left[\frac{m_1 \sin \bar{b}E - \bar{b}\cos bE + \bar{b}\varepsilon^{-Em_1}}{E[m_1^2 + \bar{b}^2][1 - \frac{\sin 2\bar{b}E}{2\bar{b}E}]} \right] \right. \right.$$

$$\left. \left. + 2K_2 \left[\frac{\bar{b} - \varepsilon^{-Em_1}(m_1 \sin \bar{b}E + \bar{b}\cos \bar{b}E)}{E(m_1^2 + \bar{b}^2)(1 - \frac{\sin 2\bar{b}E}{2\bar{b}E})} \right] \right] \right\}^{1/2} \tag{4.47}$$

The signal energy E_s is given by

$$E_s = \frac{A^2 T}{2}[1 - \frac{\sin 2\bar{b}E}{2\bar{b}E}] \tag{4.48}$$

Substituting Eqs. (4.48) and (4.40) into Eq. (4.47) yields

$$P_e = \text{ERFC}_* \left\{ \frac{2\text{SNR}}{\frac{4(\text{JSR})(\text{SNR})}{E(1+\bar{b}^2)} + 1} \left[1 + 2K_1 \frac{m_1 \sin\bar{b}E - \bar{b}\cos\bar{b}E + \bar{b}\varepsilon^{-Em_1}}{E(m_1^2+\bar{b}^2)\left(1 - \frac{\sin 2\bar{b}E}{2\bar{b}E}\right)} \right.\right.$$

$$\left.\left. + 2K_2 \frac{\bar{b} - \varepsilon^{-Em_1}(m_1 \sin\bar{b}E + \bar{b}\cos\bar{b}E)}{E(m_1^2+\bar{b}^2)\left(1 - \frac{\sin 2\bar{b}E}{2\bar{b}E}\right)} \right] \right\}^{1/2} \qquad (4.49)$$

The constants K_1, K_2 are defined by Eqs. (4.23) and (4.24). Eq. (4.49) is a rather formidable expression. It can be calculated by a computer.

Figs. 4.17 and 4.18 show the performance of the colored noise receiver matched to sinusoidal waveforms, for SNR = 10 and E = 1.0 as a function of $\bar{b}$. They also show for comparison purposes the performance of the colored noise receiver matched to rectangular pulse waveforms. The important conclusion one can draw is that by increasing $\bar{b}$, the performance of the colored noise receiver matched to sinusoidal waveforms improves significantly.

Consider the following numerical example by referring to Fig. 4.17. For SNR = 10 and JSR = 1 the colored noise receiver matched to rectangular pulses has $P_e = 0.15$. The colored noise receiver matched to sinusoidal pulses has a $P_e = 0.065$ for the same JSR and SNR values and $\bar{b} = 1$. This represents a significant improvement however neither receiver can function properly at such a high P_e. Increasing the signal frequency up to $\bar{b} = 6$ causes P_e to drop to a value of 10^{-3}. Now the

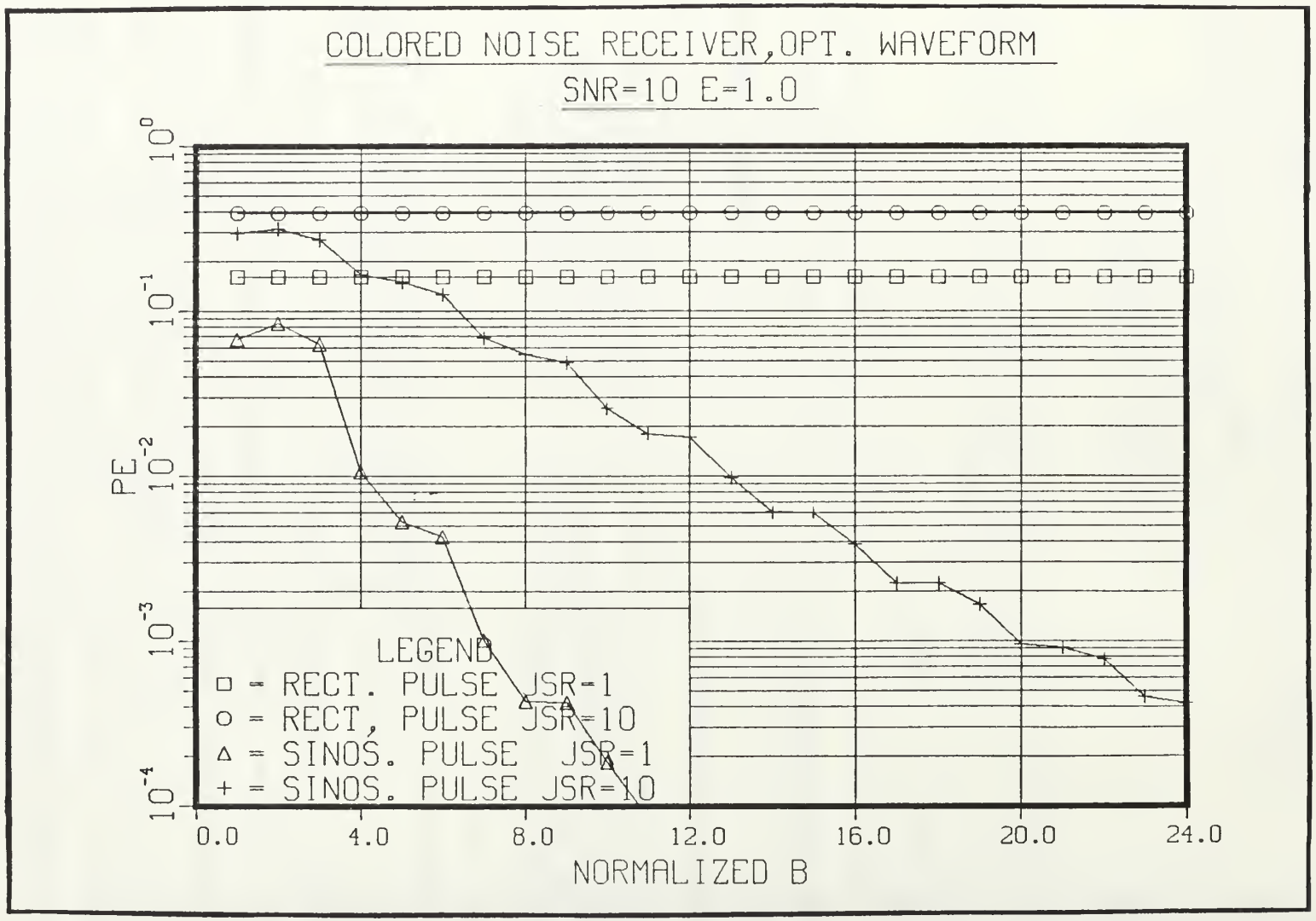

Figure 4.17 P_e for Colored Noise Receiver with Optimum Waveform, E = 1

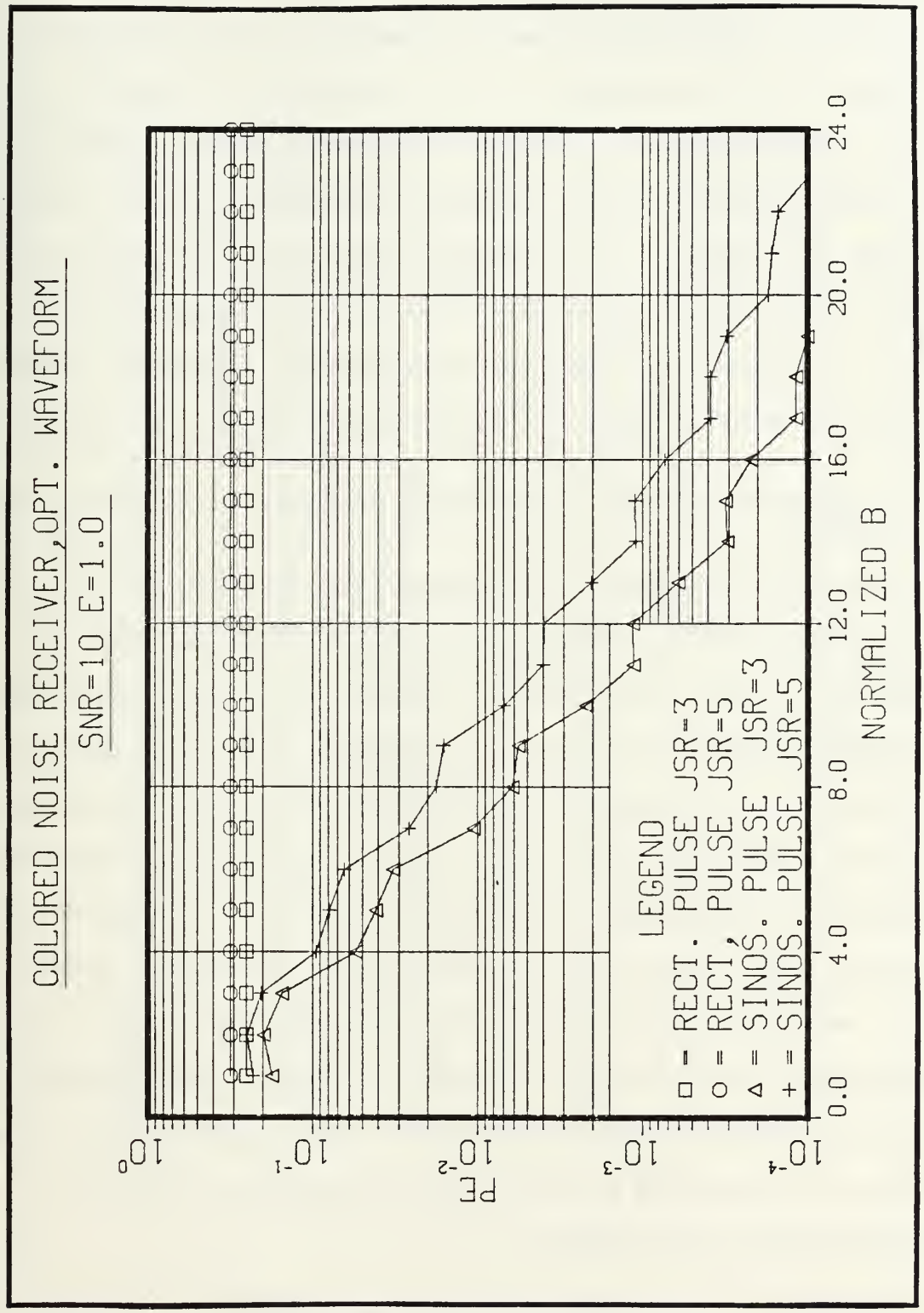

Figure 4.18 P_e for Colored Noise Receiver with Optimum Waveform, E = 1

latter receiver can operate properly even under severe jamming conditions. Notice that in spite of the fact that the signal frequency has been increased, the signal energy collected by the receiver is not decreased by as much as that of the interference. Thus receiver performance improves. One must conclude that it is best to increase signal frequency as much as possible until hardware constraints are reached. Figs. 4.19 and 4.20 show data similar to that presented in Fig. 4.17 except that now the interference bandwidth is much smaller. Nevertheless, similar conclusions can be reached.

H. PERFORMANCE OF THE WHITE NOISE RECEIVER WITH SINUSOIDAL PULSES

As was demonstrated in the previous section, the use of sinusoidal optimum pulses significantly improved the performance of the colored noise receiver in comparison to the performance when rectangular suboptimum pulses are used. In this section we evaluate the performance of the white noise receiver with sinusoidal pulse signals in order to determine whether the improvement discussed above for the colored noise receiver also occurs for the white noise receiver. The white noise receiver performance in the presence of white noise is independent of the signal waveform. However when an additional (colored) interference is introduced, the performance of the receiver is affected by the signal waveforms as will be demonstrated in the sequel.

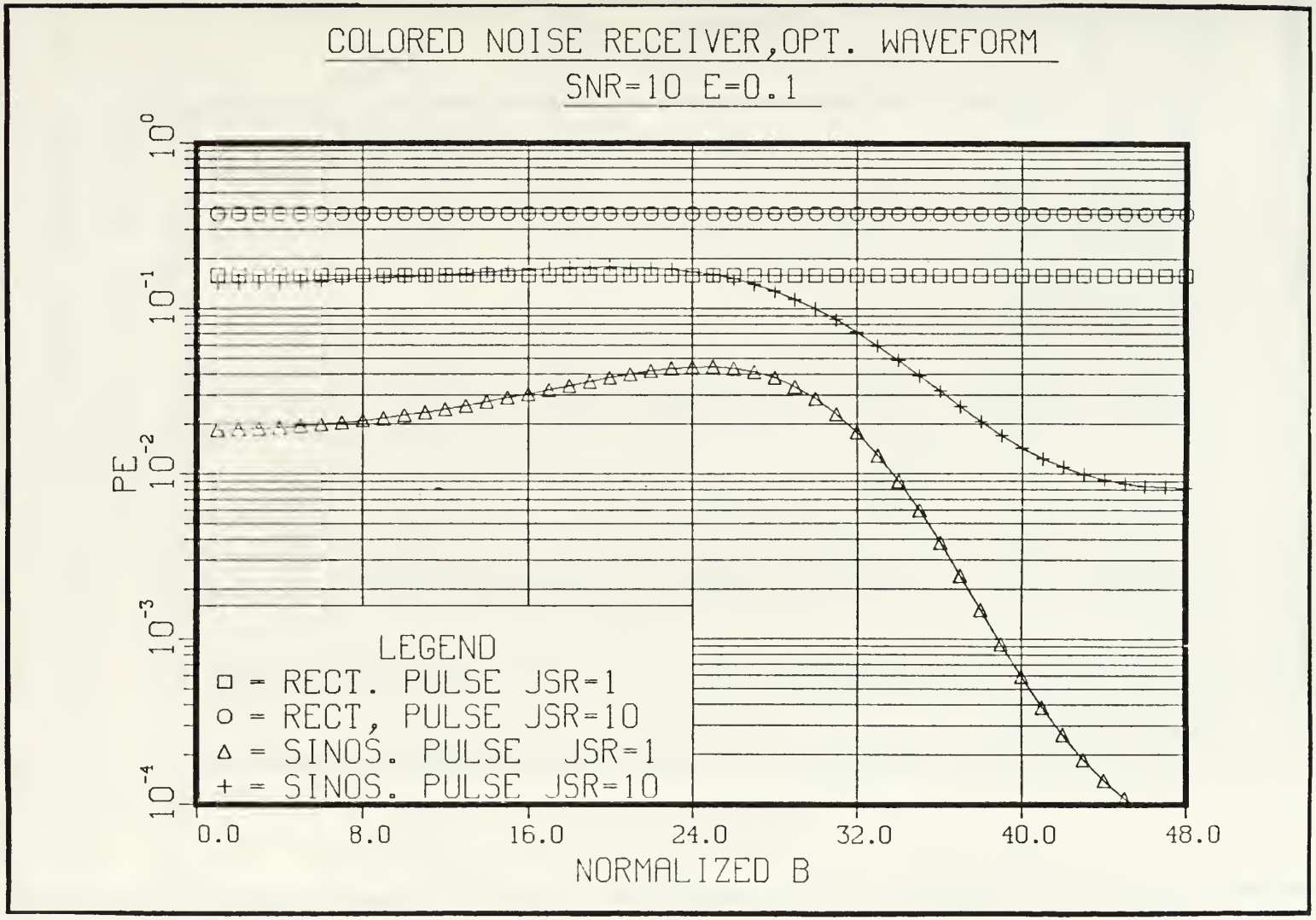

Figure 4.19 P_e for Colored Noise Receiver with Optimum Waveforms, E = 0.1

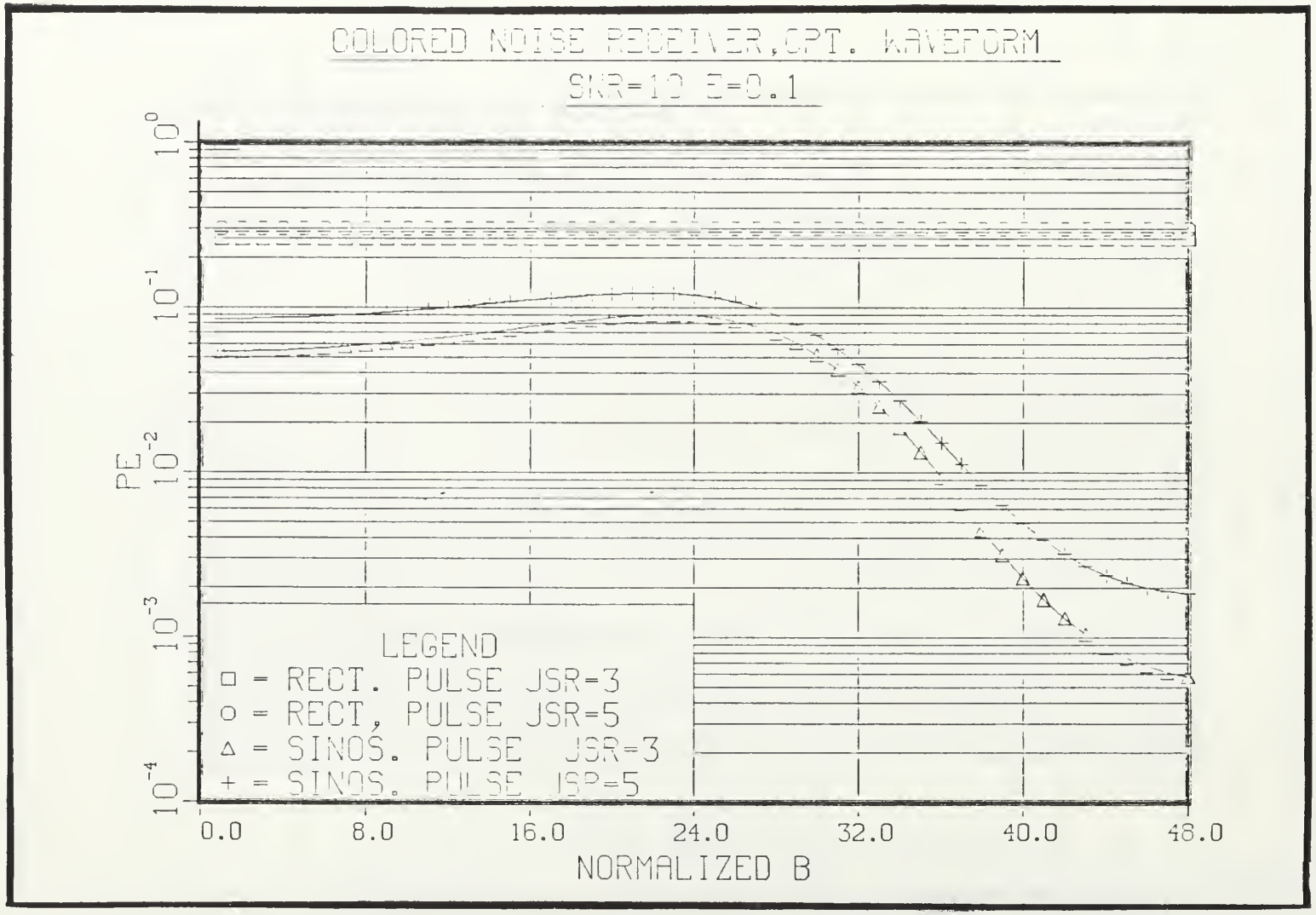

Figure 4.20 P_e for Colored Noise Receiver with Optimum Waveforms, E = 0.1

The inputs to the receiver are:

$$\text{Hypothesis } H_0: \quad z(t) = y_0(t) + n_c(t) + n_w(t)$$

$$\text{Hypothesis } H_1: \quad z(t) = y_1(t) + n_c(t) + n_w(t) \qquad 0 \leq t \leq T$$

The signal waveforms are

$$y_1(t) = A \sin bt$$

$$y_0(t) = -A \sin bt \tag{4.50}$$

so that

$$y_d(t) = 2A \sin bt \tag{4.51}$$

The energy per bit is given by

$$E_s = \int_0^T y_1^2(t)\,dt = \int_0^T y_0^2(t)\,dt = \int_0^T A^2 \sin^2 bt\,dt$$

$$= \frac{A^2 T}{2}\left[1 - \frac{\sin 2bT}{2bT}\right] \tag{4.52}$$

The statistic ℓ generated by the receiver has a conditional mean given by Eqs. (4.29) and (4.30).

The conditional variance is given by substituting Eqs. (4.33), (4.34), (4.35) and (4.50) into (4.32). Performing the substitution yields

$$\text{Var}[\ell|H_1] = \frac{1}{E_s}\int_0^T\int_0^T A^2 \sin bt \sin b\tau\left[\frac{N_0\beta}{4}\varepsilon^{-\beta|t-\tau|} + \frac{N_1}{2}\delta(t-\tau)\right]dtd\tau$$

$$= \frac{N_1}{2} + \int_0^T\int_0^T A^2 \sin bt \sin b\tau \frac{N_0\beta}{4}\varepsilon^{-\beta|t-\tau|}dtd\tau$$

$$= \frac{N_1}{2} + \frac{A^2N_0\beta}{4E_s}\int_0^T \sin bt\left[\int_0^t \sin b\tau\ \varepsilon^{-\beta(t-\tau)}d\tau\right.$$

$$\left. + \int_t^T \sin b\tau\ \varepsilon^{-\beta(\tau-t)}d\tau\right]dt \ . \qquad (4.53)$$

Performing the integration and substituting Eq. (4.52) yields

$$\text{Var}[\ell|H_1] = \frac{N_1}{2} + \frac{N_0}{2}\frac{\beta^2}{\beta^2+b^2}\left[1 + \frac{\sin^2 bT}{E\left(1 - \frac{\sin bT}{2bT}\right)}\right] \qquad (4.54)$$

where E is defined by Eq. (4.12).

Applying the same procedure for $\text{Var}[\ell|H_0]$ yields the same result as Eq. (4.54). Thus

$$\text{Var}[\ell|H_1] = \text{Var}[\ell|H_0] \ . \qquad (4.38)$$

The performance of the receiver can now be calculated from

$$P_e = \text{ERFC}_* \left\{ \sqrt{\frac{E_s}{\frac{N_1}{2} + \frac{N_0}{2} \frac{\beta^2}{\beta^2+b^2}[1 + \frac{\sin^2 bT}{E(1 - \frac{\sin 2bT}{2bT})}]}} \right\} \tag{4.56}$$

$$= \text{ERFC}_* \left\{ \sqrt{\frac{2E_s/N_1}{1 + \frac{N_0}{N_1} \frac{\beta^2}{\beta^2+b^2}[1 + \frac{\sin^2 bT}{E(1 - \frac{\sin 2bT}{2bT})}]}} \right\}.$$

Substituting Eq. (4.49) yields (4.57)

$$P_e = \text{ERFC}_* \left\{ \sqrt{\frac{2(\text{SNR})}{1 + \frac{4(\text{JSR})(\text{SNR})}{E} \frac{1}{1 + (\frac{b}{\beta})^2}(1 + \frac{\sin^2 bT}{E(1 - \frac{\sin 2bT}{2bT})})}} \right\} \tag{4.57}$$

Eq. (4.57) specifies the performance of the white noise receiver with sinusoidal pulses in the presence of white and colored noise interference, as a function of SNR, JSR, E (defined by Eq. (4.12)), and $(\frac{b}{\beta})$ which is the ratio of the signal modulation frequency to the bandwidth of the interference. Figures. 4.21-4.25 show a comparison of the performance of the receivers analyzed. That is, the white noise receiver and the colored noise receiver, both with sinusoidal pulse waveform and with rectangular pulse waveform inputs.

By analyzing these figures, one can reach the following conclusions:

1. For narrow-band interference like the one shown in Fig. 4.21 (E = 0.1), the colored noise receiver matched to

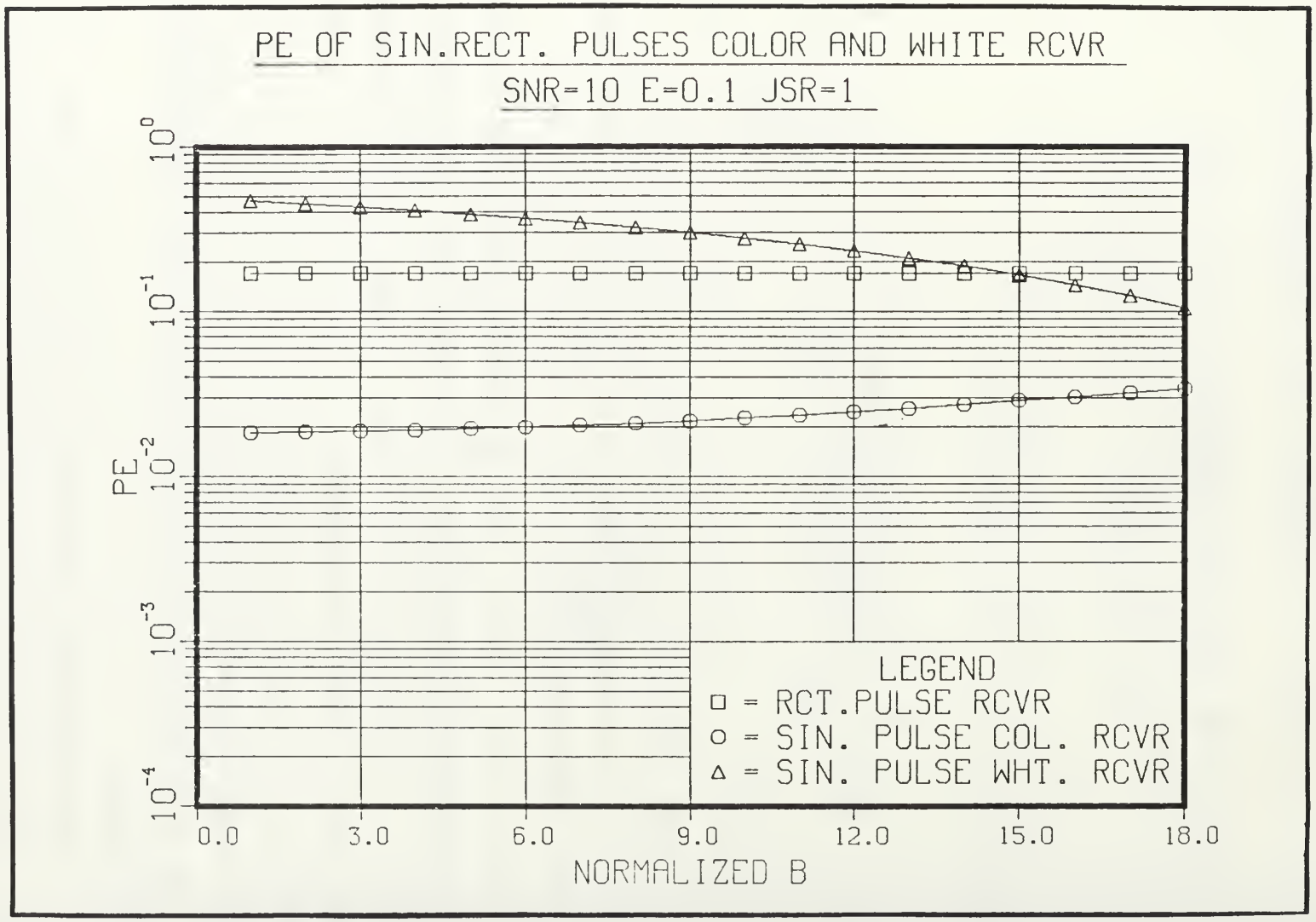

Figure 4.21 Comparison of Colored and White Noise Receivers with Sinusoidal Pulses, SNR = 10, E = 0.1, JSR = 1

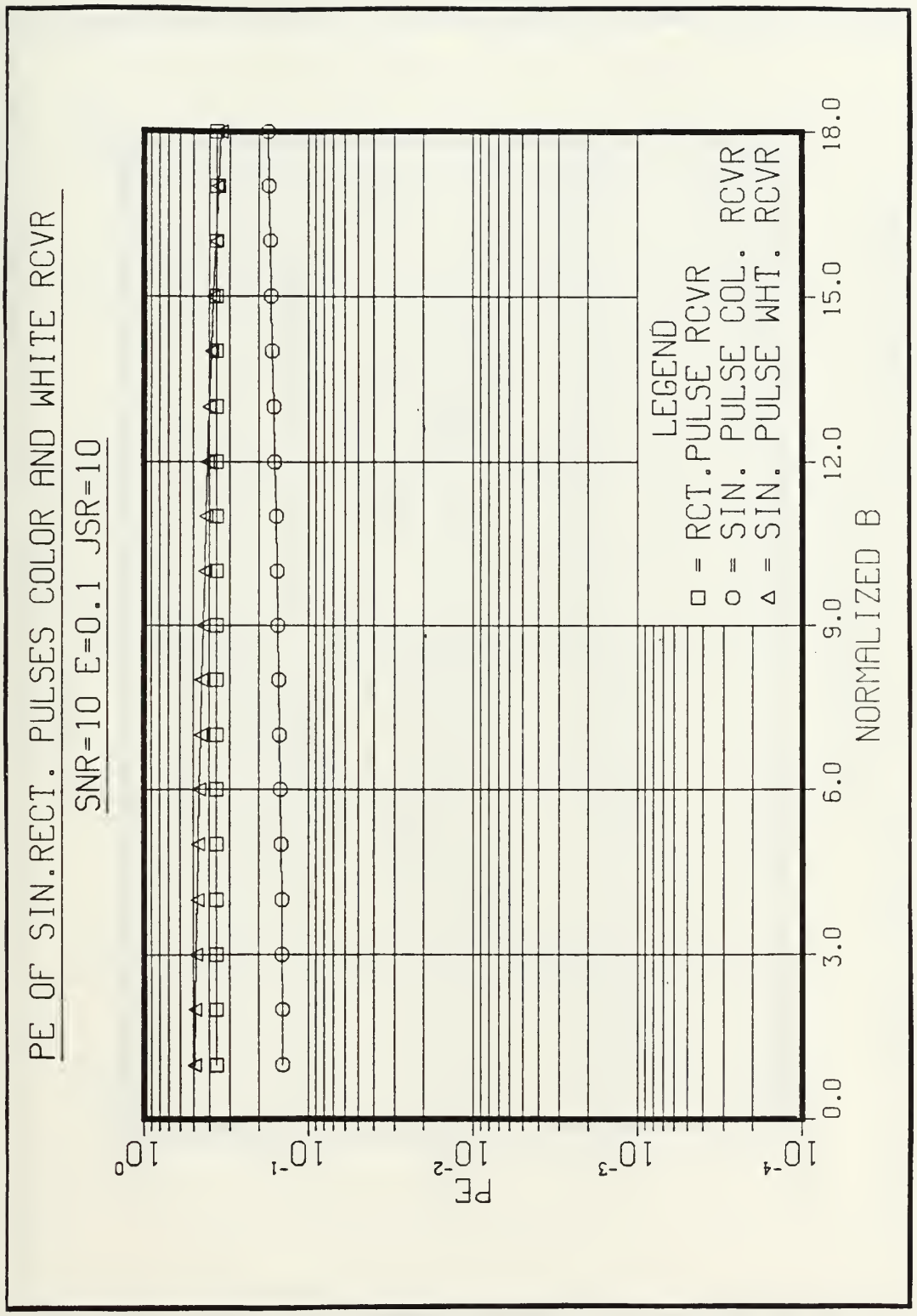

Figure 4.22 Comparison of Colored and White Noise Receivers with Sinusoidal Pulses, SNR = 10, E = 0.1, JSR = 10

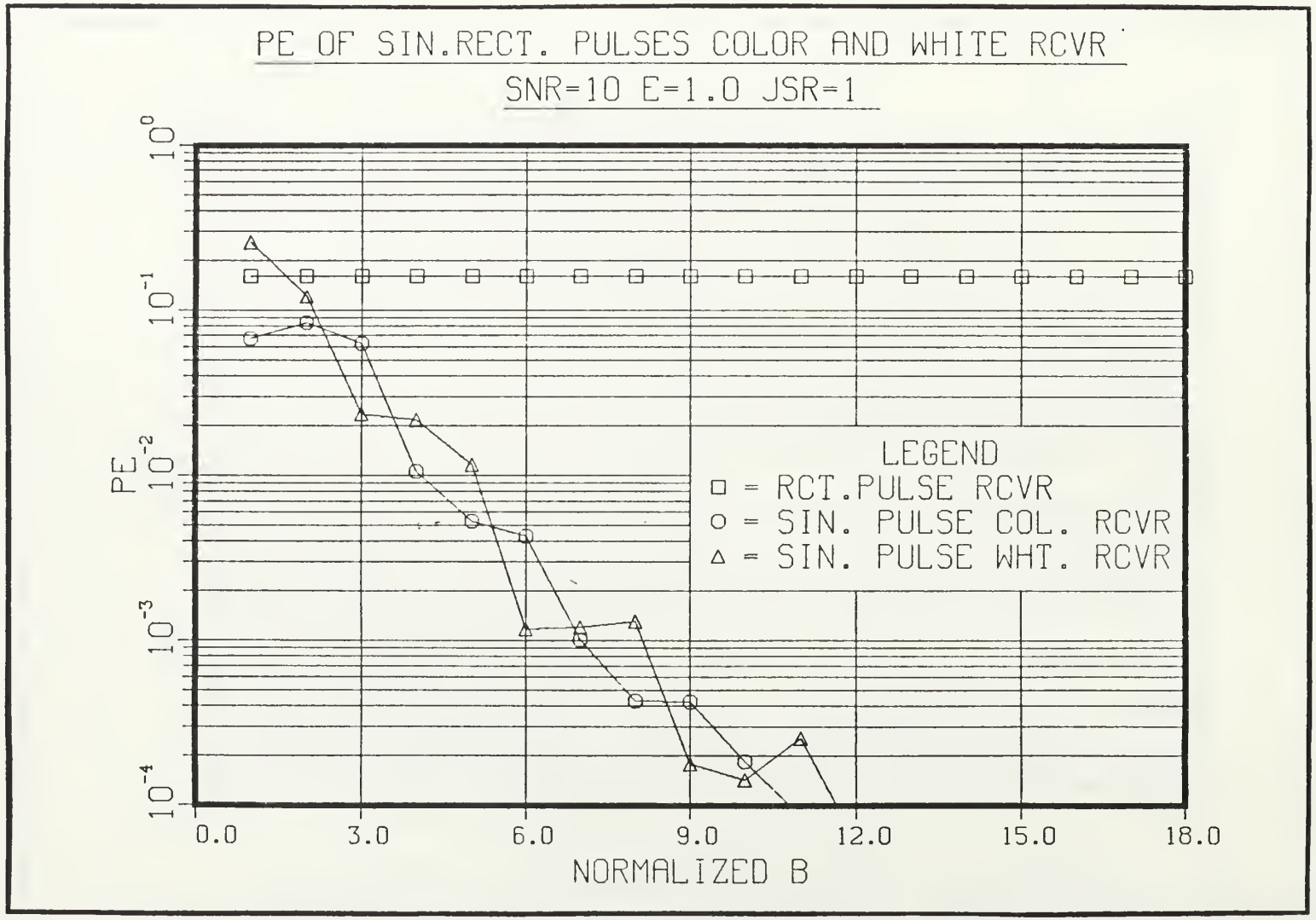

Figure 4.23 Comparison of Colored and White Noise Receivers with Sinusoidal Pulses, SNR = 10, E = 1, JSR = 1

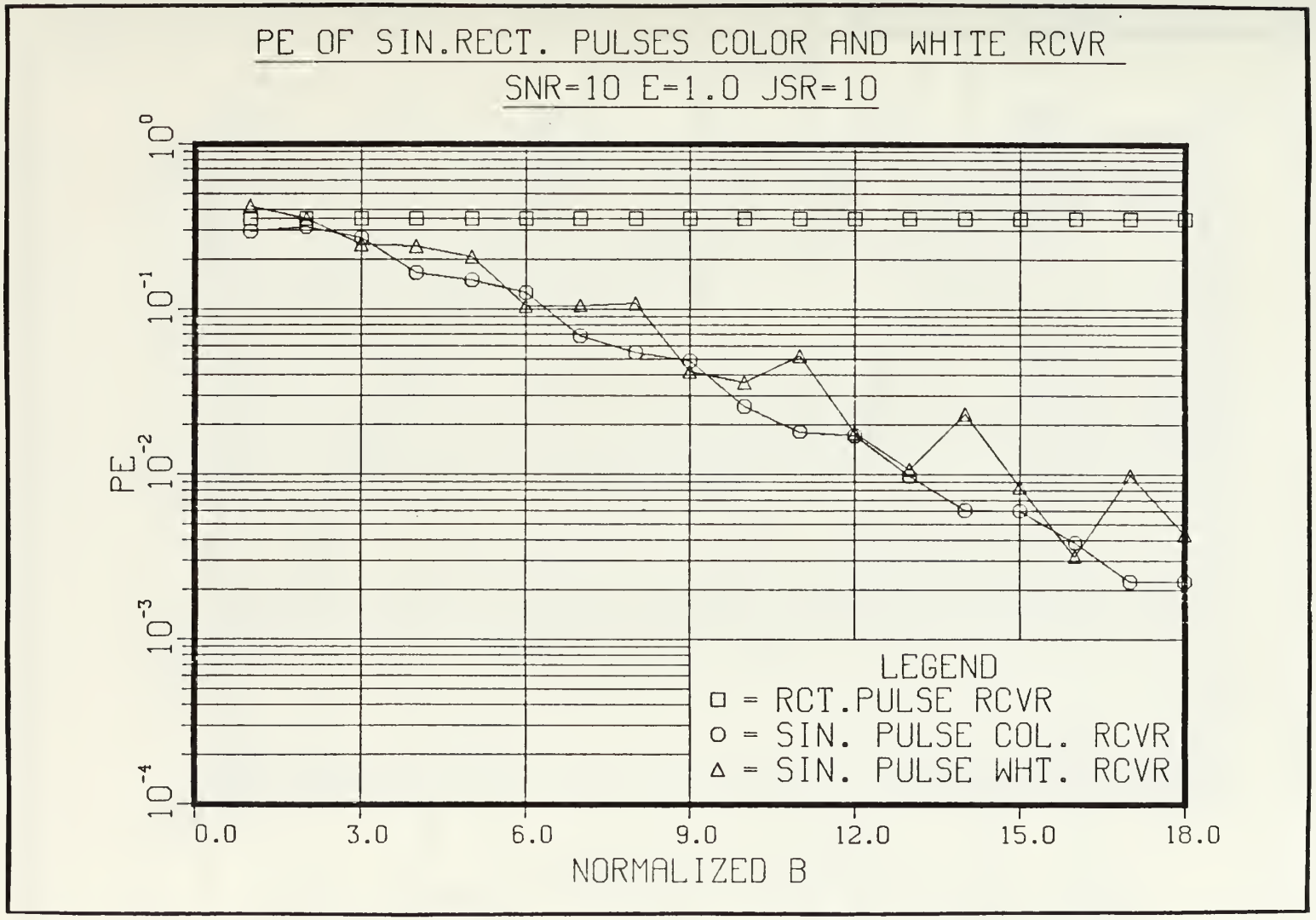

Figure 4.24 Comparison of Colored and White Noise Receivers with Sinusoidal Pulses, SNR = 10, E = 1.0, JSR = 10

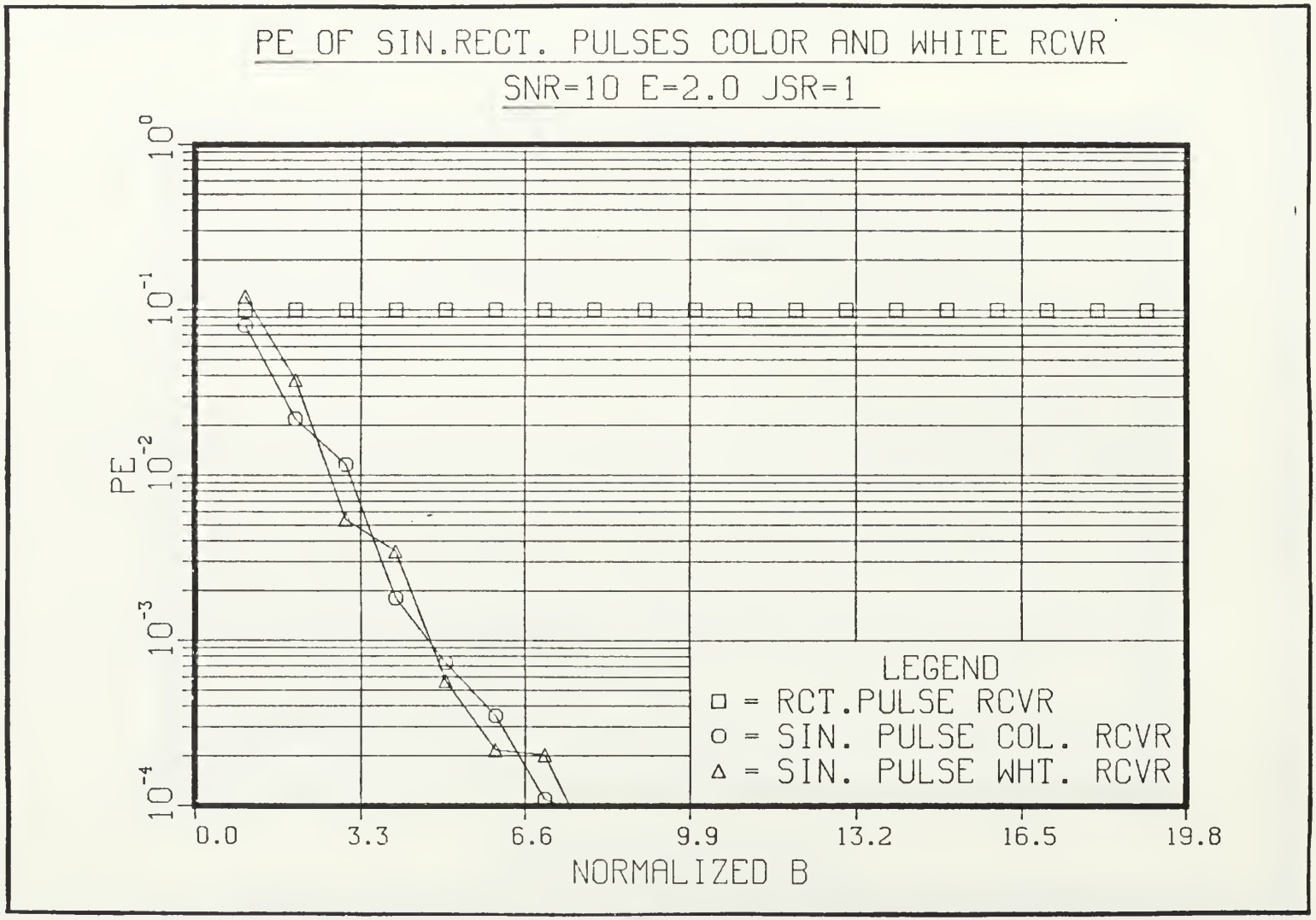

Figure 4.25 Comparison of Colored and White Noise Receivers with Sinusoidal Pulses, SNR = 10, E = 2.0, JSR = 1

sinusoidal pulses performs much better than the white noise receiver with a similar input. Let's define an improvement factor, I,

$$I = \frac{P_{e,1}}{P_{e,2}}$$

where $P_{e,1}$ is the performance of the former receiver and $P_{e,2}$ is the performance of the latter receiver.

Looking at Fig. 4.21, one can see that for low modulation frequency (b), the improvement factor is significant and can reach a value of 30. As the modulation frequency increases, the improvement factor decreases. At very high modulation frequencies both receivers have almost equal performance as can be seen in Figures 4.23, 4.24, 4.25.

2. For low modulation frequencies, the white noise receiver with sinusoidal pulse input performs worse than the white noise receiver with rectangular pulse inputs.

3. When JSR increases without bound, both receivers are driven into saturation and the improvement factor decreases as can be seen from Fig. 4.22.

4. As the bandwidth of the interference increases, the improvement factor decreases as can be seen from Figures 4.21, 4.23, 4.25. However the colored noise receiver exhibits better performance than the white noise receiver with similar inputs.

V. RF PREFILTER--COLORED NOISE THEORY ANALYSIS

A. INTRODUCTION

As discussed in Chapter II, a common source of nonwhite Gaussian noise in the communication channel is the presence of a bandpass element between the transmitter and the signal processing sections of the receiver. The most common such bandpass element is a low noise RF preamplifier used to improve the sensitivity of the receiver.

In this chapter we analyze the effect of this RF preamplifier, using some of the methods and results previously derived. The analysis will be done for two different cases.

1. The ideal case in which the noise figure of all the elements in the receiver is equal to unity.
2. The more realistic case in which the receiver components have noise figures that are greater than unity.

B. THE MODEL

In this chapter, two receivers will be analyzed and their performances will be compared. The first receiver is a binary coherent digital receiver. This receiver is optimum for discriminating between signals received in an additive white Gaussian noise environment. The input to this receiver consists of the information signals with the additive white Gaussian noise having P.S.D. level $N_0/2$. This receiver is described by Fig. 5.1. The second receiver is described by Fig. 5.2. It consists of an RF preamplifier at the front end

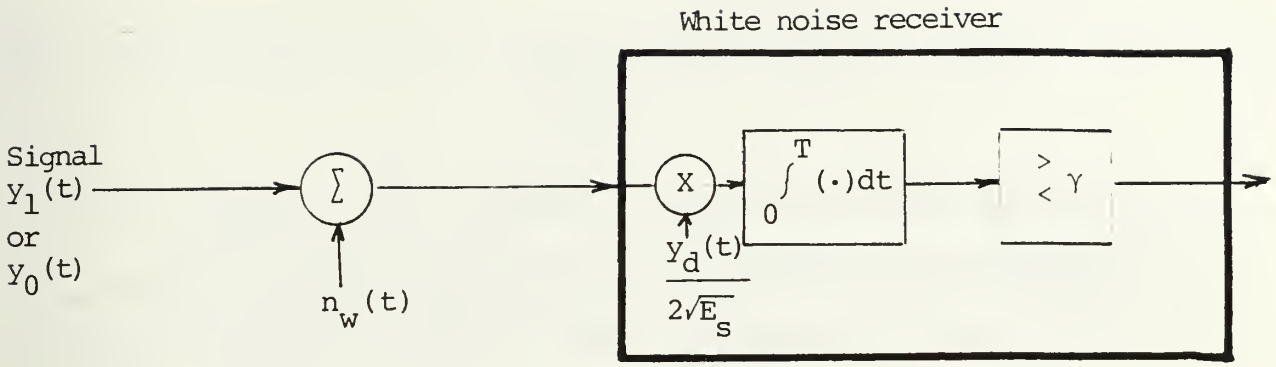

Figure 5.1

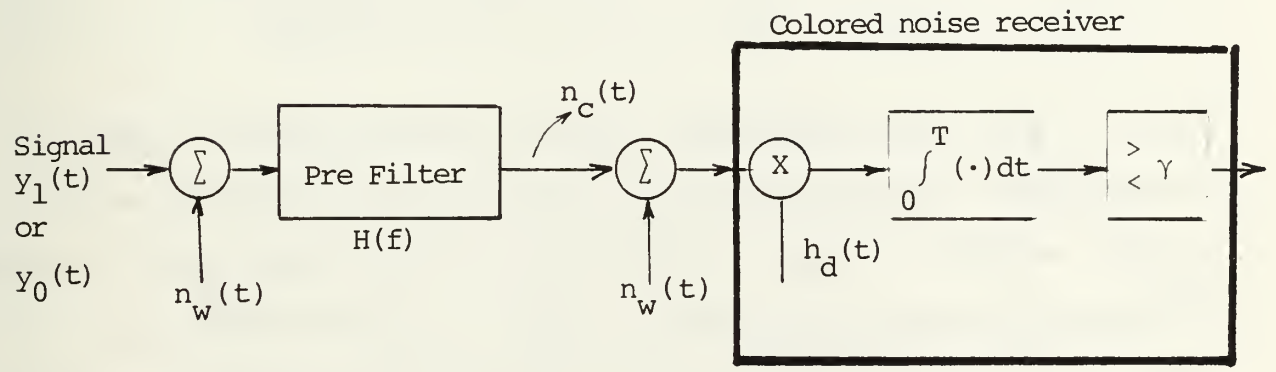

Figure 5.2 Preamplifier Receiver

of the receiver. We assume that the preamplifier has a transfer function given by

$$H(f) = \frac{G\beta}{j2\pi f + \beta} \tag{5.1}$$

The input noise power spectral density level is $N_0/2$. The RF preamplifier produces a colored noise component due to the white input noise, having power spectral density given by

$$\phi_c(s) = \frac{N_0}{2} G^2 \frac{\beta^2}{-s^2 + \beta^2} \quad (s = j2\pi f) \tag{5.2}$$

It is reasonable to assume that at the input of the correlator there is also an additive white Gaussian noise component due to the front end thermal noise. The total noise P.S.D. at the input to the correlator is thus

$$\phi(s) = \phi_c(s) + \phi_w(s) = \frac{N_0}{2} + \frac{N_0}{2} G^2 \frac{\beta^2}{-s^2 + \beta^2} \tag{5.3}$$

Observe that the information signals are distorted by the preamplifier and therefore the output of the preamplifier no longer produces signals $y_0(t)$ or $y_1(t)$, but rather $y_0'(t)$ or $y_1'(t)$. Clearly $y_1'(t)$ and $y_0'(t)$ are the result of convolving $y_1(t)$ and $y_0(t)$ respectively with the preamplifier impulse response.

The receiver described in Fig. 5.2 is optimum for discriminating between $y_0'(t)$ and $y_1'(t)$ provided $h_d(t)$ is appropriately chosen. The autocorrelation function of the total noise is given by

$$K(\tau) = \frac{N_0}{2}\delta(\tau) + \frac{N_0}{4}\beta G^2 \exp(-\beta|\tau|)$$

The power of the colored noise component is given by

$$P_c = \frac{N_0}{4}\beta G^2$$

Observe that unlike the model of Chapter IV, P_c is no longer constant. When β changes, P_c is changed also.

C. RECTANGULAR PULSE RECEIVER DESIGN

Assume the input signals to the RF preamplifier to be

$$y_1(t) = \begin{cases} A & 0 \leq t \leq T \\ 0 & T < t,\ t < 0 \end{cases} \tag{5.5}$$

$$y_0(t) = \begin{cases} -A & 0 \leq t \leq T \\ 0 & T < t,\ t < 0 \end{cases} \tag{5.6}$$

so that

$$y_d(t) = \begin{cases} 2A & 0 \leq t \leq T \\ 0 & T < t,\ t < 0 \end{cases} \tag{5.7}$$

Since the impulse response of the preamplifier is

$$h(t) = G\varepsilon^{-\beta t}u(t)$$

then

$$y_d'(t) = \begin{cases} 2AG(1-\varepsilon^{-\beta t}) & 0 \leq t \leq T \\ 0 & t < 0,\ t > T \end{cases} \tag{5.8}$$

where

$$y_d'(t) = h(t) * y_d(t)$$

The correlating signal in the colored noise receiver is the solution to the integral equation

$$\frac{N_0}{2} h_d(t) + \int_0^T \beta \frac{N_0}{4} G^2 \exp(-\beta|t-u|) h_d(u)du = y_d'(t) = 2AG(1-\varepsilon^{-\beta t}) \tag{5.9}$$

The solution to this Fredholm equation is somewhat more complicated than the one worked out in Appendix A due to the fact that the function on the right hand side of the integral equation is no longer a constant whose derivatives are zero, but rather an exponential function. The detailed solution to Eq. (5.9) is worked out in Appendix E.

The correlating signal $h_d(t)$ is given by

$$h_d(t) = C + CK_1\varepsilon^{+\beta m_1 t} + CK_2\varepsilon^{-\beta m_1 t} \tag{5.10}$$

where

$$C = \frac{4AG}{N_0(1+G^2)} \tag{5.11}$$

$$m_1 = \sqrt{1+G^2} \tag{5.12}$$

$$K_1 = \frac{(m_1+1)\left[\varepsilon^{-Em_1} - \frac{m_1-1}{m_1+1}\varepsilon^{-2Em_1}\right]}{\frac{m_1+1}{m_1-1} - \frac{m_1-1}{m_1+1}\varepsilon^{-2Em_1}} \tag{5.13}$$

$$K_2 = \frac{(m_1-1)\left[\varepsilon^{-Em_1} - \frac{m_1+1}{m_1-1}\right]}{\frac{m_1+1}{m_1-1} - \frac{m_1-1}{m_1+1}\varepsilon^{-2Em_1}} \tag{5.14}$$

Ignoring the constant of proportionality, it is easy to see that $h_d(t)$ is a function of G and E only. Recall that G is the gain of the preamplifier and E is the ratio of the preamplifier bandwidth to the receiver bandwidth.

Fig. 5.3 shows a plot of $h_d(t)$ versus time normalized to the pulse width, for various values of E and G = 20 db. In practical design, however, the preamplifier bandwidth will not be much different than the correlator bandwidth. Fig. 5.4 shows again $h_d(t)$ for various values of E with G = 0 db. The white noise component in this case is dominant causing the correlating signal $h_d(t)$ to be almost flat. This is in agreement with known results on the correlation operation for receivers operating in white noise interference only with constant pulse input.

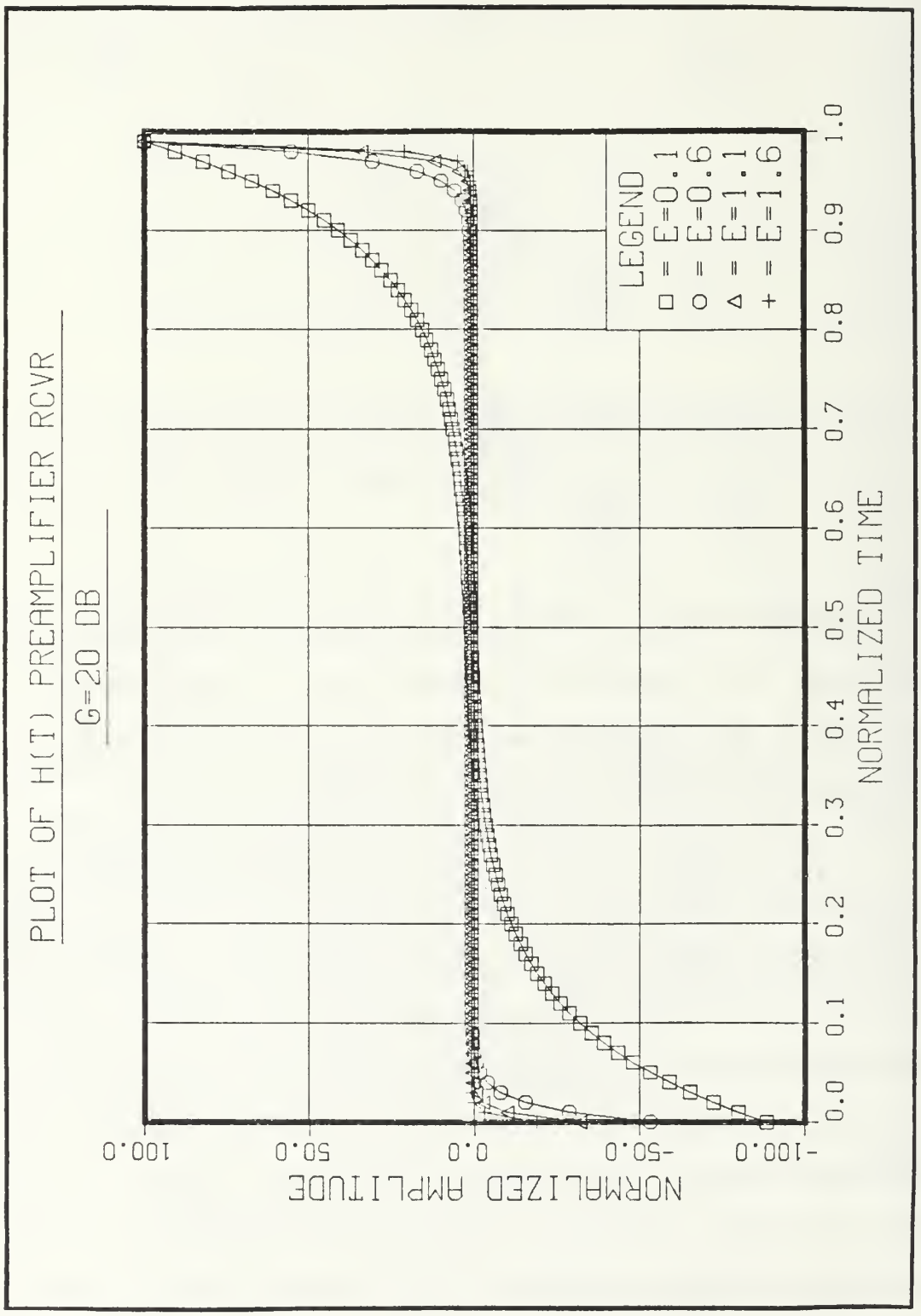

Figure 5.3 Plot of $h_d(t)$ for the Preamplifier Receiver G = 50

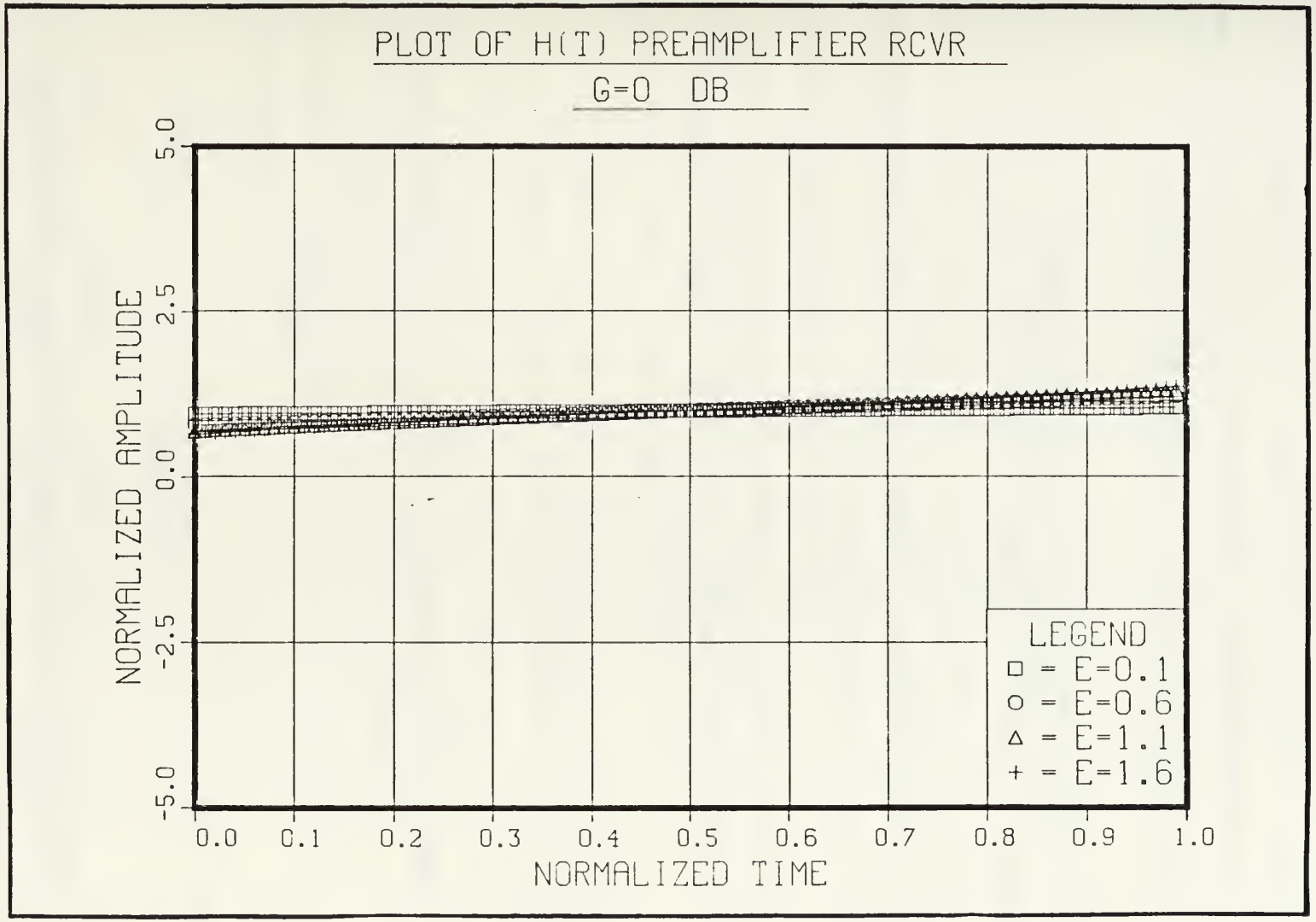

Figure 5.4 Plot of $h_d(t)$ for the Preamplifier Receiver G = 1

D. RECEIVER PERFORMANCES--THE IDEAL CASE

In this section the performance of the receivers shown in Figs. 5.1 and 5.2 is analyzed.

The performance of the colored noise receiver with equiprobable binary signals is given by Eq. (2.26).

$$P_e = \mathrm{ERFC}_*\left(\frac{1}{4}\int_0^T y_d'(t)h_d(t)dt\right)^{1/2} \tag{2.26}$$

If we substitute $y_d'(t)$ as given by Eq. (5.8) and $h_d(t)$ as given by Eqs. (5.10)-(5.14), we get

$$P_e = \mathrm{ERFC}_*\left(\frac{1}{4}\int_0^T \frac{8A^2G^2}{N_0(1+G^2)}(1-\varepsilon^{-\beta t})(1+K_1\varepsilon^{\beta m_1 t}+K_2\varepsilon^{-\beta m_1 t})dt\right)^{1/2} \tag{5.15}$$

Evaluating the integral yields

$$P_e = \mathrm{ERFC}_*\left[\frac{2A^2G^2T}{N_0(1+G^2)}\left(1-\frac{1-\varepsilon^{-E}}{E}+K_1\frac{\varepsilon^{m_1E}-1}{m_1E}-K_1\frac{\varepsilon^{(m_1-1)E}-1}{E(m_1-1)}+K_2\frac{1-\varepsilon^{-m_1E}}{Em_1}+K_2\frac{\varepsilon^{-E(m_1+1)}-1}{E(m_1+1)}\right)\right]^{1/2} \tag{5.16}$$

Since A^2T/N_0 can be interpreted as the SNR, we obtain

$$P_e = \mathrm{ERFC}_*\left[\frac{2\mathrm{SNR}G^2}{(1+G^2)}\left(1-\frac{1-\varepsilon^{-E}}{E}+K_1\frac{\varepsilon^{m_1E}-1}{m_1E}-K_1\frac{\varepsilon^{(m_1-1)E}-1}{E(m_1-1)}+K_2\frac{1-\varepsilon^{-m_1E}}{Em_1}+K_2\frac{\varepsilon^{-E(m_1+1)}-1}{E(m_1+1)}\right)\right]^{1/2} \tag{5.17}$$

where K_1 and K_2 are defined by Eqs. (5.13) and (5.14). The white noise receiver performance for equiprobable antipodal signals is given by

$$P_e = \text{ERFC}_*[\sqrt{2\text{SNR}}]$$

Fig. 5.5 shows a performance comparison between the two receivers for G = 50. It is clear that both receivers perform equally as well. The addition of the preamplifier did not improve the performance of the receiver of Fig. 5.2.

E. RECEIVER PERFORMANCES--PRACTICAL CASE

In the previous section we assumed the system analyzed consisted of only ideal components. These components didn't contribute any noise to the overall system.

In this section we discard this assumption and instead work with practical elements, so that the white noise receiver has an input noise figure NF_1. We may thus state that the power spectral density level due to the input white Gaussian noise is no longer $N_0/2$ but rather $\frac{N_0}{2} \cdot NF_1$. Therefore, the performance of the white noise receiver for equiprobable antipodal signals is

$$P_e = \text{ERFC}_*[\sqrt{2\text{SNR}/NF_1}]$$

The preamp receiver has also a non-unity noise figure associated with it, which we denote NF_2. Since the receiver input

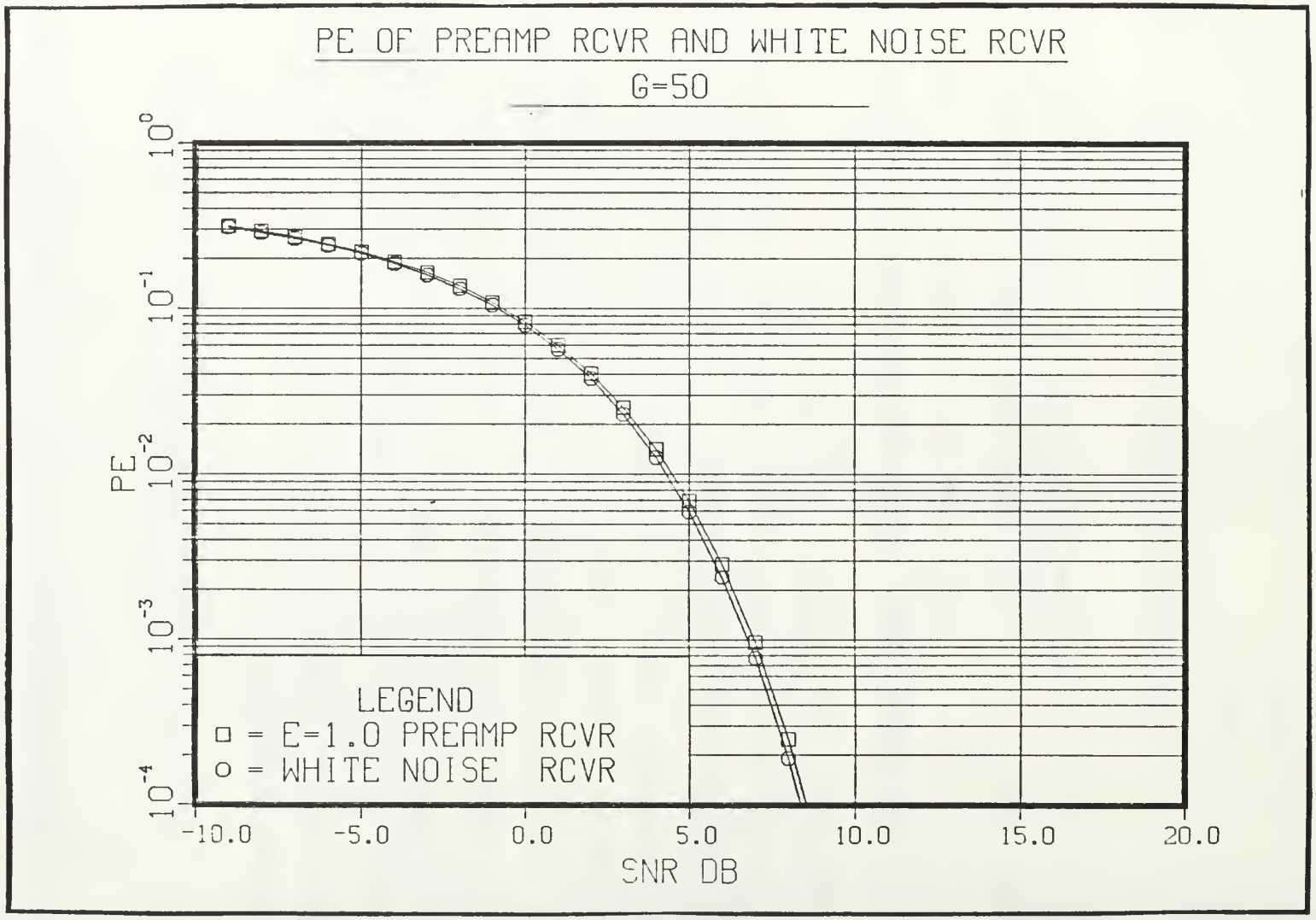

Figure 5.5 P_e of Preamplifier Receiver and White Noise Receiver

stage is assumed to be a low noise preamplifier (otherwise there is no benefit in utilizing this preamplifier), we can assume that

$$NF_2 < NF_1 .$$

The performance of the colored noise receiver is no longer given by Eq. (5.17) but must be modified accordingly to yield

$$P_e = ERFC_* \left[\frac{2SNR\,G^2}{N_0(NF_1 + NF_2 G^2)} \left[1 - \frac{1-\varepsilon^{-E}}{E} + K_1 \left(\frac{\varepsilon^{m_1 E} - 1}{m_1 E} - \frac{\varepsilon^{(m_1-1)E} - 1}{E(m_1-1)} \right) + K_2 \left(\frac{1-\varepsilon^{-m_1 E}}{Em_1} + \frac{\varepsilon^{-E(m_1+1)}}{E(m_1+1)} \right) \right] \right]^{1/2} \qquad (5.18)$$

Fig. 5.6 shows the performance of the two receivers analyzed in this section. It is clear that utilization of a low noise preamplifier improvedsignificantly the performance of the colored noise receiver. However it must be pointed out that if we design a receiver which consists of white noise receiver and a preamplifier, its performance would almost be the same as the performance of the colored noise correlator with preamplifier as described in Fig. 5.6. The major contribution to improved performance is due to the low noise amplifier and not due to the specific correlator used in the system.

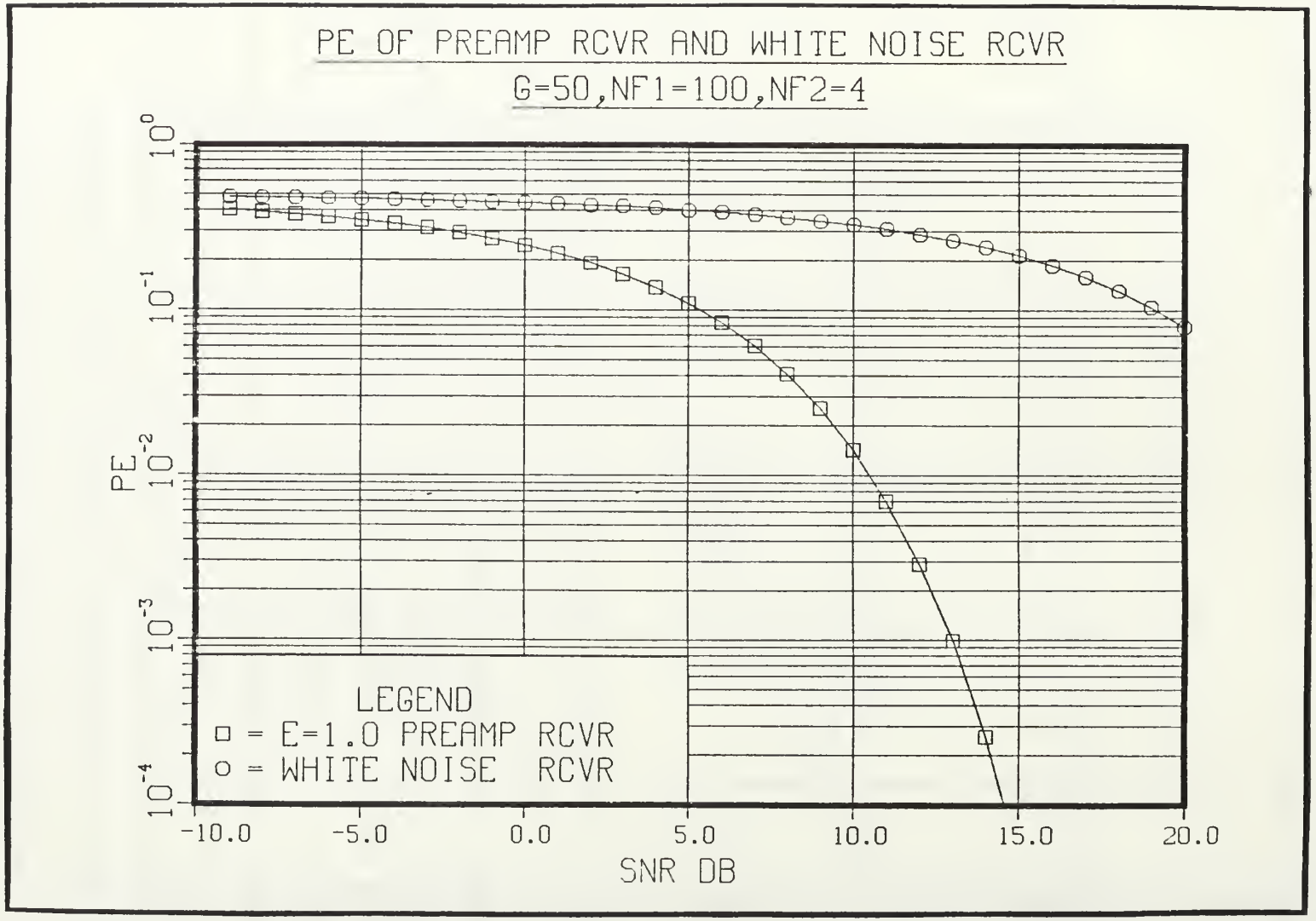

Figure 5.6 P_e of Preamplifier Receiver and Colored Noise Receiver, $NF_1 = 100$, $NF_2 = 4$

VI. JAMMING THE COLORED NOISE RECEIVER

A. INTRODUCTION

In previous chapters the design and performance of receivers operating in an environment consisting of colored noise interference were analyzed. The interference was assumed known and the receiver was optimized to the presence of that interference. In this chapter the model is expanded by considering the presence of a hostile jammer attempting to jam the communication channel. The jammer is hostile in the sense that its parameters are not known to the receiver designer. The main purpose here is to find the optimal jammer waveform that causes maximum damage to a communication channel of the type analyzed in previous chapters and to determine whether the colored noise receiver is more or less sensitive than a white noise receiver to jamming signals.

B. THE MODEL

The system model is described in Fig. 6.1. It consists of a digital coherent communication receiver operating in the presence of:

1. Colored noise interference
2. Additive white Gaussian noise
3. Jamming signal.

The digital information is transmitted via binary, baseband signals that encounter baseband interference and jamming.

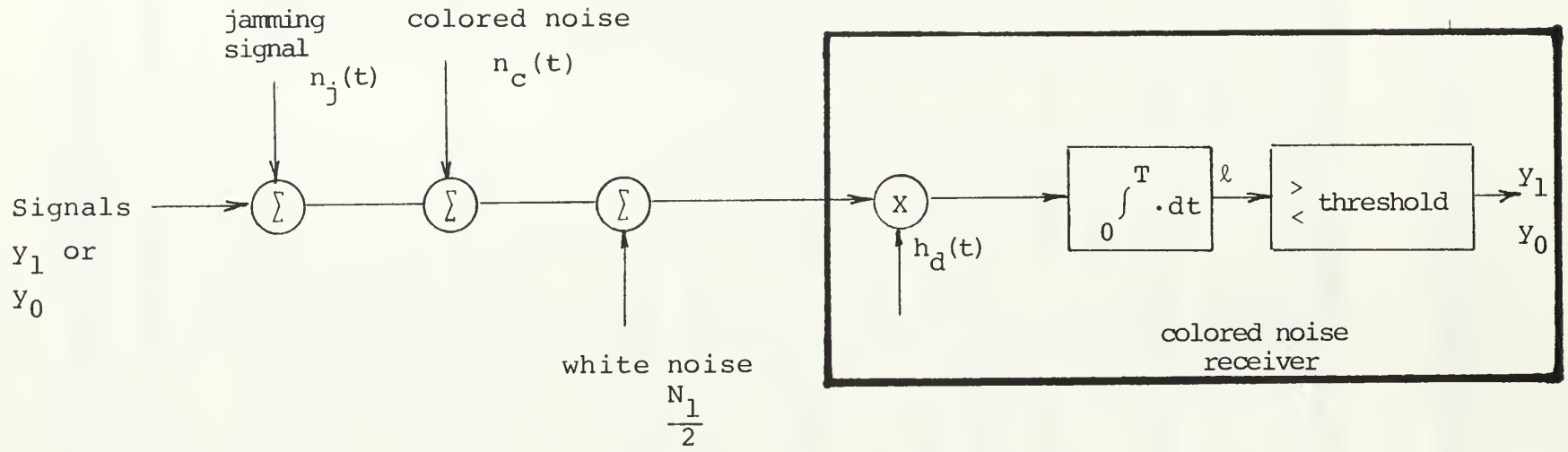

Figure 6.1 Colored Noise Receiver with Jammer

Extensions to bandpass signal analysis is straightforward in light of the results described in Chapter III, Section C.

The P.S.D. of the colored noise interference is assumed to be the same as in Chapter IV. Specifically, the colored noise P.S.D. used here is given by Eq. (4.2). Also the signals $y_1(t)$ and $y_0(t)$ are defined by Eqs. (4.8) and (4.9). The jammer is assumed to be deterministic and its specific waveshape will be determined in the solution to the optimization problem.

C. DERIVATION OF THE OPTIMAL JAMMING WAVEFORM

The decision process due to the presence of a jammer becomes

$$\text{Hypothesis } H_0: \quad z(t) = y_0(t) + n_c(t) + n_w(t) + n_j(t) \qquad (6.1)$$

$$0 \leq t \leq T$$

$$\text{Hypothesis } H_1: \quad z(t) = y_1(t) + n_c(t) + n_w(t) + n_j(t) \qquad (6.2)$$

Observe that $n_j(t)$ is modeled here as a deterministic waveform. The signals $y_0(t)$ and $y_1(t)$ are assumed to be antipodal. The energies of the signals are given by

$$E_s = \int_0^T y_1^2(t)dt = \int_0^T y_0^2(t)dt \; . \qquad (6.3)$$

The receiver generates the statistic ℓ which is a Gaussian random variable. Its conditional mean is given by

$$E[\ell|H_1] = E\{\int_0^T h_d(t)[y_1(t) + n_c(t) + n_j(t) + n_w(t)]dt\}$$

$$= \int_0^T h_d(t)[y_1(t) + n_j(t)]dt \triangleq m_1 \tag{6.4}$$

and similarly

$$E[\ell|H_0] = \int_0^T h_d(t)[y_0(t) + n_j(t)]dt \triangleq m_0 \tag{6.5}$$

The conditional variance of ℓ is given by

$$\text{Var}\{\ell|H_1\} = \text{Var}\{\ell|H_0\} = E\left\{\left[\int_0^T h_d(t)[n_w(t)+n_c(t)]dt\right]^2\right\}$$

$$\triangleq \sigma_\ell^2 \tag{6.6}$$

Note that since the jammer waveform is modeled as deterministic, it does not affect the variance of the statistic ℓ. This would not be the case if the jammer waveform were a sample function of a random process. The receiver threshold γ for antipodal equiprobable signals is equal to zero as previously demonstrated (see Eq. (2.1)).

Define now

$$\xi \triangleq \frac{1}{2}\int_0^T y_d(t)h_d(t)dt \tag{6.7}$$

From Eq. (2.23), we know that $2\xi = \sigma_\ell^2$. Introducing the shorthand notation

$$(h_d, n_j) = \int_0^T h_d(t) n_j(t)\, dt \tag{6.8}$$

the performance of the receiver of Fig. 6.1 can be shown to be given by

$$P_e = \frac{1}{2} \int_{[\xi-(h_d,n_j)]/\sigma_\ell}^{\infty} \frac{1}{\sqrt{2\pi}} \varepsilon^{-x^2/2} dx + \frac{1}{2} \int_{-\infty}^{[-\xi-(h_d,n_j)]/\sigma_\ell} \frac{1}{\sqrt{2\pi}} \varepsilon^{-x^2/2} dx \tag{6.9}$$

$$= \frac{1}{2} \mathrm{ERFC}_*\left[\frac{\xi-(h_d,n_j)}{\sqrt{2\xi}}\right] + \frac{1}{2} \mathrm{ERFC}_*\left[\frac{\xi+(h_d,n_j)}{\sqrt{2\xi}}\right]$$

where $P\{H_0\} = P\{H_1\} = \frac{1}{2}$ has been assumed.

Define

$$\alpha \triangleq (h_d, n_j)$$

and differentiate P_e with respect to α. This yields

$$\frac{\partial P_e}{\partial \alpha} = \frac{\varepsilon^{-(\xi^2+\alpha^2)/4\xi}}{\sqrt{2\pi 2\xi}}\left[\frac{\varepsilon^{\xi\alpha/\sqrt{2\xi}} - \varepsilon^{-\xi\alpha/\sqrt{2\xi}}}{2}\right] = \frac{\varepsilon^{-(\xi^2+\alpha^2)/4\xi}}{\sqrt{4\pi\xi}} \sinh\sqrt{\xi/2}\,\alpha \tag{6.11}$$

Since ξ is non-negative, it is clear that

$$\frac{\partial \bar{P}_e}{\partial \alpha} = \begin{cases} > 0 & \alpha > 0 \\ = 0 & \alpha = 0 \\ < 0 & \alpha < 0 \end{cases} \tag{6.11}$$

Therefore $\alpha = 0$ is a minimum point of P_e, and by making $|\alpha|$ as large as possible, P_e is maximized, because Eq. (6.11) shows that P_e is monotonic in $|\alpha|$.

From the Cauchy-Schwarz inequality, it can be seen that

$$\alpha = (h_d, n_j) \leq ||h_d|| \cdot ||n_j|| \tag{6.12}$$

with equality holding if

$$n_j(t) = K\, h_d(t) \tag{6.13}$$

where K is an arbitrary constant.

The energy E_{nj} of the jammer is given by (from Eq. (6.13))

$$E_{nj} = K^2 \int_0^T h_d^2(t)\,dt = K^2 \cdot ||h_d||^2 \tag{6.14}$$

Therefore, we must have

$$K = \frac{\sqrt{E_{nj}}}{||h_d||} \tag{6.15}$$

and the optimum jammer that is energy constrained is given by

$$n_j(t) = \frac{\sqrt{E_{nj}}}{||h_d||} h_d(t) \qquad (6.16)$$

This derivation is valid for both a white noise and a colored noise coherent receiver. The only difference is in $h_d(t)$. For a white noise receiver, $h_d(t)$ is proportional to $y_d(t)$. Therefore the waveform of the optimum jammer will be related to the waveforms used to transmit the binary information. However for the colored noise receiver, $h_d(t)$ is no longer directly related to the signals $y_1(t)$ and $y_0(t)$. Thus the optimum jammer may have a waveshape that has no resemblance to the waveforms used to transmit the binary information. It is clearly feasible to implement an optimum jammer against a white noise receiver. All that must be done is to transmit the difference of the signal waveforms, or use a repeater channel [Ref. 15]. However it is almost impossible to optimize a jammer against a colored noise receiver unless all the details about the correlator receiver being used are known.

D. PERFORMANCE OF THE WHITE NOISE RECEIVER WITH OPTIMAL JAMMING

In order to properly evaluate the effect of jamming on colored noise receivers, it is necessary to first evaluate the effect of jamming on white noise receivers. The results on the latter can then be used as a reference, to which results

on the former can be compared. We assume here the model described in Fig. 6.1 with the only difference being that now a white noise receiver is used in place of the colored noise receiver. That is, $h_d(t)$ must be replaced by $y_d(t)$. The receiver performance without jamming (however with noise interference) has been evaluated in Chapter IV, Section F. A statistic ℓ is generated by the receiver of Fig. 6.1, where the conditional moments of the statistic are given by Eqs. (4.29), (4.30), (4.31) and repeated here for convenience.

$$E[\ell|H_1] = \sqrt{E_s} \tag{4.29}$$

$$E[\ell|H_0] = -\sqrt{E_s} \tag{4.30}$$

$$\text{Var}[\ell|H_1] = \text{Var}[\ell|H_0] = \frac{N_1}{2} + \frac{N_0}{2}\left(\frac{E-1+\exp(-E)}{E}\right) \triangleq \sigma_\ell^2 \tag{4.31}$$

Observe that E is defined by Eq. (4.12).

The performance of this receiver is given by Eq. (4.39), namely

$$P_e = \text{ERFC}_*\left\{\sqrt{\frac{E_s}{\frac{N_1}{2} + \frac{N_0}{2}\left[\frac{E-1+\exp(-E)}{E}\right]}}\right\} = \text{ERFC}_*\left\{\sqrt{\frac{E_s}{\sigma_\ell^2}}\right\} \tag{4.39}$$

for equiprobable signals. Here again the deterministic jammer affects the conditional means of ℓ but not its conditional variances.

We now obtain

$$E[\ell|H_1] = \int_0^T h_d(t)[y_1(t) + n_j(t)]dt$$

$$= \int_0^T h_d(t)y_1(t)dt + \int_0^T h_d(t)n_j(t)dt \qquad (6.17)$$

$$E[\ell|H_0] = -\int_0^T h_d(t)y_1(t)dt + \int_0^T h_d(t)n_j(t)dt \qquad (6.18)$$

Substituting the optimum jammer, derived in Section C and given by Eq. (6.16), yields

$$E[\ell|H_1] = \int_0^T \frac{y_d(t)}{2\sqrt{E_s}} y_1(t)dt + \int_0^T y_d(t) \frac{\sqrt{E_{nj}}}{||y_d||} \frac{y_d(t)}{2\sqrt{E_s}} dt$$

$$= \sqrt{E_s} + \sqrt{E_{nj}} \qquad (6.19)$$

$$E[\ell|H_0] = \sqrt{E_s} - \sqrt{E_{nj}}$$

Recall that for the white noise receiver $h_d(t) = y_d(t)/2\sqrt{E_s}$.

The performance of the white noise receiver becomes

$$P_e = \frac{1}{2} \text{ERFC}_*[\frac{\sqrt{E_s}}{\sigma_\ell}(1 + \frac{\sqrt{E_{nj}}}{\sqrt{E_s}})] + \frac{1}{2} \text{ERFC}_*[\frac{\sqrt{E_s}}{\sigma_\ell}(1 - \frac{\sqrt{E_{nj}}}{\sqrt{E_s}})] \qquad (6.20)$$

Observe that if no jammer is present, Eq. (6.20) takes on the form of the P_e for a white noise receiver in the presence

of noise interference only. The jammer effect can be seen from the introduction of the $(1 \pm \frac{\sqrt{E_{nj}}}{\sqrt{E_s}})$ factors.

E. PERFORMANCE OF THE COLORED NOISE RECEIVER IN THE PRESENCE OF JAMMING

The performance of the colored noise receiver in the presence of jamming was derived in Section C and the receiver P_e is given by Eq. (6.9), namely

$$P_e = \frac{1}{2} \text{ERFC}_*[\frac{\xi+(h_d,n_j)}{\sqrt{2\xi}}] + \frac{1}{2} \text{ERFC}_*[\frac{\xi-(h_d,n_j)}{\sqrt{2\xi}}] \qquad (6.9)$$

We assume that the model described in Section B is valid in the foregoing analysis.

The performance of the receiver in Fig. 6.1 when no jammer is present was analyzed in Chapter IV and its P_e given by Eq. (4.26), namely

$$P_e = \text{ERFC}_*(\sqrt{\xi/2}) = \text{ERFC}_*[\frac{2\text{SNR}}{1+(\text{JSR})(\text{SNR})\frac{4}{E}}(1 + \frac{2(m_1+1)-4\varepsilon^{-Em_1}-2\varepsilon^{-2E(m_1+1)}}{Em_1(\frac{m_1+1}{m_1-1} - \frac{m_1-1}{m_1+1}\varepsilon^{-2Em_1})}(m_1-1))]^{1/2}$$

$$= \text{ERFC}_*[\frac{2\text{SNR}}{1+(\text{JSR})(\text{SNR})\frac{4}{E}} f_1(E,m_1)]^{1/2} \qquad (6.21)$$

where E and m_1 were defined in Eq. (4.12) and Eq. (4.17) respectively and JSR is the ratio of interference power to signal power. In order to evaluate the performance of the receiver analyzed

above under jamming conditions, the factor (h_d, n_j) must be evaluated for various jamming waveforms. The analysis will be carried out for two different cases.

1. The jammer has the same waveshape as the information signal waveforms (i.e., rectangular pulses).
2. The jammer has been optimized according to the results of Section D.

Case 1:

The jammer waveform is given by

$$n_j(t) = \frac{\sqrt{E_{nj}}}{\sqrt{E_s}} y_1(t) \tag{6.22}$$

Substituting Eq. (6.22) into Eq. (6.8) yields

$$(h_d, n_j) = \int_0^T h_d(t) n_j(t) dt = \int_0^T \frac{\sqrt{E_{nj}}}{\sqrt{E_s}} y_1(t) h_d(t) dt$$

$$= \frac{\sqrt{E_{nj}}}{\sqrt{E_s}} \int_0^T y_1(t) h_d(t) dt \tag{6.23}$$

Substituting Eq. (6.7) into Eq. (6.23) yields

$$(h_d, n_j) = \frac{\sqrt{E_{nj}}}{\sqrt{E_s}} \xi \tag{6.24}$$

Furthermore, substitution of Eq. (6.21) and Eq. (6.24) into Eq. (6.9) yields finally

$$P_e = \frac{1}{2}\,\mathrm{ERFC}_*[\sqrt{\xi/2}(1 + \sqrt{E_{nj}/E_s})] + \frac{1}{2}\,\mathrm{ERFC}_*[\sqrt{\xi/2}(1 - \sqrt{E_{nj}/E_s})]$$

$$= \frac{1}{2}\,\mathrm{ERFC}_*\left[\sqrt{\frac{2\mathrm{SNR}}{1 + (\mathrm{JSR})(\mathrm{SNR})\frac{4}{E}\, f_1(E_1,m_1)}}\,(1 + \sqrt{E_{nj}/E_s})\right]$$

$$+ \frac{1}{2}\,\mathrm{ERFC}_*\left[\sqrt{\frac{2\mathrm{SNR} f_1(E,m_1)}{1 + (\mathrm{JSR})(\mathrm{SNR})\frac{4}{E}}}\,(1 - \sqrt{E_{nj}/E_s})\right] \qquad (6.25)$$

Analysis and simulation carried out on Eq. (6.25) reveals that this receiver performs at almost the same level as the white noise receiver analyzed in Chapter IV, Section F. The performance of the white noise receiver without jammer is given by Eq. (4.39). Its performance is almost the same as that of the colored noise receiver without jammer whose performance is given by Eq. (6.21). This fact was demonstrated by the numerical results presented in Tables 4.1-4.5.

When the jammer is introduced, the arguments of the error function for both receivers has to be modified by the same factor $(1 \pm \sqrt{E_{nj}}/\sqrt{E_s})$. Therefore the performance of the two receivers under jamming conditions remains almost identical.

Case 2:

The optimum waveform jammer analyzed in Section D is given by Eq. (6.16). Substituting Eq. (6.16) into Eq. (6.8) yields

$$(h_d, n_j) = \int_0^T \frac{\sqrt{E_{nj}}}{||h_d||}\, h_d(t) h_d(t)\,dt = \sqrt{E_{nj}}\;||h_d|| \;. \qquad (6.26)$$

Substituting now the appropriate $h_d(t)$ which is given by Eqs. (4.13)-(4.16) yields

$$(h_d,n_j) = \frac{\sqrt{E_{nj}}}{\sqrt{E_s}} \frac{2SNR}{1+\frac{4(JSR)(SNR)}{E}}[1 + 2K_2^2\varepsilon^{-Em_1} + K_2^2(\frac{1-\varepsilon^{-2Em_1}}{Em_1}) + 4K_2 \frac{(1-\varepsilon^{-Em_1})}{Em_1}]^{1/2} \quad (6.27)$$

where K_2 is defined by Eq. (4.15).

Equation (6.27) can be written in the form

$$(h_d,n_j) = \frac{\sqrt{E_{nj}}}{\sqrt{E_s}} \frac{2SNR}{1+\frac{4(JSR)(SNR)}{E}} \sqrt{f_2(E_1,m_1)} \quad (6.28)$$

Substituting Eq.s (6.28), (6.21) into Eq. (6.9), yields the performance of the colored noise receiver in the presence of the optimum jammer. This result is

$$P_e = \frac{1}{2} \text{ERFC}_*[\sqrt{\frac{2SNRf_1(E_1,m_1)}{1+\frac{4(JSR)(SNR)}{E}}}(1 - \frac{\sqrt{E_{nj}}}{\sqrt{E_s}} \frac{\sqrt{f_2(E_1,m_1)}}{\sqrt{f_1(E_1,m_1)}})]$$

$$+ \frac{1}{2} \text{ERFC}_*[\sqrt{\frac{2SNRf_1(E_1,m_1)}{1+\frac{4(JSR)(SNR)}{E}}}(1 + \sqrt{E_{nj}/E_s}\sqrt{\frac{f_2(E_1,m_1)}{f_1(E_1,m_1)}})] \quad (6.29)$$

where f_1 and f_2 are defined by Eqs. (6.21) and (6.28) respectively.

In Figures 6.2-6.5, a comparison between the performance of the colored noise receivers analyzed under the two jamming

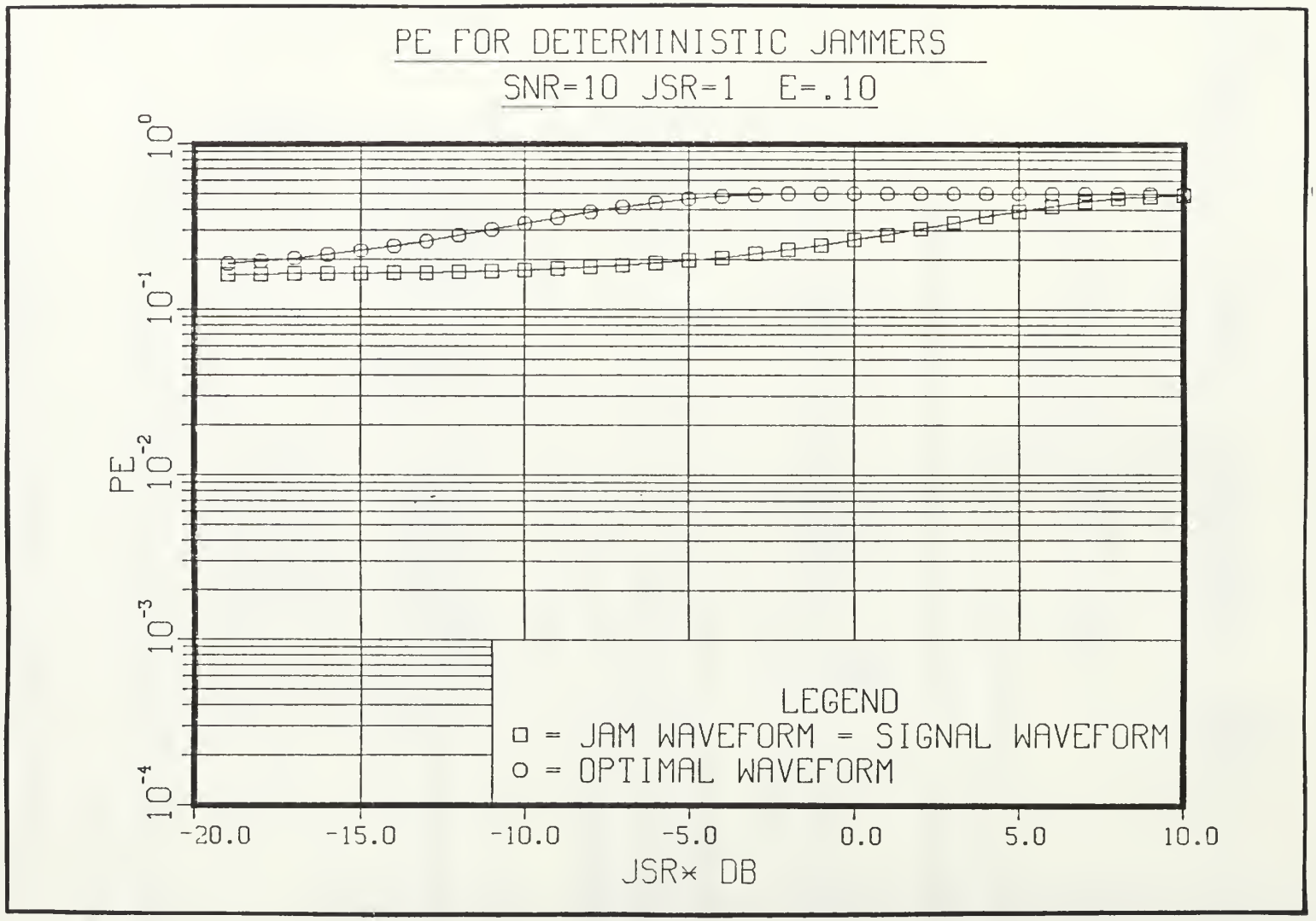

Figure 6.2 P_e For Deterministic Jammers, JSR = 1, E = 0.1

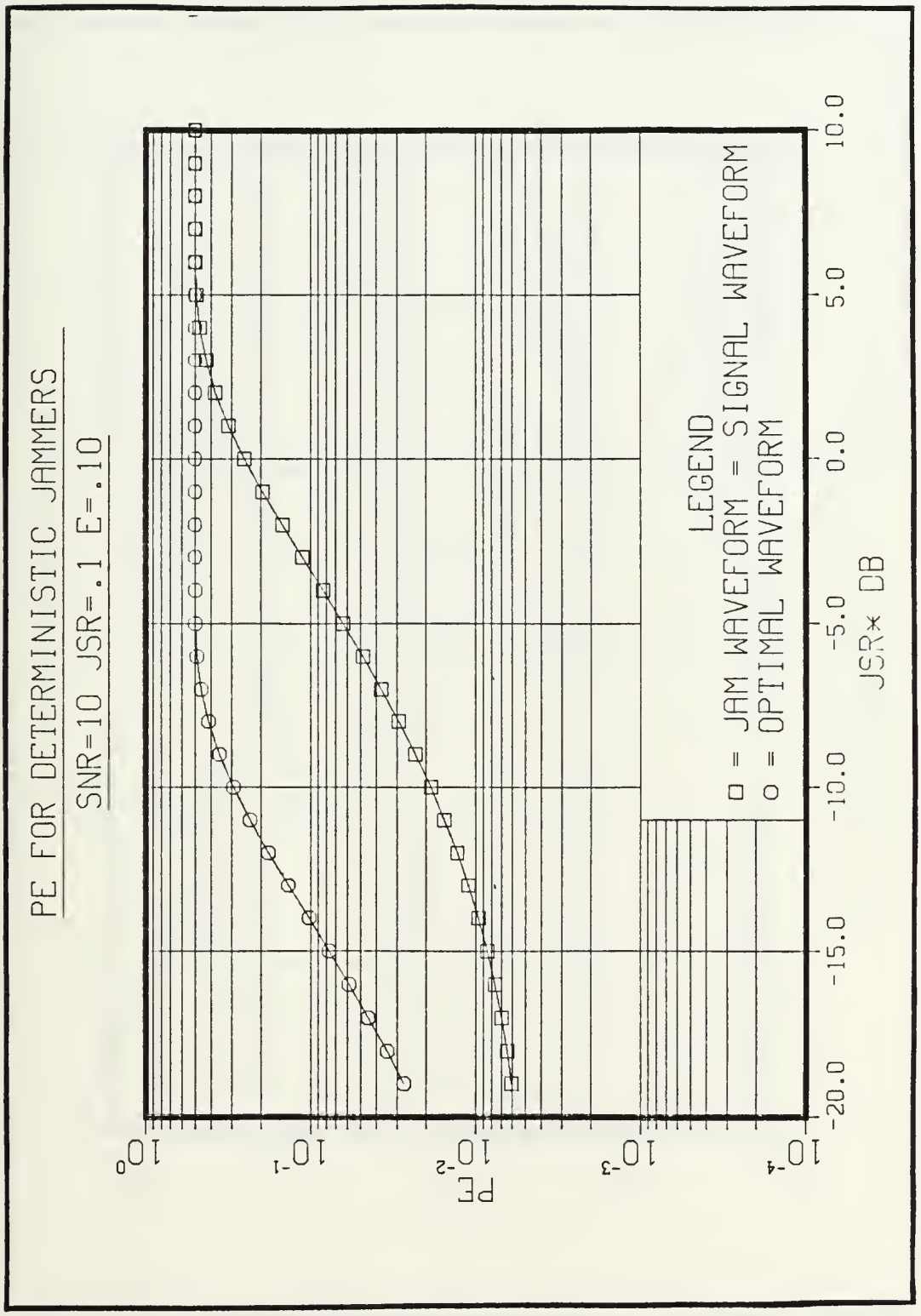

Figure 6.3 P_e for Deterministic Jammers, JSR = 0.1, E = 0.1

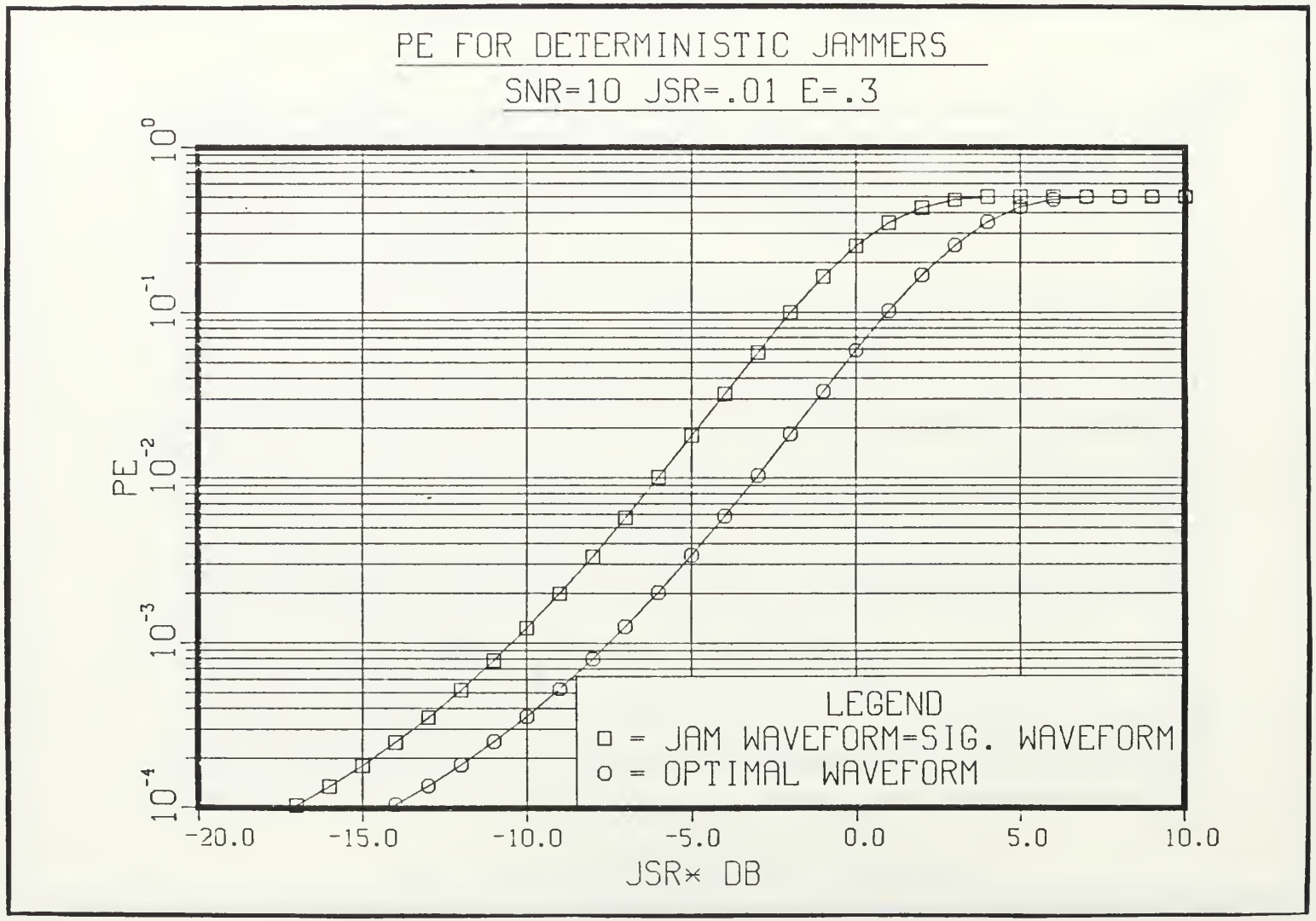

Figure 6.4 P_e for Deterministic Jammers, JSR = 0.01, E = 0.3

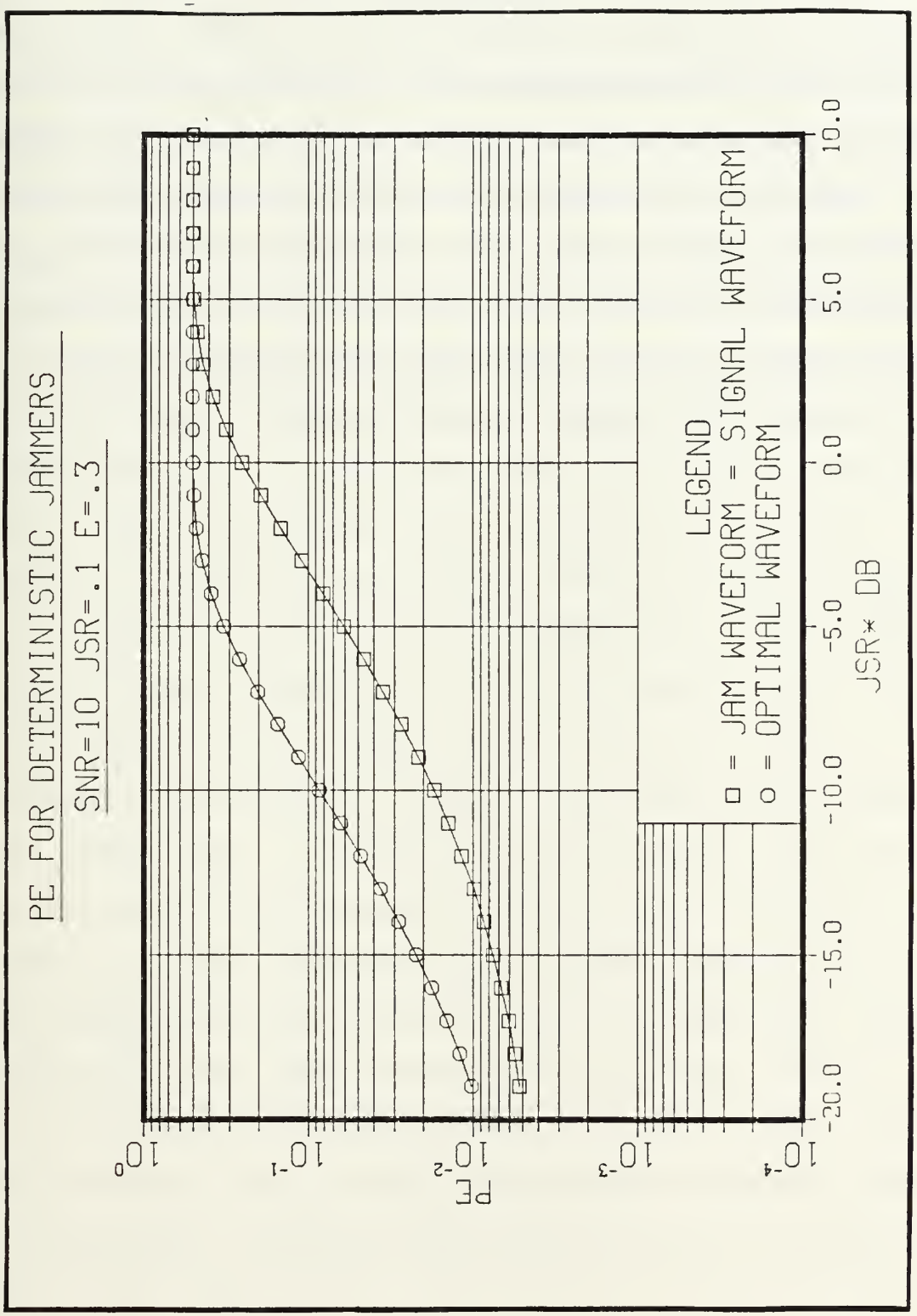

Figure 6.5 P_e for Deterministic Jammers, JSR = 0.1, E = 0.3

conditions is shown. The pertinent equations are Eq. (6.29) and Eq. (6.25). All results are a function of the jammer to signal energy ratio, E_{nj}/E_s, denoted as JSR*. The figures show that the optimum jammer ($n_j(t) = Kh_d(t)$) causes much more damage to the receiver performance than the suboptimum jammer ($n_j(t) = Ky_d(t)$). If one tries to determine what JSR value is required to cause the receiver to operate at a certain P_e, it can be seen that when the optimal jammer is used, less jamming power is needed (somewhere between 6-12 db less jammer power) than if the suboptimum jammer of Case 1 is used.

VII. CONCLUSION

This thesis presents several applications of the theory of signal detection in the presence of colored noise. In it, the analysis of practical design implications of the theory is carried out and the evaluation of the performance of receivers designed according to this theory is undertaken. The design of a digital receiver operating in a colored noise environment requires the solution of a specific Fredholm integral equation. In order to solve the Fredholm integral equation, the designer must have available an analytical expression for the autocorrelation function of the colored noise and also know the signal waveforms being used to transmit the digital information. Once this information is available, solution of the Fredholm integral equation must be attempted. As discussed in Chapter III, analytical solutions do not always exist. Even if solutions do exist, the procedure for solving the integral equation is at best tedious. In most of the work undertaken, a relatively simple case in which the colored noise was the output of an amplifier stage followed by a first order Butterworth filter was analyzed. This leads to an analytical expression for the noise autocorrelation for which the solution of the integral equation exists and is tractable. Several cases were presented in Appendices A-E.

The receiver structure and correlator signal waveform were derived in Chapter IV for the cases in which the binary information was transmitted using either rectangular or sinusoidal pulses. As shown in Appendix D, the design of such a receiver was quite feasible once the noise autocorrelation was specified and an analytical solution to the Fredholm integral equation was obtained. Next, the performance of this receiver was evaluated and compared to that of a white noise receiver operating in the same environment. The results showed that both receivers performed almost identically with only a few percent difference in receiver error probabilities when rectangular pulses were used for signaling. Only when optimum sinusoidal pulses were used in place of the rectangular pulses, a major improvement in the performance of the colored noise receiver in comparison to the performance of the white noise receiver was achieved. Low noise preamplifiers used to improve receiver sensitivity are also a source of colored noise. The effect such preamplifiers have on practical receivers was discussed in Chapter V. The conclusion of such analysis indicated again that receivers designed to operate in a colored noise environment do not perform significantly better than white noise receivers, operating in a similar environment. Improvement is achieved only due to the fact that the low noise preamplifier isolates the front-end of the receiver from the "noisy" correlator.

Although these results were obtained using a first order Butterworth filter amplifier excited by white noise as a

model for the colored noise source, it is reasonable to expect (based on the results of Ref. 16) that using a more complicated model for the colored noise generation will not change significantly the results and the conclusions obtained.

The ECM vulnerability of the colored noise receiver versus that of the white noise receiver was analyzed in Chapter VI. Both receivers were found to be equally sensitive to a deterministic waveform jammer. However when the jammer used an optimum waveform which was related to the signals used in the correlation operation in the receivers, a significant deterioration in the performance of the colored noise receiver was observed. It must be noted however that the jammer waveform designer has in practice almost no chance to accurately determine what this optimum waveform should be and how to appropriately use it.

This thesis has demonstrated the relative robustness of the white noise receiver. In most practical cases, even when colored noise interferences are present, the white noise receiver performs nearly as well as the colored noise receiver designed for specific interference models. Only in very special cases in which optimum signal waveforms were used to transmit the binary information did the colored noise receiver perform better than a white noise receiver.

Table 7.1 presents a quantitative summary of the performances of the colored noise receivers and white noise receivers. Table 7.2 presents the effect of jammers on the performances of the white noise and the colored noise receiver.

Table 7.1

The Receiver	P_e SNR = 10, JSR = 1, E = 1
White noise receiver rectangular pulses	0.129
Colored noise receiver rectangular pulses	0.125
Colored noise receiver sinusoidal pulses $\bar{b} = 1$(*)	0.07
Colored noise receiver sinusoidal pulses $\bar{b} = 4$	0.01
Colored noise receiver sinusoidal pulses $\bar{b} = 8$	0.00045
White noise receiver sinusoidal pulses $\bar{b} = 1$	0.28
White noise receiver sinusoidal pulses $\bar{b} = 4$	0.03
White noise receiver sinusoidal pulses $\bar{b} = 6$	0.002

(*) $\bar{b}$ is defined by Eq. (4.44) and is the ratio of the signal frequency to interference noise bandwidth.

Table 7.2

The Receiver	P_e Jammer waveform equals signal waveform SNR = 10, JSR = 1, E = 0.1 JSR* = -5 db	P_e Optimal jammer SNR = 10, JSR = 1 E = 0.1 JSR* = -5 db
White noise receiver rectangular pulses	0.05	0.05
Colored noise receiver rectangular pulses	0.05	0.4

* JSR* is related to the jammer and defined as E_{nj}/E_s, namely the ratio of interference energy to signal energy.

APPENDIX A

DETAILED SOLUTION OF A FREDHOLM II EQUATION FOR COLORED NOISE WITH RATIONAL SPECTRA AND RECTANGULAR PULSES

The Fredholm II equation to be solved is

$$\frac{N_1}{2} h_d(t) + \int_0^T K_c(t-u) h_d(u) du = y_d(t) \quad 0 \leq t \leq T \tag{A.1}$$

The noise is assumed to be a sample function from a W.S.S. process whose P.S.D. is given by

$$\phi_c(s) = \frac{2\alpha\beta}{-s^2 + \beta^2} = \frac{N(s^2)}{D(s^2)} \tag{A.2}$$

The autocorrelation function corresponding to this P.S.D. is given by

$$K_c(\tau) = \alpha\varepsilon^{-\beta|\tau|} \tag{A.3}$$

The signal $y_d(t)$ is defined by

$$y_d(t) = \begin{cases} 2A & 0 \leq t \leq T \\ 0 & t < 0,\ t > T \end{cases} \tag{A.4}$$

Equation (A.2) can be written as follows

$$D(s^2)[\phi_c(s)] = N(s^2) = 2\alpha\beta \tag{A.5}$$

Multiplying $\phi_c(s)$ by $D(s^2)$ corresponds to operating on $K_c(t)$ with $D(p^2)$ in the time domain where p is the derivative operator.

Eq. (A.5) can be written as

$$D(p^2)[K_c(t)] = 2\alpha\beta\delta(t) \tag{A.6}$$

Operating with $D(p^2)$ on Eq. (A.1) yields

$$D(p^2)\frac{N_1}{2}h_d(t) + \int_0^T D(p^2)[K_c(t-\sigma)h_d(\sigma)]d\sigma = D(p^2)[y_d(t)] \tag{A.7}$$

Substituting Eq. (A.6) in Eq. (A.7) and performing the operation specified by $D(p^2)$, yields the differential equation

$$-\frac{N_1}{2}\ddot{h}_d(t) + \frac{N_1}{2}\beta^2 h_d(t) + 2\alpha\beta h_d(t) = -\ddot{y}_d(t) + \beta^2 y_d(t) \tag{A.8}$$

Substituting $y_d(t)$ as defined by Eq. (A.4) yields

$$-\frac{N_1}{2}\ddot{h}_d(t) + \beta^{*2}h_d(t) = \beta^2 A \qquad 0 \leq t \leq T \tag{A.9}$$

where

$$\beta^{*2} = \frac{N_1}{2}\beta^2 + 2\alpha\beta \ .$$

Eq. (A.9) is a differential equation. Its particular solution is given by a constant C, where

$$C = \left(\frac{\beta}{\beta^*}\right)^2 2A \tag{A.10}$$

Its homogeneous solution is

$$K_1 \varepsilon^{\gamma t} + K_2 \varepsilon^{-\gamma t} \tag{A.11}$$

where

$$\gamma = \sqrt{2/N_1}\, \beta^* \tag{A.12}$$

The complete solution is of the form

$$h_d(t) = C + CK_1 \varepsilon^{\gamma t} + CK_2 \varepsilon^{-\gamma t} \tag{A.13}$$

where the constants K_1 and K_2 are obtained by plugging this solution into the Fredholm II equation.

This process is very long and tedious and involves a great deal of algebraic manipulations. At the end of this process two linear equations are obtained which define K_1 and K_2, namely

$$\left.\begin{aligned} \frac{-K_1}{\gamma + \beta} + \frac{K_2}{\gamma - \beta} &= \frac{1}{\beta} \\ \frac{K_1 \varepsilon^{\gamma T}}{\gamma - \beta} - \frac{K_2 \varepsilon^{-\gamma T}}{\gamma + \beta} &= \frac{1}{\beta} \end{aligned}\right\} \tag{A.14}$$

The simultaneous solution of Eq. (A.14) is

$$K_1 = \frac{\frac{1}{\beta}(\gamma^2 - \beta^2)[(\gamma - \beta)\varepsilon^{-\beta T} + (\gamma + \beta)]}{(\gamma + \beta)^2\varepsilon^{\gamma T} - (\gamma - \beta)^2\varepsilon^{-\gamma T}}$$

(A.15)

$$K_2 = \frac{\frac{1}{\beta}(\gamma^2 - \beta^2)[(\gamma - \beta) + (\gamma + \beta)\varepsilon^{\gamma T}]}{(\gamma + \beta)^2\varepsilon^{\gamma T} - (\gamma - \beta)^2\varepsilon^{-\gamma T}}$$

where

$$C = \left(\frac{\beta}{\beta^*}\right)^2 2A = \frac{2A\beta^2}{\frac{N_1}{2}\beta^2 + 2\alpha\beta} \tag{A.16}$$

and

$$\gamma = \sqrt{2/N_1}\,\beta^* = \sqrt{\frac{2}{N_1}\left(\frac{N_1}{2}\beta^2 + 2\alpha\beta\right)}$$

$$= \beta\sqrt{1 + N_0/N_1} \tag{A.17}$$

APPENDIX B

DETAILED SOLUTION OF A FREDHOLM II EQUATION FOR COLORED NOISE WITH RATIONAL SPECTRA AND SINUSOIDAL PULSE INPUT

The Fredholm II equation to be solved is

$$\frac{N_1}{2} h_d(t) + \int_0^T K_c(t-u) h_d(u) du = y_d(t) \quad 0 \leq t \leq T \tag{B.1}$$

The colored noise P.S.D. and autocorrelation function are the same as defined in Appendix A, Eqs. (A.2), (A.3). The signal is however different and is defined as

$$y_d(t) = \begin{cases} 2A \sin bt & 0 \leq t \leq T \\ 0 & 0 > t,\ t > T \end{cases} \tag{B.2}$$

The procedure outlined in Appendix A, Eqs. (A.5)-(A.8) is applicable here. Using Eq. (A.8) and using $y_d(t)$ as derived by Eq. (B.2) yields

$$-\frac{N_1}{2} \ddot{h}_d(t) + \beta^{*2} h_d(t) = 2A(b^2 + \beta^2) \sin bt \tag{B.3}$$

The homogeneous solution is not affected by the sinusoidal driving function in this equation. Thus, the homogeneous solution is given by Eq. (A.11). The particular solution is given by

$$h_p(t) = C \sin bt \tag{B.4}$$

where C is given by

$$C = \frac{2A[b^2 + \beta^2]}{\frac{N_1}{2} b^2 + \beta^{*2}} \tag{B.5}$$

The complete solution is therefore

$$h_d(t) = C \sin bt + CK_1 \varepsilon^{\gamma t} + CK_2 \varepsilon^{-\gamma t} \quad 0 \leq t \leq T \tag{B.6}$$

where the constants K_1 and K_2 are obtained by plugging this solution into the Fredholm II equation. This process is very long and tedious and involves a great deal of algebraic manipulations. At the end of this process two linear equations are obtained which define K_1 and K_2, namely

$$\begin{cases} \dfrac{-K_1}{\gamma + \beta} + \dfrac{K_2}{\gamma - \beta} = \dfrac{-b}{\beta^2 + b^2} \\ \dfrac{K_1}{\gamma - \beta} \varepsilon^{\gamma T} - \dfrac{K_2 \varepsilon^{-\gamma T}}{\gamma + \beta} = \dfrac{1}{\beta^2 + b^2}[\beta \sin bT + b \cos bT] \end{cases} \tag{B.7}$$

The solution for K_1 and K_2 is

$$K_1 = \frac{(\frac{b}{\beta})(\frac{\gamma}{\beta}-1)\varepsilon^{-2\gamma T} + (\sin bT + \frac{b}{\beta}\cos bT)(\frac{\gamma}{\beta}+1)\varepsilon^{-\gamma T}}{[1 + (\frac{b}{\beta})^2][-\frac{\frac{\gamma}{\beta}-1}{\frac{\gamma}{\beta}+1}\varepsilon^{-2\gamma T} + \frac{\frac{\gamma}{\beta}+1}{\frac{\gamma}{\beta}-1}]} \qquad (B.8)$$

$$K_2 = \frac{-\frac{b}{\beta}(\frac{\gamma}{\beta}+1) + (\sin bT + (\frac{b}{\beta})\cos bT)(\frac{\gamma}{\beta}-1)\varepsilon^{-\gamma T}}{[1 + (\frac{b}{\beta})^2][\frac{\frac{\gamma}{\beta}+1}{\frac{\gamma}{\beta}-1} - \frac{\frac{\gamma}{\beta}-1}{\frac{\gamma}{\beta}+1}\varepsilon^{-2\gamma T}]} \qquad (B.9)$$

APPENDIX C

THE FREDHOLM II EQUATION FOR BANDPASS SIGNALS

The Fredholm II equation for bandpass signals and spectra is given by

$$\frac{N_1}{2}\tilde{h}_d(t) + \int_0^T \tilde{K}_c(t-u)\tilde{h}_d(u)du = \tilde{y}_d(t) \quad 0 \leq t \leq T \tag{C.1}$$

where

$$\tilde{y}_d(t) = y_d(t)\cos\omega_0 t \tag{C.2}$$

$$\tilde{K}_c(t) = K_c(t)\cos\omega_0 t \tag{C.3}$$

We assume that the solution of Eq. (C.1) is of the form

$$\tilde{h}_d(t) = h_d(t)\cos\omega_0 t \tag{C.4}$$

and check the conditions under which this assumption is valid. Substituting Eqs. (C.2), (C.3), and (C.4) into Eq. (C.1) yields

$$\frac{N_1}{2}h_d(t)\cos\omega_0 t + \int_0^T K_c(t-u)\cos\omega_0(t-u)h_d(u)\cos\omega_0 u\,du$$

$$= y_d(t)\cos\omega_0 t \tag{C.5}$$

Using trigonometric identities yields the following equation

$$\frac{N_1}{2}h_d(t)\cos\omega_0 t + \int_0^T \cos\omega_0 t K_c(t-u)h_d(u)du$$

$$+ \int_0^T \cos\omega_0(t-2u)K_c(t-u)h_d(u)du$$

$$= y_d(t)\cos\omega_0 t \qquad (C.6)$$

We now denote

$$\int_0^T \cos\omega_0(t-2u)K_c(t-u)h_d(u)du = \alpha(t) \qquad (C.7)$$

and check the conditions under which $\alpha(t)$ is negligible. We may write

$$h_d^*(t) = h_d(t)[u(t) - u(t-T)] \qquad (C.8)$$

Substituting $h_d^*(t)$ in Eq. (C.7) enables changing the limits of integration

$$\int_{-\infty}^{\infty} K_c(t-u)\cos\omega_0(t-2u)h_d^*(u)du = \alpha(t) \qquad (C.9)$$

Taking the Fourier transform of Eq. (C.9) yields

$$F[\alpha(t)] = \int_{-\infty}^{\infty}\int_{-\infty}^{\infty} K_c(t-u)\cos\omega_0(t-2u)h_d^*(u)\varepsilon^{-j\omega t}dudt \qquad (C.10)$$

with

$$t-u = \sigma \tag{C.11}$$

substituting in Eq. (C.10) yields

$$F\{\alpha(t)\} = \int_{-\infty}^{\infty} h_d^*(u)\left[\int_{-\infty}^{\infty} K_c(\sigma)\cos\omega_0(\sigma-u)\varepsilon^{-j\omega\sigma}d\sigma\right]\varepsilon^{-j\omega u}du \tag{C.12}$$

The expression inside the parenthesis is the Fourier transform of $K_c(\sigma)\cos\omega_0(\sigma-u)$ and is given by the convolution of the Fourier transform of $K_c(\sigma)$ and $\cos\omega_0(\sigma-u)$. Performing the convolution yields

$$\frac{1}{2}\phi_c(\omega-\omega_0)\varepsilon^{-j\omega_0 u} + \frac{1}{2}\phi_c(\omega+\omega_0)\varepsilon^{j\omega_0 u} \tag{C.13}$$

where $\phi_c(\omega)$ is the P.S.D. or equivalently the Fourier Transform of $K_c(t)$.

Substituting Eq. (C.13) into Eq. (C.12) yields

$$F[\alpha(t)] = \frac{1}{2}\int_{-\infty}^{\infty} h_d^*(u)\left(\phi_c(\omega-\omega_0)\varepsilon^{-j\omega_0 u} + \phi_c(\omega+\omega_0)\varepsilon^{j\omega_0 u}\right)\varepsilon^{-j\omega u}du \tag{C.14}$$

Evaluating the integral yields

$$\frac{1}{2}H_d^*(\omega+\omega_0)\phi_c(\omega-\omega_0) + \frac{1}{2}\phi_c(\omega+\omega_0)H_d^*(\omega-\omega_0) \tag{C.15}$$

Eq. (C.15) is a cross product of two low pass functions at high frequencies. If

$$\omega_0 \gg \frac{1}{T}$$

then Eq. (C.15) represents a negligible small value. Under these conditions, $\alpha(t)$ is a small number.

The bandpass Eq. (C.6) can be written as

$$\frac{N}{2}h_d(t)\cos\omega_0 t + \cos\omega_0 t \int_0^T K_c(t-u)h_d(u)du = y_d(t)\cos\omega_0 t \tag{C.16}$$

The solution to Eq. (C.16) is the solution to the lowpass equation multiplied by $\cos\omega_0 t$.

The conclusion is that if the communication channel center frequency is much bigger than the channel bandwidth, then the solution to Eq. (C.1) can be written as a solution to a baseband equation multiplied by $\cos\omega_0 t$ where ω_0 is the channel center frequency.

APPENDIX D

BLOCK DIAGRAM OF A SIGNAL GENERATOR FOR $h_d(t)$

A suggested block diagram for generating $h_d(t)$ in the correlator unit is shown in Fig. D.1.

The desired waveform is sampled at a high enough rate. The samples are digitized and stored in the PROM. When the sync pulse is received, the proper addresses of the PROM are read sequentially and the output is converted to an analog signal $h_d(t)$. The PROM can store several waveforms for various types of transmission signals or interferences.

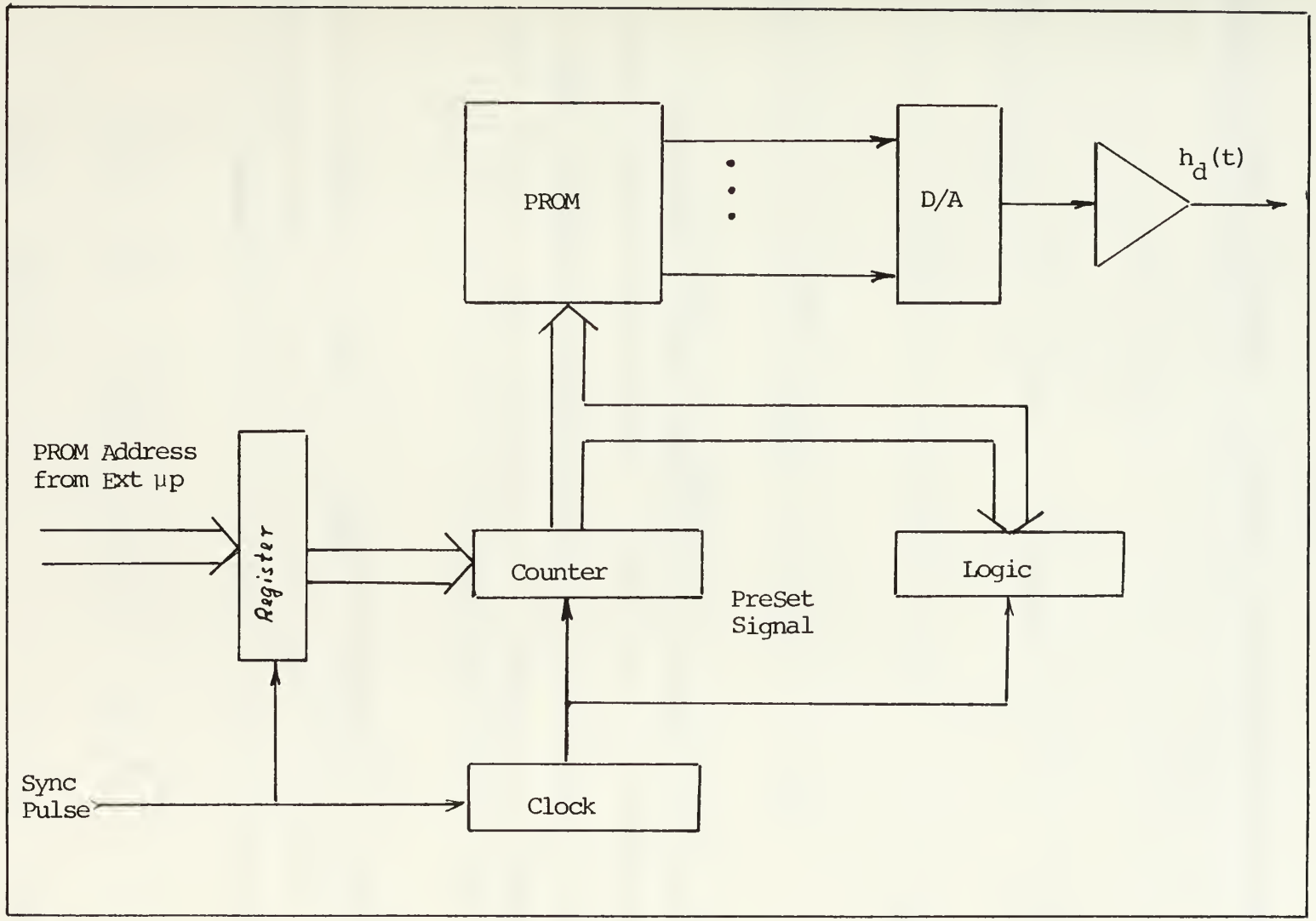

Figure D.1. Block Diagram of $h_d(t)$ Waveform Generator

APPENDIX E

DETAILED SOLUTION OF THE FREDHOLM II EQUATION GIVEN BY EQ. (5.9)

The Fredholm II equation to be solved is

$$\frac{N_0}{2} h_d(t) + \int_0^T K_c(t-u) h_d(u)\,du = 2AG(1-\varepsilon^{-\beta t}) = y_d(t) \qquad (E.1)$$

$$0 \leq t \leq T$$

where

$$K_c(\tau) = \alpha\varepsilon^{-\beta|\tau|} = \frac{N_0}{4}\beta G^2\, \varepsilon^{-\beta|\tau|} \qquad (E.2)$$

The solution follows the procedure shown in Appendix A except that y_d is no longer a constant and therefore modification to the particular solution will be necessary. The procedure of Appendix A is applicable here up to Eq. (A.8), so that our starting point is

$$-\frac{N_0}{2}\ddot{h}_d(t) + \frac{N_0}{2}\beta^2 h_d(t) + 2\alpha\beta h_d(t) = -\ddot{y}_d(t) + \beta^2 y_d(t) \qquad (E.3)$$

Substituting $y_d(t)$ as defined by Eq. (E.1) yields

$$-\frac{N_0}{2}\ddot{h}_d(t) + \beta^{*2} h_d(t) = 2A\beta^2 G \qquad (E.4)$$

where

$$\beta^{*2} = \frac{N_0}{2}\beta^2 + 2\alpha\beta = \frac{N_0}{2}\beta^2 + \frac{N_0}{2}\beta^2 G^2 = \frac{N_0}{2}\beta^2(1+G^2) \qquad (E.5)$$

The homogeneous solution to Eq. (E.4) is

$$CK_1\varepsilon^{\gamma t} + CK_2\varepsilon^{-\gamma t} \qquad (E.6)$$

where γ is given by

$$\gamma = \sqrt{2/N_0}\,\beta^* = \beta\sqrt{1+G^2} = \beta m_1 \qquad (E.7)$$

The particular solution is given by

$$C = \left(\frac{\beta}{\beta^*}\right)^2 2AG = \frac{4AG}{N_0(1+G^2)} \qquad (E.8)$$

The complete solution therefore is

$$h_d(t) = C + CK_1\varepsilon^{\gamma t} + CK_2\varepsilon^{-\gamma t}$$

The next step is to plug this solution into Eq. (E.1). This substitution leads to two equations that must be solved for K_1, and K_2, that is,

$$\frac{-K_1}{\gamma+\beta} + \frac{K_2}{\gamma-\beta} = -\frac{1}{\beta}$$

$$\frac{K_1\varepsilon^{\gamma T}}{\gamma-\beta} - \frac{K_2\varepsilon^{-\gamma T}}{\gamma+\beta} = \frac{1}{\beta} \qquad (E.9)$$

The simultaneous solution to these equations is

$$K_1 = \frac{\frac{1}{\beta}[(\gamma+\beta) - (\gamma-\beta)\varepsilon^{-\gamma T}](\gamma^2-\beta^2)}{\varepsilon^{\gamma T}(\gamma+\beta)^2 - (\gamma-\beta)^2\varepsilon^{-\gamma T}} \tag{E.10}$$

$$K_2 = \frac{\frac{1}{\beta}(\gamma^2-\beta^2)[(\gamma-\beta) - (\gamma+\beta)\varepsilon^{-\gamma T}]}{(\gamma+\beta)^2\varepsilon^{\gamma T} - (\gamma-\beta)^2\varepsilon^{-\gamma T}} \tag{E.11}$$

Substituting Eq. (E.7) into Eqs. (E.10) and (E.11), and introducing the notation

$$E = \beta T$$

yields

$$K_1 = \frac{(m_1+1)[\varepsilon^{-Em_1} - \frac{m_1-1}{m_1+1}\varepsilon^{-2Em_1}]}{\frac{m_1+1}{m_1-1} - \frac{m_1-1}{m_1+1}\varepsilon^{-2Em_1}} \tag{E.12}$$

$$K_2 = \frac{(m_1-1)[\varepsilon^{-Em_1} - \frac{m_1+1}{m_1-1}]}{\frac{m_1+1}{m_1-1} - \frac{m_1-1}{m_1+1}\varepsilon^{-2Em_1}} \tag{E.13}$$

LIST OF REFERENCES

1. Van Trees, Harry L., Detection Estimation and Modulation Theory, Part I, pp. 287-307, Wiley, 1968.

2. Srinath, M., P.K. Rajasekaran, An Introduction to Statistical Signal Processing With Applications, pp. 120-141, John Wiley, 1979.

3. Loeve, M., Probability Theory, D. Van Nostrand Co., Princeton, N.J., 1955.

4. Low Cost Anti-Jam Digital Data Link, Department of Electrical Engineering, University of Texas, Technical Report AFAL-TR-77-104, June 1977.

5. Orchnnikov, A.V. and A.F. Terpugov, Optimal Coherent Signal Systems for Information Transmission in the Presence of Colored Gaussian Noise, Report Number AST 1700I-029-76, March 1977.

6. Brewer, H., C.T. Leondes, A Treatment of Nonwhite Measurement Noise in Discrete Linear Systems, University of California at Los Angeles, Department of Engineering Systems, July 1975.

7. Van Trees, Harry L., Detection, Estimation and Modulation Theory, Part I, pp. 246-287, Wiley, 1968.

8. Srinath, M., P.K. Rajasekaran, An Introduction to Statistical Signal Processing With Applications, pp. 104-120, John Wiley, 1979.

9. Wozencraft, J., I.M. Jacobs, Principles of Communication Engineering, pp. 211-273, John Wiley, 1965.

10. Whalen, Anthony D., "Statistical Theory of Signal Detection and Parameter Estimation," IEEE Communication Magazine, Vol. 22, No. 6, June 1984.

11. Chambers, Li. G., Integral Equations--A Short Course, pp. 22-81, International Textbook Company, Limited, 1976.

12. Van Trees, Harry L., Detection Estimation and Modulation Theory, Part I, pp. 309-325, John Wiley, 1968.

13. Van Brundt, Applied ECM Countermeasures Handbook, pp. 464-470, EW Engineering, Inc., Vol. I, 1982.

14. Van Trees, Harry L., Detection Estimation and Modulation Theory, Part I, pp. 187-190, John Wiley, 1968.

15. Van Brundt, Applied ECM Countermeasures Handbook, Part I, pp. 356-376, EW Engineering, Inc., 1982.

16. Kassam, Saleem A., H. Vincent Poor, "Robust Signal Processing for Communication Systems," IEEE Communication Magazine, 1983.

INITIAL DISTRIBUTION LIST

		No. Copies
1.	Defense Technical Information Center Cameron Station Alexandria, Virginia 22304-6145	2
2.	Library, Code 0142 Naval Postgraduate School Monterey, California 93943-5100	2
3.	Prof. D. Bukofzer, Code 62Bh Naval Postgraduate School Monterey, California 93943-5100	5
4.	Prof. Jin Fu Chang, Code 62Cn Naval Postgraduate School Monterey, California 93943-5100	2
5.	Maj Avraham Hasarchi 42 Galit. st Nave Ilan Yavne - 70600 Israel	3

214298

Thesis
H29684
c.1

Hasarchi
An analysis of coherent digital receivers in the presence of colored noise interferences.